



HAL
open science

Standardisation and automatisisation of the diagnosis of patients with disorders of consciousness : a machine learning approach applied to electrophysiological brain and body signals

Federico Raimondo

► **To cite this version:**

Federico Raimondo. Standardisation and automatisisation of the diagnosis of patients with disorders of consciousness : a machine learning approach applied to electrophysiological brain and body signals. *Neurons and Cognition [q-bio.NC]*. Sorbonne Université; Universidad de Buenos Aires, 2018. English. NNT : 2018SORUS321 . tel-02864837

HAL Id: tel-02864837

<https://theses.hal.science/tel-02864837>

Submitted on 11 Jun 2020

HAL is a multi-disciplinary open access archive for the deposit and dissemination of scientific research documents, whether they are published or not. The documents may come from teaching and research institutions in France or abroad, or from public or private research centers.

L'archive ouverte pluridisciplinaire **HAL**, est destinée au dépôt et à la diffusion de documents scientifiques de niveau recherche, publiés ou non, émanant des établissements d'enseignement et de recherche français ou étrangers, des laboratoires publics ou privés.



Sorbonne Université
Universidad de Buenos Aires

Ecole Doctorale Cerveau Cognition Comportement (ED3C)
*Institut du Cerveau et de la Moelle épinière - PICNIC Lab et
Laboratorio de Inteligencia Artificial - DC, FCEyN*

Normalisation et automatisisation du diagnostic des patients atteints de troubles de la conscience: une approche par apprentissage automatique appliquée aux signaux électrophysiologiques du cerveau et du corps.

Standardisation and automatisisation of the diagnosis of patients with disorders of consciousness: a machine learning approach applied to electrophysiological brain and body signals.

par Federico RAIMONDO

Thèse de doctorat de Neurosciences

Dirigé para Laurent COHEN, Diego FERNÁNDEZ SLEZAK et Jacobo Diego SITT

Présentée et soutenue publiquement le 27/11/2018

Devant un jury composé de :

M Joaquin NAVAJAS AHUMADA	PU, Universidad Torcuato Di Tella	Rapporteur
M Enzo TAGLIAZUCCHI	CR, Instituto de Física de Buenos Aires	Rapporteur
M Pablo Miguel GRANITTO	PU, CIFASIS - CONICET	Examinateur
M Salvador Martin GUINJOAN	PU, FLENI - CONICET	Examinateur
M Jacobo Diego SITT	CR, INSERM	Directeur
M Diego FERNÁNDEZ SLEZAK	PU, Departamento de Computación, UBA	Directeur
M Laurent COHEN	PU-PH, Sorbonne Université	Directeur

Contents

Acknowledgments	vii
Abstract	ix
Résumé	xi
Resumen	xiii
1 Introduction	1
1.1 The study of Consciousness	2
1.1.1 Conscious Access vs Conscious States	2
1.1.2 Disorders of Consciousness	2
1.1.3 Why diagnosis is important?	3
1.2 State of the art of DOC diagnosis	5
1.2.1 Current tools for DOC diagnosis	5
1.3 Electroencephalography	9
1.3.1 What is EEG?	9
1.3.2 What do we analyse in EEG?	11
1.4 Electroencephalography in DOC patients	15
1.5 Methods used in this thesis	17
1.5.1 The Coma Recovery Scale (Revised)	17
1.5.2 The <i>Local-Global</i> paradigm	18
1.5.3 Machine Learning	19
1.5.4 Statistics	22
1.6 This work	23
1.6.1 Purpose	23
1.6.2 Description of chapters	23

2	Automation and identification of robust EEG-extracted markers for the diagnosis of DOC	25
2.1	Background	26
2.2	Objectives	27
2.3	Automation	27
2.3.1	Reasons to rewrite the code and automate the process	27
2.3.2	Software Implementation	28
2.3.3	Preprocessing	28
2.3.4	Optimisations and Performance	29
2.4	Replication	30
2.4.1	Methods	30
2.4.2	Results	35
2.5	Validation	36
2.5.1	Methods	36
2.5.2	Results	36
2.6	Clinical application	38
2.6.1	Report	38
2.7	Further steps: towards a universal tool	39
2.7.1	Generalisation to difference EEG recording configurations	40
2.7.2	Generalisation to Resting State	43
2.7.3	Discussion	45
2.8	Insights from Machine Learning	47
2.8.1	Methods	47
2.8.2	Results	48
2.8.3	Discussion	48
2.9	Summary	50
3	Towards cross-modal integration as a measure of consciousness	51
3.1	Background	52
3.2	Hypotheses	54
3.3	Methods	55
3.3.1	Cross-modal Local-Global	55
3.3.2	Subjects	58
3.3.3	EEG acquisition	58
3.3.4	Analysis	59
3.3.5	Group-Level analysis	59
3.3.6	Statistics	60
3.4	Results	60
3.4.1	ERP analysis	60

<i>CONTENTS</i>	v
3.4.2 ERP characterisation through MVPA	61
3.5 Discussion	61
4 Brain-Body interactions as a diagnostic marker for DOC	69
4.1 Background	70
4.2 Hypotheses	71
4.3 Baseline cardiac activity	72
4.3.1 Methods	72
4.3.2 Results	75
4.4 Cardiac markers of cognitive processing	78
4.4.1 Methods	78
4.4.2 Results	82
4.5 EEG and EKG Multivariate Pattern Analysis	82
4.5.1 Methods	82
4.5.2 Results	84
4.6 Discussion	86
5 Summary and final remarks	91

Acknowledgments

Despite that it is at the beginning, this is the last page that I wrote about this work. I have been thinking in this text since the moment that I opened the first file and started writing. It has been a bit more than five years, three countries, five summers, seven winters, three labs, and in each one of those moments, countless persons that have been part of this present in which I am. It is my wish to thank all these people that were and are part of my life.

I want to thank my parents, Martha and Dicky, who pushed me since I was little, but let me free to choose my future (although they never gave me the chance to live from rock).

To my sisters and brother, Nina, María y Tomás, who had to put up with moves, formalities, orders and favours. Who were always there, in good and bad times, even when I was not present enough.

To my aunts, uncles, grandparents and cousins: Magdalena, Pepe, Diana, Leticia, Julia, Tadeo, Candela. Who in every visit to Patagonia they reminded me that family is still there. To my uncle Gustavo, who was an enormous influence in my childhood and adolescence, and continues to show that one must still fight despite the misfortunes and bad moments. Stay strong!

To my Patagonian friends, who despite the distance, were always a place of comfort and joy. In alphabetical order and without articles: Adriano, Chacha, Chiqui, Chomba, Churi, Eze, Foco, Gato, Guille, Herni, Juanpa, Pablito, Pantro, Rata, Rodri, Ruso, Topo. Without forgetting Córdoba and Rosario.

To Tut, imperceptible and present at the same time.

To Yorgos, for the mind-cleansing videogames nights.

To Abuela Lidia, that at its time provided a place of encounter and exchange between friends. But principally, to those friends, that assisted religiously to discuss new ways to change the world between wines and bondiolas.

To the Department of Computer Sciences, for the excellent education provided and for being a community that does not let go, that forms you as a student, teacher and person.

To PICNIC Lab, a team with multiple formations, but always a team, with top players like Mariam, Diana, Sami, Denis, Camille, Florence, Benjamin, Melanie, Pauline, Bertrand, Kasia, Tal and everyone that passed by when I was around, and showed me that excellent

science can also be fun.

To the Coma Science Group, the place where I am writing this, for giving me the opportunity to continue my career.

To Diego, that one day found me in the hallway and proposed a project that started me as a researcher.

To Lionel, for his trust.

To Jaco, that wore the band, took the wheel, and started to row alone in a boat that was drifting, taking this PhD to an end, and to end in a way in which I never thought possible. Who formed me as a neuroscientist, who gave me direction, who trusted me and, principally, taught me how to do good science.

And last, but without diminishing merit, to those beautiful human beings with whom I share my life every day, that stood up to everything, the good and the bad moments, and that do not stop giving me energy. To Athena and Alex.

During the development of this work, I received funds from the Department of Computer Sciences (FCEyN, UBA), ICM (France) and, in particular, a scholarship from CONICET, that supported me during 5 years. For this reason, I want to thank specially to all the people that fought and keep fighting for the Argentinian science.

Standardisation and automatisisation of the diagnosis of patients with disorders of consciousness: a machine learning approach applied to electrophysiological brain and body signals.

Advances in modern medicine have led to an increase of patients diagnosed with disorders of consciousness (DOC). In these conditions, patients are awake, but without behavioural signs of awareness. An accurate evaluation of DOC patients has medico-ethical and societal implications, and it is of crucial importance because it typically informs prognosis. Misdiagnosis of patients, however, is a major concern in clinics due to intrinsic limitations of behavioural tools. One accessible assisting methodology for clinicians is electroencephalography (EEG). In a previous study, we introduced the use of EEG-extracted markers and machine learning as a tool for the diagnosis of DOC patients. In this work, we developed an automated analysis tool, and analysed the applicability and limitations of this method. Additionally, we proposed two approaches to enhance the accuracy of this method: (1) the use of multiple stimulation modalities to include neural correlates of multisensory integration and (2) the analysis of consciousness-mediated modulations of cardiac activity. Our results exceed the current state of knowledge in two dimensions. Clinically, we found that the method can be used in heterogeneous contexts, confirming the utility of machine learning as an automated tool for clinical diagnosis. Scientifically, our results highlight that brain-body interactions might be the fundamental mechanism to support the fusion of multiple senses into a unique percept, leading to the emergence of consciousness. Taken together, this work illustrates the importance of machine learning to individualised clinical assessment, and paves the way for inclusion of bodily functions when quantifying global states of consciousness.

Normalisation et automatisation du diagnostic des patients atteints de troubles de la conscience: une approche par apprentissage automatique appliquée aux signaux électrophysiologiques du cerveau et du corps.

Les progrès de la médecine moderne ont entraîné une augmentation du nombre de patients ayant des troubles de la conscience (DOC). Ces derniers, alors qu'ils sont éveillés, ne présentent pas de signes comportementaux de conscience. L'évaluation comportementale précise de ces patients a des implications médico-éthiques et sociales cruciales, car elle conditionne généralement le pronostic. Ainsi, les erreurs diagnostiques liées aux limites intrinsèques des outils comportementaux sont une préoccupation majeure pour les cliniciens et l'électroencéphalographie (EEG) pourrait s'avérer utile. Dans une étude précédente, nous avons introduit l'utilisation de marqueurs extraits de l'EEG et l'apprentissage supervisé pour le diagnostic des patients DOC. Dans ce travail, nous avons développé cet outil et analysé son applicabilité et ses limites. De plus, nous avons proposé deux approches pour améliorer la précision de cette méthode: (1) l'utilisation de multiples modalités de stimulation pour inclure des corrélats neuronaux de l'intégration multisensorielle et (2) l'analyse des modulations de l'activité cardiaque par la conscience. Nos résultats dépassent l'état actuel des connaissances dans deux dimensions. Cliniquement, nous avons constaté que la méthode pouvait être utilisée dans des contextes hétérogènes, confirmant l'utilité de l'apprentissage automatique en tant qu'outil automatisé de diagnostic clinique. Scientifiquement, nos résultats soulignent que les interactions cerveau-corps pourraient être le mécanisme fondamental pour soutenir l'intégration multisensorielle en un percept unique, conduisant à l'émergence de la conscience. Au total, ces travaux illustrent l'importance de l'apprentissage automatique pour une évaluation individualisée de la conscience et ouvrent la voie à l'inclusion des fonctions corporelles pour la quantification des états de conscience.

Estandarización y automatización en el diagnóstico de pacientes con desordenes de conciencia: aprendizaje automático aplicado a señales electrofisiológicas del cerebro y el cuerpo.

Avances en la medicina moderna han llevado a un incremento en el número de pacientes diagnosticados con desordenes de conciencia (DOC). En estas condiciones, los pacientes se encuentran despiertos, pero no muestran signos de entendimiento acerca de si mismos o el lugar donde se encuentran. Una evaluación precisa de los pacientes tiene implicaciones medico-éticas y sociales, y es de suma importancia porque típicamente informa el pronóstico. Los diagnósticos erróneos, no obstante, es una gran preocupación en las clínicas debido a las limitaciones intrínsecas de las herramientas de diagnóstico basados en comportamiento. Una tecnología accesible para asistir a los médicos es la electroencefalografía (EEG). En un estudio previo, introducimos el uso de marcadores extraídos de EEG en combinación con aprendizaje automático como una herramienta para el diagnóstico de pacientes DOC. En este trabajo, desarrollamos una herramienta de análisis automatizado, y analizamos la aplicabilidad y limitaciones de este método. Adicionalmente, proponemos dos enfoques para incrementar la precisión del diagnóstico: (1) el uso de múltiples modalidades de estimulación para incluir los correlatos neuronales de la integración multisensorial y (2) el análisis de las modulaciones de la actividad cardíaca mediadas por la conciencia. Nuestros resultados exceden el conocimiento actual en dos dimensiones. Clínicamente, encontramos que el método puede ser utilizada en contextos heterogéneos, confirmando la utilidad del aprendizaje automático como una herramienta para el diagnóstico clínico. Científicamente, nuestros resultados resaltan que las interacciones entre el cerebro y el cuerpo pueden ser el mecanismo fundamental para sostener la fusión de múltiples sentidos en una única percepción, conduciendo a la emergencia de la conciencia. En conjunto, este trabajo ilustra la importancia del aprendizaje automático para la evaluación clínica individualizada, y crea un punto de partida para la inclusión de las funciones corporales en la cuantificación de los estados de conciencia globales.

Chapter 1

Introduction

Contents

1.1	The study of Consciousness	2
1.1.1	Conscious Access vs Conscious States	2
1.1.2	Disorders of Consciousness	2
1.1.3	Why diagnosis is important?	3
1.2	State of the art of DOC diagnosis	5
1.2.1	Current tools for DOC diagnosis	5
1.3	Electroencephalography	9
1.3.1	What is EEG?	9
1.3.2	What do we analyse in EEG?	11
1.4	Electroencephalography in DOC patients	15
1.5	Methods used in this thesis	17
1.5.1	The Coma Recovery Scale (Revised)	17
1.5.2	The <i>Local-Global</i> paradigm	18
1.5.3	Machine Learning	19
1.5.4	Statistics	22
1.6	This work	23
1.6.1	Purpose	23
1.6.2	Description of chapters	23

1.1 The study of Consciousness

1.1.1 Conscious Access vs Conscious States

Throughout history, the term *consciousness* has been studied from disciplines as philosophy, psychology and biomedical sciences. Nowadays, there is still no universal definition for such an ambiguous concept (Baars, 2015). Depending on the use of the word *conscious*, it can refer to the *state of consciousness* or to *conscious access* or *processing*. In its intransitive use (e.g. “the patient is still conscious”), it refers to the state of consciousness, also called *wakefulness* or *vigilance*. In its transitive use (e.g. “I was not conscious of the red light”), it refers to access or processing of a specific piece of information. The information accessed consciously at a given moment defines the *conscious content*, which can be reported (Dehaene and Changeux, 2011).

1.1.2 Disorders of Consciousness

The state of consciousness, at the same time, is a multidimensional construct (Bayne et al., 2016). This means that it can be expressed in several distinct states which describe arousal level, cognitive function, and bodily states. In lack of a full description of these dimensions of each state of consciousness, we will here adopt a simplified definition coming from clinical practice (Posner et al., 2007). Clinical neurologists typically evaluate consciousness on two dimensions, *arousal* and *awareness*. Arousal refers to the level of wakefulness and is clinically indicated by eyes-opening. Awareness refers to the contents of consciousness and it is clinically evaluated by command following and by observing nonreflex behaviours. What is further known from clinics is that the relationship between these two dimensions is not always a positive one. The introduction of the mechanical ventilator in the 1950s and the development of intensive care in the 1960s made it possible for many patients to sustain their vegetative functions and allowed them to survive their severe injuries. Despite such advancement, many patients were found to suffer from altered states of consciousness, which had never been encountered before as these patients would normally die from apnea (Laureys and Boly, 2007). Patients in a vegetative state/unresponsive wakefulness syndrome (VS/UWS), although they show intermittent periods of wakefulness, they do not respond to stimulation

evidencing awareness of self and the environment (Jennett and Plum, 1972). Even when patients show discernible signs of behavioural non-reflex activity, coined as the minimally conscious state (MCS), they remain unable to communicate and are considered with impaired consciousness (Giacino et al., 2002). When patients regain the capacity of functional communication or object user are considered to be emerged from MCS (EMCS). An illustration comparing the different consciousness states is shown in Figure 1.1 on the following page.

1.1.3 Why diagnosis is important?

The impact of such profound states of unconsciousness is reflected in the composition of the first bioethical committees discussing the redefinition of life and death, hence predicting the medico-ethical legal, and societal debates that were to follow (Beecher et al., 1968). Debates of this kind mainly stem from how consciousness is considered in these conditions (Racine et al., 2008). For example, with a wide European survey among healthcare professionals there was a unanimous support for pain perception in MCS (96%) but less for the VS/UWS (56%) (Demertzi et al., 2009). Similarly, the majority (66%) of healthcare professionals agreed to withdraw life-sustaining treatment from chronic VS/UWS patients whereas only 28% agreed so for the chronic MCS (Demertzi et al., 2011). Additionally, disorders of consciousness have required the mediation of legal authorities in order to regulate end-of-life decisions (Quill, 2005): in the absence of a written statement about end-of-life preference from patients' behalf (advance directive), a surrogate decision maker is eligible to mediate trying to maximise patients' self-determination and protect their interests (Bernat, 2002, 2004). As such, conflicts of interest among caregivers can arise leading to wide societal debates (Quill, 2005; Striano et al., 2009). Also, treatment resources are not unlimited. The allocation of medical resources and the economics at the end of life have not yet been fully determined for patients for whom the dilemma on treating becomes crucial either because treatments are not guaranteed as successful (i.e., the condition is too bad to be treated) or unkind (i.e., the quality of life of those surviving is not acceptable) (Fins, 2003). Finally, the ethical significance of consciousness has raised many discussions as to whether greater sentience entails greater quality of life. As being conscious entails being conscious both of wellbeing and suffering (Kahane and Savulescu, 2009), it might hence not be in patients' best interest to preserve life-sustaining aids (Horne, 2009).

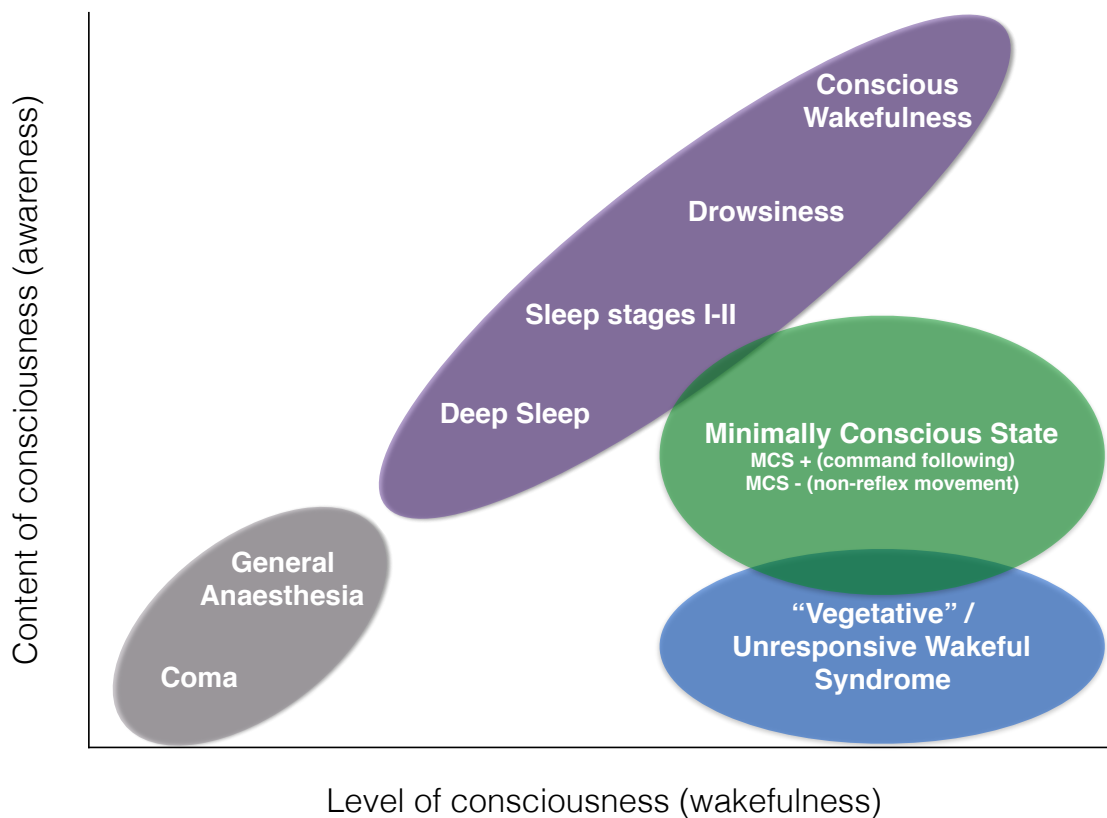


Figure 1.1: Simplified illustration of the two major components of consciousness: the level (wakefulness) and the content of consciousness (awareness). Normal physiological states (purple) present a positive correlation. Patients in coma or anaesthesia (gray) are unconscious and they cannot be awakened. DOC patients are awake but do not present signs of awareness (VS/UWS patients; blue) or show inconsistent but discernible signs of behavioural activity (MCS patients; green). Adapted from [Laureys 2005b](#)

Taken collectively, to evaluate consciousness in noncommunicating patients has medico-ethical significance. To date, efforts are focused on determining reliable diagnostic labels. Diagnosis is considered a crucial level, because it typically informs about patients' prognosis, i.e., unresponsive patients have less favourable outcome as compared to those in MCS (Faugeras et al., 2017), and may influence clinical management and treatment options (Jox et al., 2012).

1.2 State of the art of DOC diagnosis

1.2.1 Current tools for DOC diagnosis

Behavioural evaluation

Voluntary and reflexive behaviours are difficult to distinguish. Clinicians and caregivers could miss the subtle signs of consciousness behaviour present in MCS patients. Despite the specification of a diagnostic criteria for MCS (Giacino et al., 2002), a study showed that non-standardised observation presented a 41% misdiagnosis of VS/UWS patients when compared with a standardised scale (Schnakers et al., 2009). Among the several sources of variance that contribute to this misdiagnosis, the patient's fluctuations in terms of arousal, fatigue, illness, pain, cortical sensory deficits, motor impairments or cognitive disturbance decreases the probability of observing signs of consciousness (Schnakers et al., 2015). Taking this fact into account, behavioural evaluations should occur repeatedly over time and should be sensitive enough to detect this subtle but meaningful fluctuations.

Conventional bedside assessment procedures as the Glasgow Coma Scale (GCS; Teasdale and Jennett 1974) are designed to detect gross changes in behaviour rather than reflexive from voluntary behaviour. An alternative scale which present higher sensitivity in detecting levels of brainstem function in the acute stage of brain injury is the Full Outline of UnResponsiveness score (FOUR score) (Wijdicks et al., 2005). Nevertheless, this score does not include a systematic assessment of signs of consciousness (Giacino et al., 2002) and it may not capture the transition from VS to MCS (Schnakers et al., 2006; Bruno et al., 2011).

Standardised neurobehavioral assessment measures tailored for DOC patients include the Coma Recovery Scale – Revised (CRS-R) (Giacino et al., 2004), the Coma-Near Coma Scale

(CNC) (Rappaport et al., 1992), the Western Neurosensory Stimulation Profile (WNSSP) (Ansell and Keenan, 1989), the Western Head Injury Matrix (WHIM) (Shiel et al., 2000), and the Sensory Modality Assessment and Rehabilitation Technique (SMART) (Wilson and Gill-Thwaites, 2000). Although item content varies across measures, all evaluate behavioural responses to a variety of auditory, visual, motor, and communication prompts.

Neuroimaging

Nowadays, behavioural assessment of DOC remains the ‘gold standard’ due to the lack of an objective test of consciousness. Nevertheless, neuroimaging permits objective documentation of central nervous system damage after acquired brain injury. Scientifically, neuroimaging studies contributes to a better understanding of the neural correlates of human consciousness. Clinically, they provide additional information concerning diagnosis, prognosis and the course of recovery of consciousness, and can serve as surrogate markers for novel therapeutic interventions (Giacino et al., 2014).

Structural neuroimaging techniques used in DOC comprises Magnetic Resonance Imaging (MRI) and Computed Tomography (CT). These images allow the visualisation of the location and extent of brain damage, but cannot reliably differentiate VS/UWS from MCS patients. A previous study showed that structural MRI can predict the outcome of DOC patients; for example, the presence of corpus callosum and dorsolateral brain-stem lesions correlates with the lack of recovery at the group level (Kampfl et al., 1998). However, the recently developed quantitative diffusion tensor imaging (DTI) techniques, which permit assessment of structural white matter damage, have been shown to outperform clinical markers in predicting 1-year functional outcome at the individual-patient level in patients with traumatic (Galanaud et al., 2012) or anoxic (Luyt et al., 2012) brain injury.

Functional neuroimaging can measure brain function, either in active or passive (resting) states. Among the available technologies, functional MRI (fMRI), F-fluorodeoxyglucose PET (FDG-PET) and Electroencephalography (EEG) have helped understanding DOC. Each technique measures different aspects: FDG-PET measures the brain’s metabolic activity, fMRI the haemodynamic activity and EEG the electrical activity.

A recent study used FDG-PET to measure whole-brain glucose metabolic state, concluding that this quantification allows accurate diagnosis and prediction of disorders of conscious-

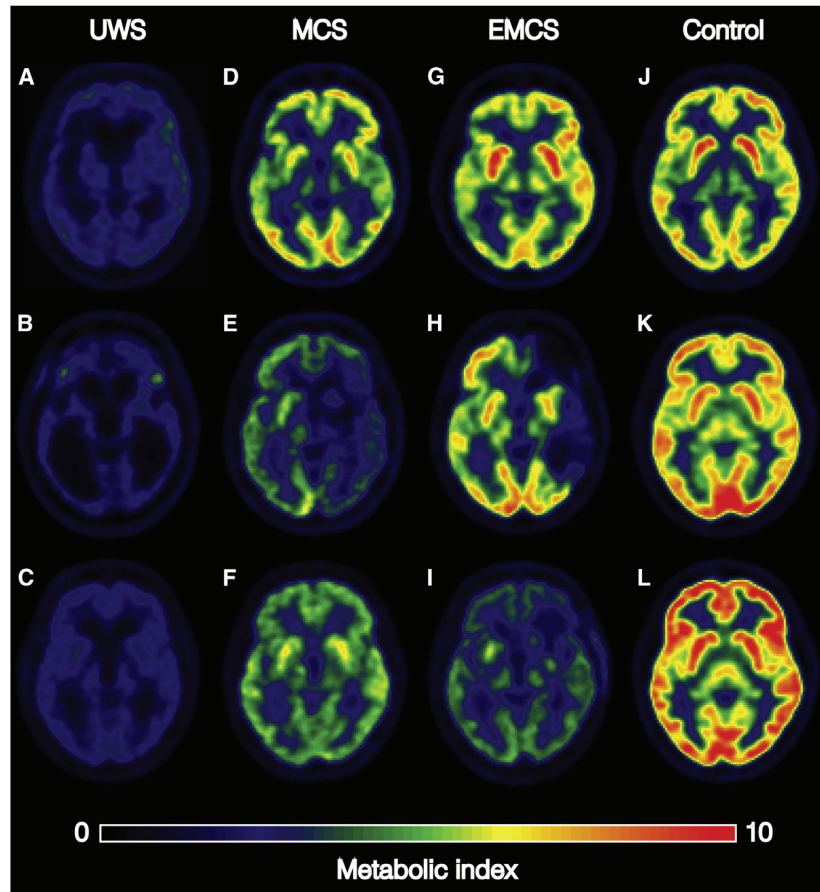


Figure 1.2: FDG-PET images for representative group samples as extracted from [Stender et al. 2016](#).

ness (Figure 1.2; [Stender et al. 2014](#)). Nevertheless, in the same work, the authors depict the need for high standards in image quality and registration.

Using fMRI, studies have been carried using auditory, tactile or visual stimuli, depicting near-normal cortical activation patterns in MCS patients contrary to the low-level activations in VS/UWS patients ([Laureys and Schiff, 2012](#)). Despite their potential value as prognostic markers, the diagnostic value and interpretation of activation fMRI studies in DOC in terms of the presence or absence of residual consciousness have remained controversial. Indeed, in the absence of a full understanding of the neural correlates of consciousness, deficient cortical activation to external stimuli does not necessarily prove the absence of consciousness ([Laureys, 2005a](#)). On the other hand, task-free *resting-state* fMRI measurements are also used for

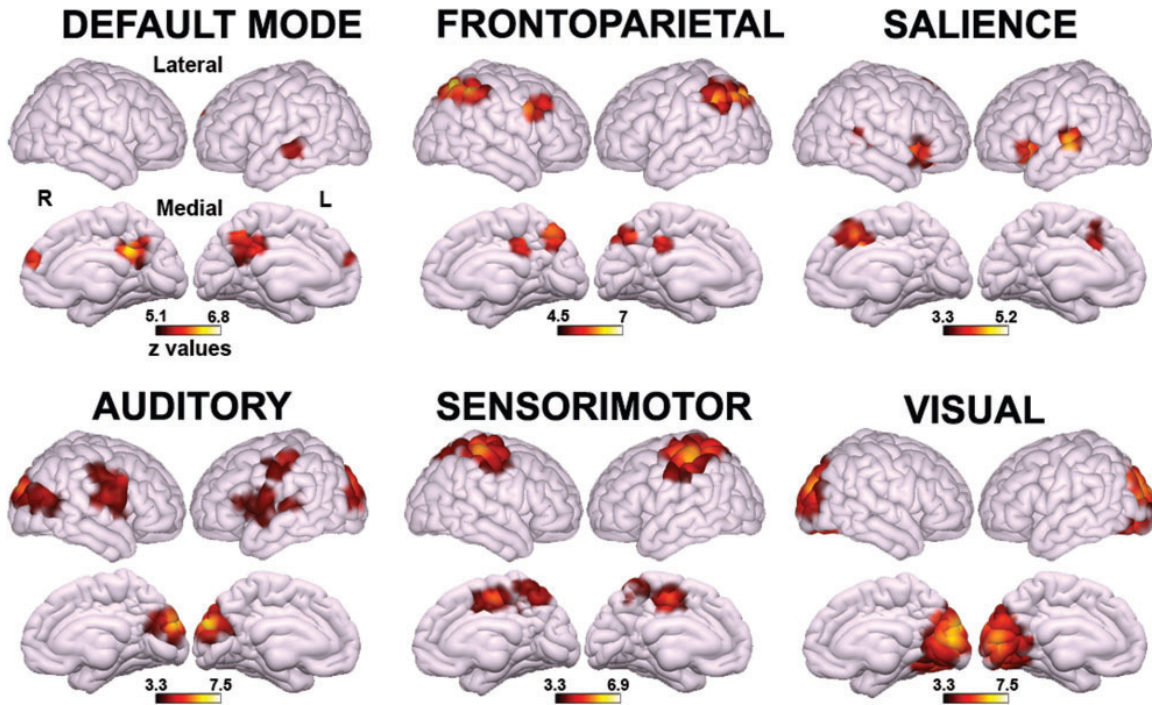


Figure 1.3: Regions showing higher functional connectivity in MCS patients as compared to VS/UWS patients (extracted from [Demertzi et al. 2015](#)).

diagnosis of DOC. In a recent study, automatic classification using functional connectivity between left auditory, right auditory and occipital cortex was able to determine the conscious state of 20 out of 22 patients (figure 1.3; [Demertzi et al. 2015](#)).

Electrophysiology

Another technique consists of studying the electrical activity of neurons or muscles. The term electrophysiology encompasses several particular techniques, depending on the source of the signals. A common technique used throughout this entire thesis is electroencephalography (EEG) which focuses on measuring the electrical activity of the cerebral cortex.

1.3 Electroencephalography

1.3.1 What is EEG?

How does it work?

Electroencephalography (EEG) is an electrophysiological technique for the recording of electrical activity arising from the human brain. The history of EEG goes back to the 19th century, starting by Richard Caton in 1875 who performed the first known neurophysiologic recording of animals using a galvanometer. It was not until 1924 when the first studies in human began, made by Hans Berger, a German psychiatrist ([St. Louis and Frey, 2016](#)).

EEG uses the principle of differential amplification, or recording voltage differences between different points using a pair of electrodes that compares one active exploring electrode site with another neighbouring or distant reference electrode. These differences are measured in volts (typically microvolts or μV).

An EEG acquisition system consists of a set of delicate electrodes connected to a set of differential amplifiers (one for each channel), followed by filters. Before the digital era, these amplified signals were written by a mechanical pen directly into a rolling paper, leaving ink traces of waveforms that mirrored the electrical potential differences on the scalp. Modern systems contain analog-to-digital converters (ADC) that transform the analog signal into discrete digital data, readable by a computer or microprocessor which can be used to store the acquired signals ([Sanei and Chambers, 2007](#)).

The electrodes used to sense the voltage differences are crucial for acquiring high quality data. Nowadays, electrodes can be used to record neuronal activity in the scalp (EEG), brain cortex (Electrocorticography; ECoG), brain tissue (Local Field Potentials; LFP) or single neurons (single-unit recordings). Nevertheless, except for scalp EEG, the mentioned techniques are invasive and require surgical procedures. Scalp EEG electrodes are pasted or glued to the scalp. For multichannel recordings with a large number of electrodes, caps are often used.

What do we measure?

The nerve cells in the brain produce signals that are called action potentials. These action potentials move from one cell to another across a gap called the synapse. Special chemicals called neurotransmitters help the signals to move across the gap. There are two types of neurotransmitters, one will help the action potential to move to the next cell (excitatory), the other will stop it moving to another nerve cell (inhibitory).

The electrical activity measured by scalp EEG recordings is generated by similarly oriented groups of cerebral cortical neurons near the scalp where the recording electrodes are placed. Each scalp electrode collects, at a minimum, an estimated 6 cm² synchronous cortical activity. The majority of the electrical activity collected in the EEG is generated by groups of pyramidal neurons. These cells have cell bodies primarily in layers three and five of the cerebral cortex. The electrical activity recorded on the scalp represents the summation of the inhibitory or excitatory postsynaptic potentials (not action potentials, they are too short to be recordable) from thousands of pyramidal cells near each recording electrode. This summated activity can be represented as a field with positive and negative poles (dipole).

There are systematic interconnections between cortical neurons, as well as cortical to subcortical connections to structures such as the thalamus, that have well-developed feedback linkages. Any sinusoidal rhythmic activity seen on the EEG is thought to represent oscillatory communications between the cortex and deeper, subcortical structures. These communication loops occur when the cortex is at rest or is not performing any specific task. Once the cortex has a task to perform, the electrical activity of the cortex desynchronises, and lower amplitude, faster electrical rhythms take predominance until the cortex completes its task and returns to a resting state ([St. Louis and Frey, 2016](#)).

Resolution, precision and accuracy of EEG

The differences between precision, resolution and accuracy are subtle but important. Resolution refers to the number of data samples by unit time, precision refers to the certainty of the measurements at each time point and accuracy to the relationship between the timing of the EEG signal and the biophysical event that lead to that signal.

The temporal resolution of the EEG is given by the sampling rate of the acquisition, generally between 100 Hz and 20 Khz, depending on the purpose of the acquisition. For most

analysis on scalp EEG, resolutions between 250 Hz and 1000 Hz are sufficient and appropriate. In contrast, the temporal precision depends on the analysis applied. Raw (unprocessed data) have the highest temporal precision because each sample was taken at a precise time point. Nevertheless, filtered data is a weighted average of the temporal surrounding activity, which reduces the temporal precision. In terms of accuracy, the EEG is extremely accurate because brain electrical activity travels instantaneously from the neurons generating the electrical field to the electrodes measuring them.

Although EEG has high temporal precision, resolution and accuracy, it is not the case for spatial properties, as they are considered low compared to neuroimaging techniques such as fMRI. The spatial resolution of EEG is determined by the number of electrodes. Common configurations consists on 21 electrodes (10-20 standard; [Jasper 1958](#)), 32, 64, 128 and 256. The spatial precision of the EEG is considered low, although it can be improved by spatial filters. In terms of accuracy, the problem is that one electrode does not reflect the activity from neurons directly below that electrode, but rather a complex mixture of activities from many brain regions close to and distant from it. Furthermore, the extent to which one brain region contributes to the signal recorded from each EEG electrode depends on cortical anatomy and to what extent that brain region is active at a given point in time ([Cohen, 2014](#)).

1.3.2 What do we analyse in EEG?

Oscillations

An oscillation is a rhythmic alternation of states. They can occur in time or in space, and are commonly seen in physical and biological systems. In the brain, they refer to fluctuations in the excitability of neurons or populations of neurons. Neural oscillations are observed on many spatial and temporal scales ([Varela et al., 2001](#)) and have been linked to many neurobiological events ranging from long-term potentiation to conscious perception ([Buzsáki, 2009](#); [Engel et al., 2001](#); [Herrmann et al., 2010](#); [Kistler et al., 2000](#); [Klimesch et al., 2007](#); [McBain and Kauer, 2009](#)). These neurobiological mechanisms are fairly well understood ([Buzsáki et al., 2012](#); [Wang, 2010](#)) although uncertainties remain in the extent to which different factors contribute to the signal recoded by EEG, in part due to the complexity of the models and the difference in spatial scale between individual neurons and scalp EEG.

Brain rhythmic activity contains multiple frequencies simultaneously, which can be separated through signal processing techniques. These rhythms are grouped into bands, defined as delta (2-4 Hz), theta (4-8 Hz), alpha (8-12 Hz), beta (15-30 Hz), lower gamma (30-80 Hz), upper gamma (80-150 Hz). Although there are more oscillations, these bands are most typically associated with cognitive processes, defined from neurobiological mechanisms of brain oscillations, including synaptic decay and signal transmission dynamics (Buzsáki, 2009; Buzsáki and Draguhn, 2004; Kopell et al., 2010; Niedermeyer and Silva, 2004; Wang, 2010)

Changes in rhythmic activity correlate with task demands, including perceptual, cognitive, motor, linguistic, social, emotional, mnemonic and other functional processes (Cohen, 2014).

Event-related Potentials (ERPs)

One way to study the human brain function is by analysing the reactions of the brain to a variety of stimuli. Some of these reactions may be associated with clear cut changes in the EEG; some others, however, consist of changes that are difficult to visualise. These EEG changes may be treated globally under the common term event-related potentials (ERPs); a subset of the ERPs are sensory (visual, auditory, somatosensory) evoked potentials (ERPs).

ERPs are usually defined in the time domain as the brain electrical activity that is triggered by the occurrence of particular events or stimuli. A basic problem of analysis is how to detect ERP activity within the often much larger ongoing EEG or background activity. According to the most widely accepted model, ERPs are signals generated by neural populations that are time-locked to the stimulus; these signals would be summed to the ongoing EEG activity. According to another model, however, ERPs are assumed to result, at least partially, from a reorganisation of the ongoing activity (Sayers et al., 1974). More recently, a study demonstrated that ERPs could be generated by stimulus-induced phase resetting of ongoing EEG components (Makeig et al., 2004).

The ERP waveform can be quantitatively characterised across three main dimensions: amplitude, latency, and scalp distribution. In addition, an ERP signal may also be analysed with respect to the relative latencies between its subcomponents. The amplitude provides an index of the extent of neural activity (and how it responds functionally to experimental variables), the latency (i.e. the time point at which peak amplitude occurs) reveals the timing

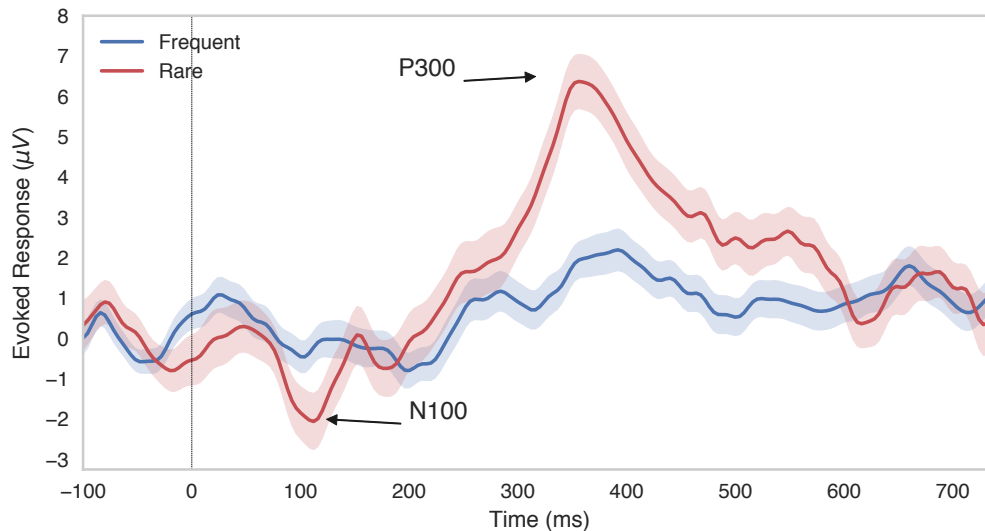


Figure 1.4: Timeseries of two auditory evoked responses corresponding to an oddball paradigm. Rare trials (blue) present distinct evoked responses when compared to frequent trials (red). This classic paradigm elicits a P300 wave. The two main components of the wave are a negative deflection 100 ms after the stimuli (N100) and a positivity 300ms after the stimuli (P300).

of this activation, and the scalp distribution provides the pattern of the voltage gradient of a component over the scalp at any time instant (Sanei and Chambers, 2007).

The ERP signals are either positive, represented by the letter P, such as P300, or negative, represented by the letter N, such as N100 and N400 (see figure 1.4 for an example). The digits indicate the time in terms of milliseconds after the stimuli (audio, visual, or somatosensory). The amplitude and latency of the components occurring within 100 ms after stimulus onset are labelled exogenous, and are influenced by physical attributes of stimuli such as intensity, modality, and presentation rate. On the other hand, endogenous components such as P300 are nonobligatory responses to stimuli, and vary in amplitude, latency, and scalp distribution with strategies, expectancies, and other mental activities triggered by the event eliciting the ERP. These components are not influenced by the physical attributes of the stimuli (Sanei and Chambers, 2007).

The ERP parameters such as amplitude and latency are the indicators of the function of the brain neurochemical systems. ERPs are also related to the circumscribed cognitive process. For example, there are interesting correlations between late-evoked positivities and

memory, N400 and semantic processes, or the latencies of ERPs and the timing of cognitive processes. Therefore, the ERP parameters can be used as indicators of cognitive processes and dysfunctions not accessible to behavioural testing.

Nevertheless, there are overlapping components within ERPs, which represent specific stages of information processing, which are difficult to distinguish (Frodl-Bauch et al., 1999; Dien et al., 2003). An example is the composite P300 wave, a positive ERP component, which occurs with a latency of about 300 ms after novel stimuli, or task-relevant stimuli, which requires an effortful response on the part of the individual under test (Frodl-Bauch et al., 1999; Dien et al., 2003; Kok et al., 2004; Friedman and Cycowicz, 2001).

In the P300 wave (figure 1.4 on the preceding page), the elicited ERPs are comprised of two main components: the mismatch negativity (MMN) and the P300 complex. The MMN is the earliest ERP activity that indicates that the brain has detected a change in a background of brain homogeneous events, and it has been detected even when the stimuli are unattended or ignored. Because the MMN is evoked by stimuli that fall outside the focus of attention, it is considered to be a relatively automatic, pre-attentive response to stimulus deviance (Friedman and Cycowicz, 2001). The P300 complex represents cognitive functions involved in orientation of attention, contextual updating, response modulation, and response resolution (Dien et al., 2003; Kok et al., 2004), and consists mainly of two overlapping subcomponents P3a and P3b (Frodl-Bauch et al., 1999; Friedman and Cycowicz, 2001; Comerchero and Polich, 1999). P3a reflects an automatic orientation of attention to novel or salient stimuli independent of task relevance. Profrontal, frontal, and anterior temporal brain regions play the main role in generating P3a, giving it a frontocentral distribution (Friedman and Cycowicz, 2001). In contrast, P3b has a greater centroparietal distribution due to its reliance on posterior temporal, parietal, and posterior cingulate cortex mechanisms (Frodl-Bauch et al., 1999; Dien et al., 2003). The P3b wave is thought to reflect a higher-order violation of subject's expectations of a given rule, constructed over a longer time period than the MMN, and has been closely linked to working memory (Goldstein et al., 2002; Polich, 2007) and conscious access (Dehaene et al., 2006; Dehaene and Changeux, 2011).

According to the classic view, ERP analysis is based on two basic assumptions: (1) the electrical response evoked from the brain is invariably delayed relative to the stimulus and (2) the ongoing activity is a stationary noise, the samples of which may or may not be corre-

lated. Thus, ERP detection becomes a question of improving signal-to-noise ratio. A simple method to detect ERPs is to average across many repetitions (trials) with the main objective, of course, to increase the signal-to-noise ratio so that the EEG background activity is attenuated (Niedermeyer and Silva, 2004). Nevertheless, quantifying ERPs can be difficult for several reasons, including environmental artifacts and intra-subject variability. This problem of classification can be solved using multivariate statistical methods (Donchin, 1969) and multivariate pattern (MVP) analysis King et al. (2013a).

1.4 Electroencephalography in DOC patients

Regarding EEG, we must differentiate between the ERP-based or active, passive and resting state methods used for the diagnosis of disorders of consciousness. The multidimensional construct of consciousness can be assessed through a variety of stimulation and recording paradigms, each one addressing particular aspects of consciousness across the spectrum of pathologies with disorders of consciousness.

For example, in case of comatose state, Brainstem Auditory Evoked Potentials (BAEPs), Middle Latency Auditory Evoked Potentials (MLAEPs), Somatosensory Evoked Potentials (SEPs) and Visual Evoked Potentials (VEP) are general indicators of prognosis. The presence of these potentials indicate preserved brainstem, sensory pathways and primary cortex function (Garcia-Larrea et al., 1992; Litscher, 1995). Nevertheless, these potentials are not related to cognition or high order function, hence they only indicate a bad prognosis with the absence of responses. Contrarily, cognitive ERPs are used to assess and predict higher order functions as language, attention and working memory.

The N400 (negative deflection 400 ms after the stimuli) ERP is found in healthy subjects when they see or hear semantically anomalous sentences like “The coffee is too hot to fly” versus “The coffee is too hot to drink” (Schoenle and Witzke, 2004), hence used a test to probe linguistic capabilities. When applied to DOC patients, the presence of an N400 due to semantic processing indicates preserved cognitive function and has only been detected in MCS patients (Rohaut et al., 2015).

Neural responses to motor imagery and spatial navigation tasks have proven to detect consciousness (Goldfine et al., 2011; Cruse et al., 2011, 2012) by asking subjects to imag-

ine movements or navigate spatially and analysing the oscillatory responses. However, the specificity and sensitivity of this marker is still under discussion ([Goldfine et al., 2013](#)).

Another classic ERP used in DOC is the MMN (mismatch negativity, see 1.3.2 on page 12). In comatose patients, these evoked potential elicited by novelty detection (oddball paradigms) has been reported as a highly specific (>90%) predictor of awakening ([Kane et al., 1993](#); [Fischer et al., 2004](#); [Naccache et al., 2005](#)). Highly associated with the novelty P300, and with several flavours ranging from auditory beeps ([Naccache et al., 2005](#)) to the subject's own name ([Fischer et al., 2010](#); [Schnakers and Laureys, 2009](#)), this ERPs has not proved to be always specific in regard to diagnosis of DOC in post-comatose states as MCS or VS/UWS: they have been detected in both MCS and VS/UWS patients ([Faugeras et al., 2011](#); [Naccache et al., 2005](#); [Fischer et al., 2010](#)).

The main reason for the specificity failure of the novelty P300 ERPs is that this particular complex represents several cognitive functions and consists of two overlapping subcomponents (P3a, P3b, see 1.3.2 on page 12). In 2009, [Bekinschtein et al. 2009](#) proposed a two-level hierarchical oddball paradigm designed to differentiate the MMN and P3b responses (for details, see 1.5.2 on page 18). This new paradigm named *Local-Global* presented an effect when subjects were able to maintain conscious attention, thus implying capacity for conscious access. When applied to DOC patients, it was only detected in EMCS and MCS patients, with an exception of two VS/UWS patients that later recovered ([Faugeras et al., 2012](#)). Nevertheless, the main caveat of this test is its low sensitivity: it was detected in 53.8% of the EMCS patients and only 14.3% of the MCS patients.

Interestingly, a recent work proposed a multidimensional cognitive evaluation of DOC patients using ERPs ([Sergent et al., 2017](#)). During a 1.5 hour session, patients were probed for own name recognition, temporal attention, spatial attention, detection of spatial incongruence, motor planning and modulation of these effects by global context, reflecting higher-level function. This proof-of-concept study revealed that the combination of several ERP markers increased diagnostic sensitivity, particularly in the detection of minimally conscious states with the presence of high-level effects.

So far, these ERPs are mainly elicited by auditory, somatosensory and in less frequency, visual stimuli. The main reason behind this unbalance is the difficulty to force patients to open their eyes and fixate in the case of visual stimuli. An alternative stimulation is the use

of Transcranial Magnetic Stimulation (TMS).

The Integrated Information Theory of consciousness (Tononi et al., 2016) states that, phenomenologically, each conscious experience is both differentiated (composed of several phenomenal distinctions that exist within it) and integrated (the distinctions are bound together in various ways). These properties, from a neurophysiological point of view, rely on the ability of multiple, functionally specialised areas of the brain to interact rapidly to form an integrated whole (Dehaene and Changeux, 2011; Friston, 2002; Laureys, 2005b; Tononi and Koch, 2008). In Information Theory, integration and differentiation is also defined as complexity. Under this premises, the spatio-temporal complexity of an EEG can act as a proxy to the combination of integration and segregation. Casali et al. 2013 proposed a marker of brain complexity that quantifies the response to direct cortical stimulation using TMS and measured by EEG, named Perturbational Complexity Index (PCI). In a follow-up study on a cohort of 38 MCS and 43 VS/UWS patients, authors reported a sensitivity of 94.7% and a specificity of 80% (Casarotto et al., 2016).

In a recent review, Bai et al. 2017 report several common aspects among various studies on resting state (or spontaneous) EEG recordings in DOC patients: spectrum power differences in alpha, delta and theta bands between MCS and VS/UWS patients; ratios between higher and lower frequencies correlates with CRS-R scores; spectral entropy, markers of EEG complexity and functional connectivity differentiates patients groups.

One particular work, analysed in this thesis, is the one presented by Sitt et al. 2014 which combines EEG-extracted markers from diverse theoretical frameworks and uses machine learning to predict the diagnosis of individual patients. In particular, they analyse dozens of markers including ERPs from the *Local-Global* paradigm and markers of information, complexity, connectivity and spectral power, obtaining an AUC of 78% when used to diagnose a cohort of 68 MCS and 75 VS/UWS patients.

1.5 Methods used in this thesis

1.5.1 The Coma Recovery Scale (Revised)

The current *gold standard* for the behavioural diagnosis of DOC patients is the Coma Recovery Scale - Revised (CRS-R). This scale, initially described in Giacino et al. 1991 and later

revised in [Giacino et al. 2004](#) was developed to characterise and monitor patients, detecting subtle but potentially meaningful changes in neurobehavioural function, while ensuring proper interrater reliability.

The CRS-R consists of 26 hierarchically arranged items that comprise 6 subscales addressing auditory, visual, motor, oromotor, communication, and arousal processes. Scoring is based on the presence or absence of specific behavioural responses to sensory stimuli administered in a standardised manner. The lowest item on each subscale represents reflexive activity, whereas the highest items represent cognitively mediated behaviours. Depending on the different scores in the subscales, the CRS-R will diagnose the patient as VS/UWS, MCS or EMCS.

1.5.2 The *Local-Global* paradigm

As described previously in 1.4 on page 15, the MMN and P3b events are close in time and extremely difficult to differentiate in individual subjects. For that purpose, [Bekinschtein et al. 2009](#) propose a new paradigm named *Local-Global* which adds a second level of novelties to a classic oddball paradigm. A first level of regularities is defined at a local (or within trial) level, while the second level is defined at a global (or across trial) level. While disruptions of the local level regularities elicits the MMN and P3a ERPs, disruptions of the global regularities elicits a P3b ERP.

Each trial of the paradigm is formed by 5 consecutive sounds lasting 50 ms, with a 150-millisecond gap between the sounds' onsets and an intertrial interval ranging from 1,350 to 1,650 milliseconds. The fifth sound can be either equal to or different from the first four; this defines whether the trial is standard or deviant at the local level. The second level of regularities is defined across trials (or at a global level); frequent trials (80%) define the regularity, and rare ones (20%) violate this regularity.

Two types of stimulation blocks are played to the subjects; in the XX blocks, the frequent stimulus corresponds to five equal sounds (local standard and global standard [LSGS]). In contrast, the infrequent stimulus corresponds to four equal sounds followed by a fifth different sound (local deviant and global deviant [LDGD]). In the XY blocks, the frequent stimulus corresponds to four equal sounds and a fifth different sound (local deviant and global standard [LDGS]). The infrequent stimulus corresponds to 5 equal sounds (local standard and global

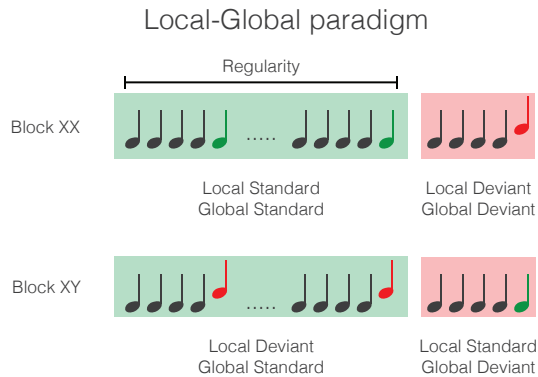


Figure 1.5: Illustration of the Local-Global paradigm. Each trial of the auditory paradigm was composed by 5 consecutive sounds. Four equal sounds define a local regularity (music notes). The fifth sound could be equal or different, defining a local standard or deviant trial, respectively. At a second level, frequent trials (80%, green shaded area) defined a global regularity and rare trials (20%, red shaded area) violated this regularity.

deviant [LSGD]). For more details see figure 1.5.

The local effect is quantified by contrasting all local deviant (LD) trials (LDGS+LDGD) versus all local standard (LS) trials (LSGS+LSGD). The global effect is quantified by contrasting all global deviant (GD) trials (LSGD+LDGD) versus all global standard (GS) trials (LSGS+LDGS). All subjects were presented with these four conditions, twice for each block type. Each block started with 20–30 global standard trials to establish the global regularity before the occurrence of the first global deviant trial. An example of the neural response to the Local-Global paradigm is shown in 1.6 on the next page.

Subjects were instructed to count the GD trials and asked after each stimulation block (3.5 minutes). For patients, if they appeared asleep, they were stimulated with pressure as recommended in the *arousal facilitation protocol* in the CRS-R.

1.5.3 Machine Learning

According to [Mitchell 1997](#), “the field of machine learning is concerned with the question on how to construct computer programs that automatically improve with experience”. Throughout this thesis, we will focus on a specific type of learning named *supervised learning*, that is, algorithms that could learn from examples provided by a *supervisor*. In this case, the algorithm is first presented with a set of samples and its corresponding labels (*training set*). Once the algorithm has learnt from the examples, one can feed it with an independent set of samples (*test set*) and ask the algorithm to classify the samples based on the knowledge obtained from the training set. The performance of the algorithm can be assessed by comparing the

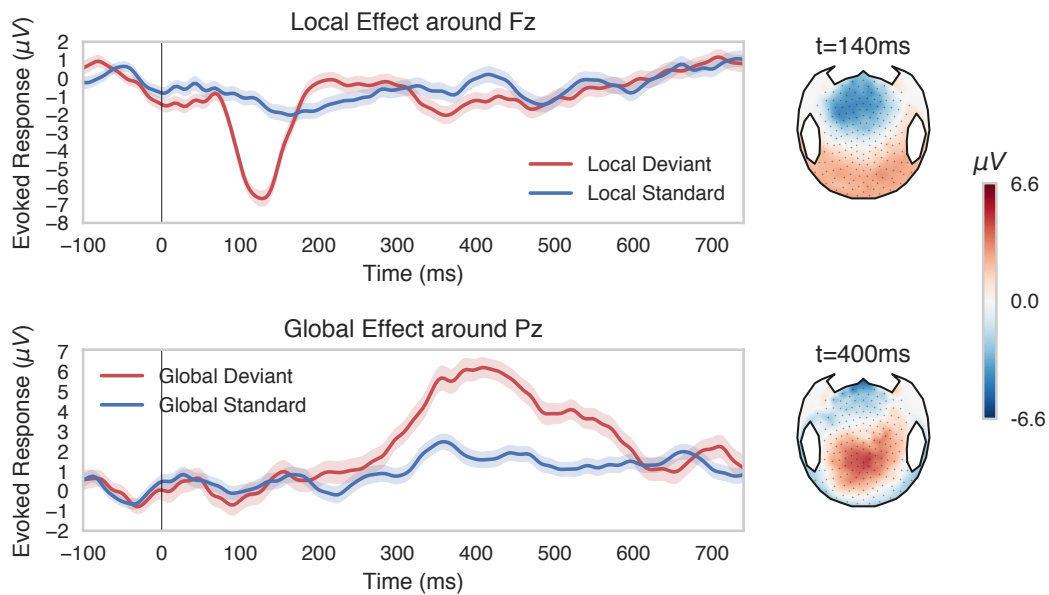


Figure 1.6: Local and Global effects as measured with EEG in one of the directors of this thesis. Timeseries of the Local Effect around the Fz electrode (top left) present the MMN around 140ms after the onset of the 5th sound only when it is different from the first four. The associated scalp map (top right) shows a frontal/central negativity and a posterior positivity. Timeseries of the Global Effect around the Pz electrode (bottom left) depict the P3b component starting around 350ms after the onset of the 5th sound. The associated scalp map (bottom right) presents a central/posterior positivity.

labels provided by the algorithm and the ones provided by the supervisor. An good algorithm is the one who provides accurate labels within some reasonable error.

A classification algorithm can be univariate or multivariate. In the first case, a single variable or *feature* is provided for each sample. Multivariate Pattern Analysis (MVPA) classifiers refers to classification algorithms that uses more than one feature for each sample. Depending on the algorithm and the number of features, some of them could be discarded to reduce dimensionality. This is called *feature selection*.

Cross Validation

In order to test the real performance of a classification algorithm, one must provide two sets of representative data from the underlying real population distribution. For the train set, it should be big enough so the algorithm learns generalizable rules and not particular and specific to the available samples. For the test set, its size will have a direct impact on the variance of the estimated performance.

A common problem we face when evaluating models in neuroimaging and clinical applications is that the number of available samples is severely limited. For example, data from DOC patients in the Pitié-Salpêtrière hospital in Paris is acquired weekly: 52 samples a year in the best case scenario. To address this issue, a widely used validation technique is to partition the available data into independent sets and use them for training and testing the algorithm. In order to reduce variability, this action can be repeated with different partitions. This method is called *cross-validation* and there are several partitioning schemes. We here focus on two particular methods: Stratified Shuffle Split (also called Monte Carlo cross-validation) and Stratified K-Fold.

The Stratified Shuffle Split method consists on randomly shuffling the data and splitting the data into two partitions for training and testing the algorithm. The sizes of the partition are determined by the user, but both of them respects the label distributions of the original set. This action is repeated several times and the performance is estimated across the repetitions. A disadvantage of this methods is that there is no guarantee that a sample will be used for the validation set, and that validation sets overlap.

In the Stratified K-fold cross validation, samples are split into K different groups (folds) that respects the original label distributions. The algorithm is then trained on $K - 1$ folds and

tested on the remaining one. This action is repeated K times with a different testing fold. An advantage of this method is that it guarantees that each samples is used for validation exactly once.

Area under the ROC curve (ROC-AUC)

Univariate and multivariate discrimination performance was summarised with Area Under the Curve (AUC) calculated from the receiver operator characteristic (ROC). For a binary classification system, the ROC pits the detection probability, commonly referred to as sensitivity against the probability of false alarm ($1 - \text{sensitivity}$). These probabilities are empirically estimated by moving the decision cut-off along the sorted values of a continuous variable, e.g. a score, and evaluating its relation to the true label. In the case of traditional model-free univariate analysis, the score is the EEG-marker itself, in the case of univariate or multivariate machine learning it is the predicted probability of a given sample to belong to the target class. The AUC can then be conveniently used to summarise the performance, where a score of 0.5 is uninformative and equals to random guessing whereas a score of 1 amounts to perfect classification and 0 to total confusion, indicating negative correlation between the score and the label.

1.5.4 Statistics

Statistical analysis encompassed correlations using Pearson product–moment correlation coefficient (r) and Spearman rank correlation coefficient (ρ) with corresponding probability values. Pearson chi-square and Wilcoxon rank sum test were used to test for independence between the diagnosis and the demographic information of the patients. Bayesian ANOVA was performed to test the differences between groups using the BayesFactor R package (JZS Bayes factor with “medium” default prior setting $r = 0.5$; [Rouder et al. 2012](#); [Morey et al. 2014](#); [R Development Core Team 2016](#). Bayes factor (BF) interpretation was done according to the Kass & Raftery scale ([Kass and Raftery, 1995](#)). Differences between groups were also tested using 2-sided paired samples signed tests. Different between conditions at single subjects and group level were tested using paired t-tests. Performance of MVPA models was assessed using the Area Under the Curve (AUC). MVPA models were tested using nonparametric Kruskal–Wallis test adjusted for multiple comparisons. We extended our visualisations

into hypothesis tests by employing the percentile bootstrap (Efron and Tibshirani, 1994). Accordingly, we generated 2000 bootstrap samples by drawing with uniform probability and replacement n samples from the dataset. The test-statistic of interest was then evaluated on each bootstrap sample. Two-sided 95% confidence intervals were obtained by querying the 2.5 and 97.5 percentiles and the significance-level was then obtained by inversion of the confidence interval that excluded the value under H_0 .

1.6 This work

1.6.1 Purpose

The purpose of this thesis is to analyse the current EEG-based tools used to diagnose disorders of consciousness with two major objectives: (1) validate and standardise the usage of state-of-the-art tools based on machine learning methods and (2) analyse and propose novel tests in order to increase the sensitivity of the current tool and improve the diagnostic accuracy.

1.6.2 Description of chapters

Chapter 2: Automation and identification of robust EEG-extracted markers for the diagnosis of DOC. As a first step, we analyse the validity and clinical usage of a previous publication which combines EEG-extracted markers and a Support Vector Machine classifier to diagnose DOC patients. In order to develop an online clinical tool, we automate the process and analyse the application across different clinical setups.

Chapter 3: Towards cross-modal integration as a measure of consciousness. Previous works on diagnosis of DOC using auditory ERP analyses show high specificity but low sensitivity. Past research on multimodal stimulation suggest the existence of a variety of neural responses that can be measured using EEG. In this chapter, we analyse the possibility of using the neural responses to multimodal stimulation and cross-modal integration for the diagnosis of DOC.

Chapter 4: Brain-Body interactions as a diagnostic marker for DOC. So far, all the assisting technologies used to diagnose DOC patients are based on a strict neuro-centric approach. Nevertheless, past research on healthy subjects demonstrate interactions between the body and the brain, which are also affected by cognitive processes. In this chapter, we shift away from this neuro-centric approach and analyse the possibility of evaluating DOC patients via the embodied paradigm, according to which body-brain functions contribute to a holistic approach to conscious processing.

Chapter 5: Summary and final remarks. In this chapter, we summarise the findings and discuss future lines of research.

Chapter 2

Automation and identification of robust EEG-extracted markers for the diagnosis of DOC

Parts of the work described in this chapter has been accepted for publication as “Robust EEG-based cross-site and cross-protocol classification of states of consciousness”. Raimondo F., Engemann DA.*, King JR., Rohaut B., Louppe G., Faugeras F., Annen J., Cassol H., Gosseries O., Fernandez Slezak D., Laureys S., Naccache L., Dehaene S., Sitt JD. Brain, to be published in Volume 141, Issue 11, November 2018.*

Additionally, this work was the basis for a case report published as “Probing consciousness in a sensory-disconnected paralysed patient”. Rohaut B., Raimondo F., Galanaud D., Valente M., Sitt JD., Naccache L. Brain Injury, Volume 31, Issue 8, Pages 1-6. 2017.

Contents

2.1	Background	26
2.2	Objectives	27
2.3	Automation	27
2.3.1	Reasons to rewrite the code and automate the process	27
2.3.2	Software Implementation	28
2.3.3	Preprocessing	28
2.3.4	Optimisations and Performance	29
2.4	Replication	30
2.4.1	Methods	30
2.4.2	Results	35

2.5	Validation	36
2.5.1	Methods	36
2.5.2	Results	36
2.6	Clinical application	38
2.6.1	Report	38
2.7	Further steps: towards a universal tool	39
2.7.1	Generalisation to difference EEG recording configurations	40
2.7.2	Generalisation to Resting State	43
2.7.3	Discussion	45
2.8	Insights from Machine Learning	47
2.8.1	Methods	47
2.8.2	Results	48
2.8.3	Discussion	48
2.9	Summary	50

2.1 Background

Over the last decade, several electrophysiological signatures of consciousness has been proposed, varying from simple quantifications of ERPs or oscillations, to complex topological summaries of connectivity. This chapter is based on one of the key studies in EEG-based DOC diagnosis ([Sitt et al., 2014](#)). This work analysed dozens of EEG-markers obtained from more than 150 EEG recordings of the Local-Global paradigm. The authors demonstrated that by using a Support Vector Machine (SVM) classifier combining several EEG-markers, the diagnostic precision was higher than any of the individual markers. Furthermore, when the clinical (behavioural) diagnosed VS/UWS patients where classified by the SVM as MCS patients, the proportion of those who later showed signs of consciousness significantly increased ([Sitt et al., 2014](#)).

The main result, a gain in diagnostic precision by combining several EEG measures, has both theoretical and clinical implications. Theoretically, the results indicate that the markers addresses distinct and dissociable features of conscious states. Clinically, they depict the usefulness of combining EEG measures for the diagnosis. Particularly, the increase in the

probability of recovery of those clinically VS patients classified as MCS using the EEG markers, indicates that this approach is discovering information that could escape highly trained clinicians. Taken together, these results provide the basis for a reliable bedside tool to probe consciousness in DOC patients.

2.2 Objectives

In this chapter, we will focus on the follow-up analysis after the work published in [Sitt et al. 2014](#). The purpose of this work has both clinical and scientific objectives:

1. Evaluate the use of the previously developed model for the diagnosis of DOC in a clinical environment.
2. Provide a semi-supervised algorithm to obtain the results, in which there is no need for human intervention.
3. Analyse the implications of modifying data acquisition conditions in order to assess the use of the developed tool across clinical centres with heterogeneous EEG systems and acquisition protocols.
4. Obtain insight from the classification model and determine which are the markers that drives the distinction between VS/UWS and MCS patients.

2.3 Automation

2.3.1 Reasons to rewrite the code and automate the process

The development of a clinical tool that goes beyond research requires a high grade of attention to the software development processes. For example, a defect in a news website or word processor application could result on the inability to perform a certain task, the loss of data or a security breach. Nevertheless, the magnitude of this events do not directly compare to a defect in a software that predicts the diagnosis of a patient. The clinicians might take end-of-life decisions upon the wrong results due to an error in the software. It is of uttermost importance to ensure a high quality software through the development process.

Particularly in data handling for machine learning applications, it is crucial that the features are well defined and obtained in an objective manner, with no prior knowledge of the output to be predicted. When it comes to EEG, one of the first steps is to identify non-neural signals or artifacts. In addition to the neuronal activity, EEG captures the electrical activity of muscles, cardiac activity, movements and environmental noise. A common procedure is to visually inspect the recording and discard the portions of data that are contaminated by any of this artifacts. This procedure is prone to be subjective, hence a potential problem is a bias in the extracted features.

To address these potential problems, the proposed solution is to create a high quality software which extracts the features in a fully unsupervised manner.

2.3.2 Software Implementation

The software was written in Python and C, using open-source libraries. All the EEG-measures described in [Sitt et al. \(2014\)](#) were re-implemented taking advantage of the already optimised Numpy and Scipy libraries for fast algebra and scientific computing ([Jones et al., 2001](#)). For general data processing and visualisation, we used the open source MNE software package ([Gramfort et al., 2013, 2014](#)). Machine learning was performed using the scikit-learn library ([Pedregosa et al., 2012](#)). Bash scripts and GNU-parallel ([Tange, 2011](#)) were used to distribute processes and obtain results in a faster way.

2.3.3 Preprocessing

The first procedure after data acquisition, and before the computation of ERPs and EEG-extracted markers is called *preprocessing*. The objective of the preprocessing step is straightforward: convert raw and contaminated data into artifact-free data ready to analyse. Depending on the analysis to be done, the steps and tools used in preprocessing can vary.

Data was first filtered using a 0.5 Hz high-pass 6th order and a 45 Hz low-pass 8th order FFT-based Butterworth filters. The second step consisted on epoching (separate in trials) from -200ms to 1336ms relative the onset of the first sound of the Local-Global paradigm.

We then used an adaptive outlier detection algorithm specifically developed to detect and reject contaminated electrodes and epochs. This adaptive algorithm first selects bad

electrodes where more than 50 % of the epochs present a peak-to-peak amplitude higher than $100 \mu V$. The second step consists on computing the variance of each individual channel and its corresponding z-score across all channels. Channels with a z-score greater than 4 are discarded. This operation is repeated 4 times. The remaining data is then analysed at the epoch level: epochs with more than 10% of the channels outside the $100 \mu V$ peak-to-peak amplitude range are then discarded. Finally, the second step is repeated, but with the standard deviation of the channels filtered with a 4th order Butterworth high-pass filter at 25 Hz.

In order to use the same set of electrodes for every patients, electrodes marked as “bad” by the outlier algorithm are interpolated using a spherical spline interpolation. Data was finally re-referenced using an average reference and baseline corrected over the first 200 ms window preceding the onset of the first sound.

The development of the peak-to-peak amplitude rejection algorithm led to the development of an automated algorithm for rejection and repair of bad trials in EEG and MEG signals. This algorithm estimates the individual peak-to-peak threshold for each channel, rather than M/EEG system-dependent user set threshold (Jas et al., 2016). The presented method capitalises on cross-validation in conjunction with a robust evaluation metric to estimate the optimal peak-to-peak threshold, extended to a more sophisticated algorithm which estimates this threshold for each sensor yielding trial-wise bad sensors. Depending on the number of bad sensors, the trial is then repaired by interpolation or excluded from subsequent analysis.

2.3.4 Optimisations and Performance

Among the EEG-extracted measures used, three of them needed a reimplementaion in Python: Permutation Entropy (PE; Bandt and Pompe 2002), Weighted Symbolic Mutual Information (wSMI; King et al. 2013b) and Kolmogorov-Chaitin complexity (K; Sitt et al. 2014).

Due to the complexity of the algorithms, optimisations were done in C using OpenMP for multithreading, with its corresponding Python bindings. This allowed to perform the computation of all the markers for a single subject in about 30 minutes in a 16 Gb RAM Intel Core i7 type workstation.

These benchmarks are particularly relevant for the practical purpose of the system. The current implementation facilitates the computation of reference models that are estimated on EEG-measures from hundreds of clinical recordings to predict unseen patients. This not

only facilitates more frequent updates of these reference models, which may be required for research purposes. It also lowers the maintenance burdens, i.e., of detecting and fixing software bugs.

2.4 Replication

To validate, both the results from [Sitt et al. 2014](#) and our Python implementation, we computed all the markers and the main analysis of the previous study, using the same original data. After preprocessing, we analysed a final cohort of 98 patients with 142 recordings (see Paris 1 in 2.2 on page 41).

At the univariate group level, we obtained the same results. Figure 2.2 on page 32 shows the topographical maps originally published in [Sitt et al. 2014](#) (Figure 2.1 on the facing page) and the results obtained with the Python implementation.

2.4.1 Methods

For the multivariate analysis, we computed the cross-validation (CV) accuracy using the markers extracted with our implementation. We extracted 28 EEG-markers as described in detail in [Sitt et al. 2014](#). These markers can be grouped into four conceptual families, i.e., information theory, connectivity, spectral, and evoked response markers (See Table 1). In the original publication, additional markers were used but were omitted due to previously reported unsatisfying performance or redundancy. For a full list of markers and abbreviations see Table 2.1 on page 33.

For each marker, we extracted four summary statistics. Aggregations over epochs were done using an 80% trimmed mean and the standard deviation to account for the average and its fluctuations over time. Aggregations over electrodes were computed using the mean and standard deviation to account for the average and topographical fluctuations. Some markers presented additional dimensions which were aggregated using a mean or median, according to the corresponding literature. For example, we would first compute either the mean or the standard deviation across epochs, and then the mean or the standard deviation across sensors. Throughout the chapter we refer to these marker subtypes as “mean,mean”, “std,mean”,

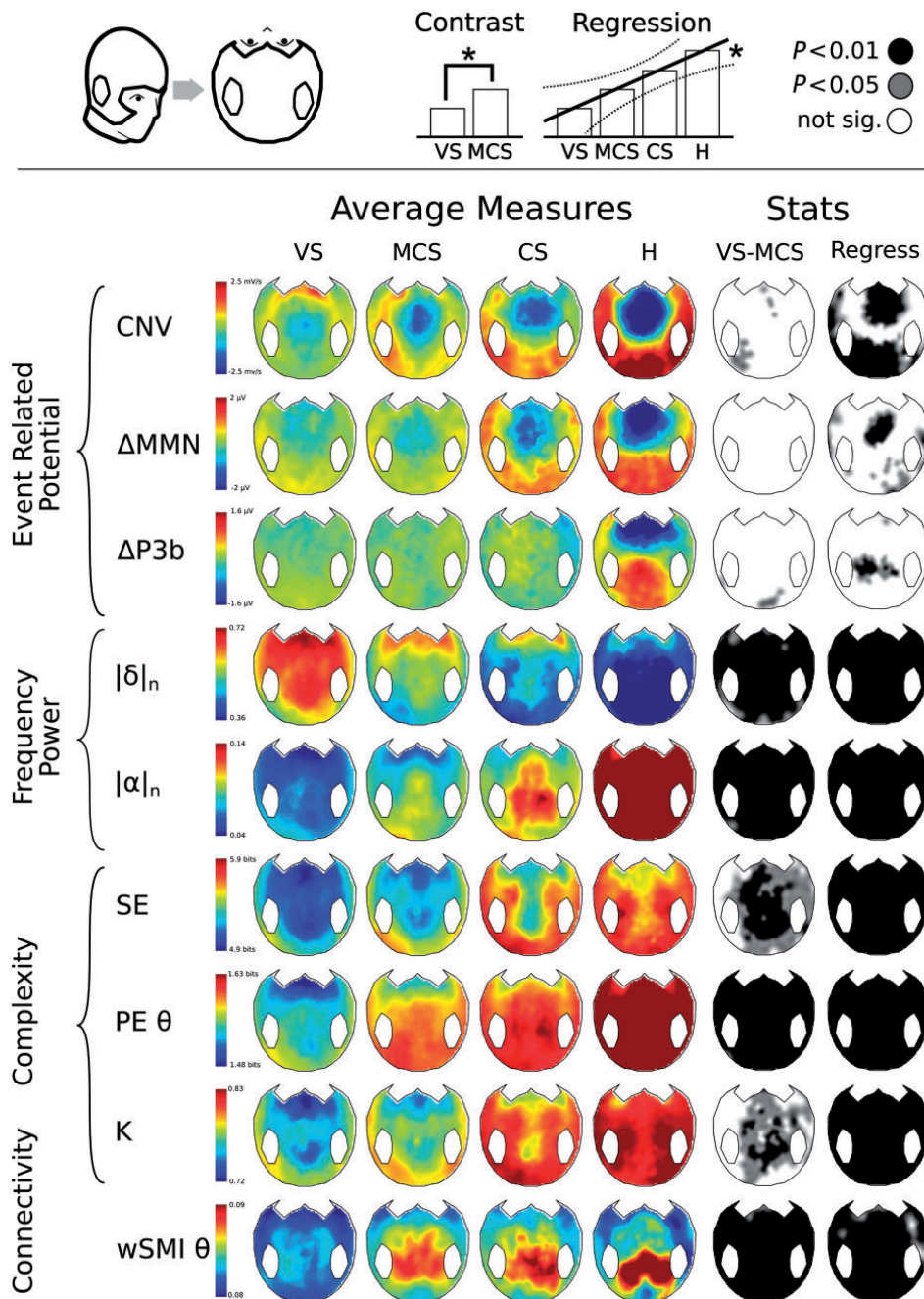


Figure 2.1: Scalp topographies of the most discriminatory measures. The fifth column indicates whether the VS and MCS patients were significantly different (Black: $p = 0.01$, light grey: $p = 0.05$, white: not significant, uncorrected). The sixth column shows the statistics of a regression analysis of the measure across the four states of consciousness (VS < MCS < CS (EMCS) < healthy controls (H)). Black: $p = 0.01$, light grey: $p = 0.05$, white: not significant, uncorrected). Extracted from [Sitt et al. 2014](#).

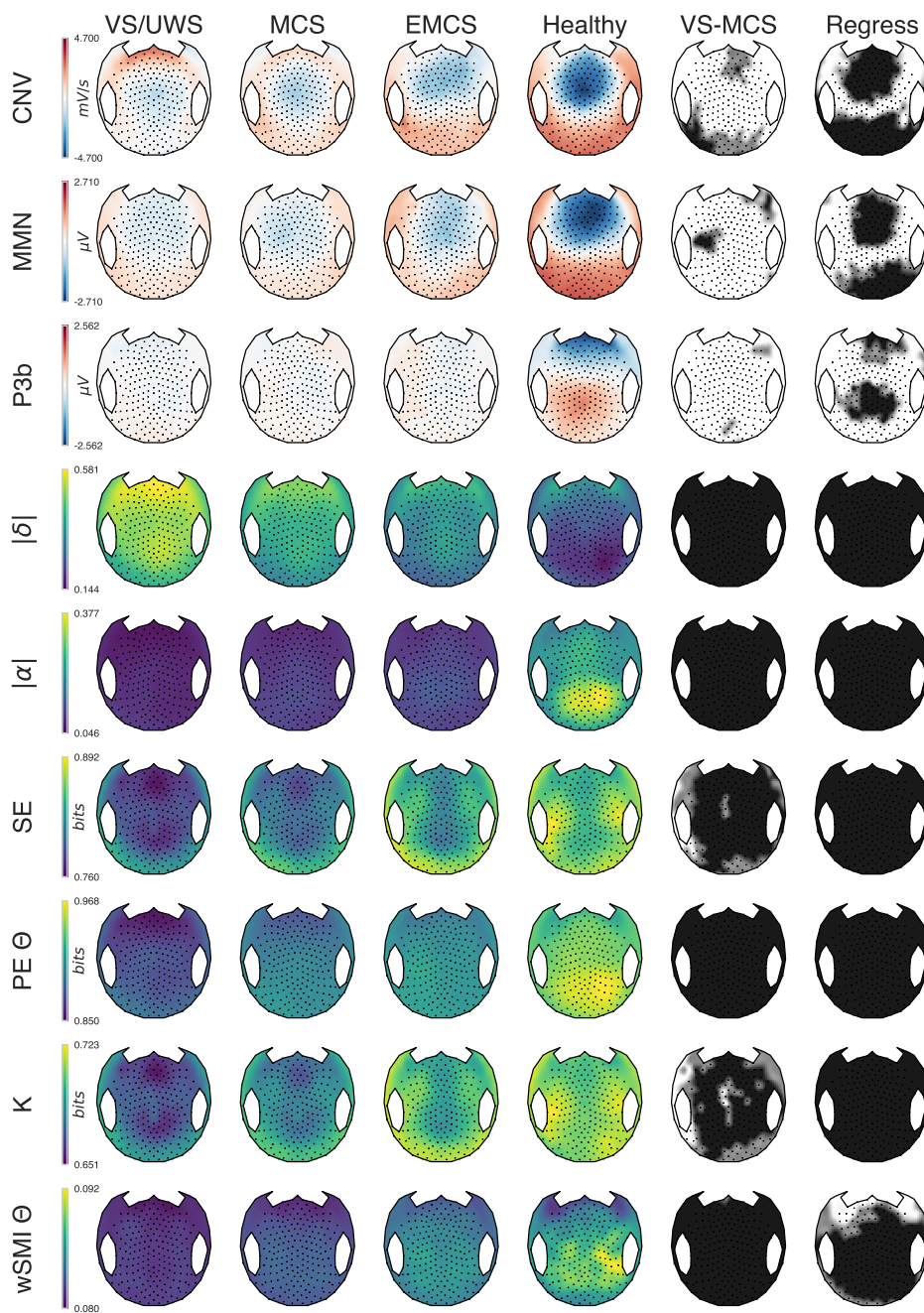


Figure 2.2: Reproduction of the figure from [Sitt et al. 2014](#) using our Python implementation.

Abbreviation	Marker	Family
PE Θ	Permutation Entropy	information theory
K	Kolmogorov Complexity	information theory
wSMI Θ	Symbolic Mutual Information (weighted)	connectivity
α	Alpha PSD	spectral
$\ \alpha\ $	Normalized Alpha PSD	spectral
β	Beta PSD	spectral
$\ \beta\ $	Normalized Beta PSD	spectral
δ	Delta PSD	spectral
$\ \delta\ $	Normalized Delta PSD	spectral
γ	Gamma PSD	spectral
$\ \gamma\ $	Normalized Gamma PSD	spectral
θ	Theta PSD	spectral
$\ \theta\ $	Normalized Theta PSD	spectral
MSF	Median Power Frequency	spectral
SE90	Spectral Edge 90	spectral
SE95	Spectral Edge 95	spectral
SE	Spectral Entropy	spectral
CNV	Contingent Negative Variation	evoked
P1	P100 evoked potential	evoked
P3A	P3a evoked potential	evoked
P3B	P3b evoked potential	evoked
GD-GS	full contrast	evoked
LD-LS	full contrast	evoked
LSGD-LDGS	full contrast	evoked
LSGS-LDGD	full contrast	evoked
Δ P3A	Contrasted P3A (LD vs LS)	evoked
Δ P3B	Contrasted P3B (GD vs GS)	evoked
Δ MMN	Contrasted MMN (LD vs LS)	evoked

Table 2.1: Acronyms used for EEG-measures

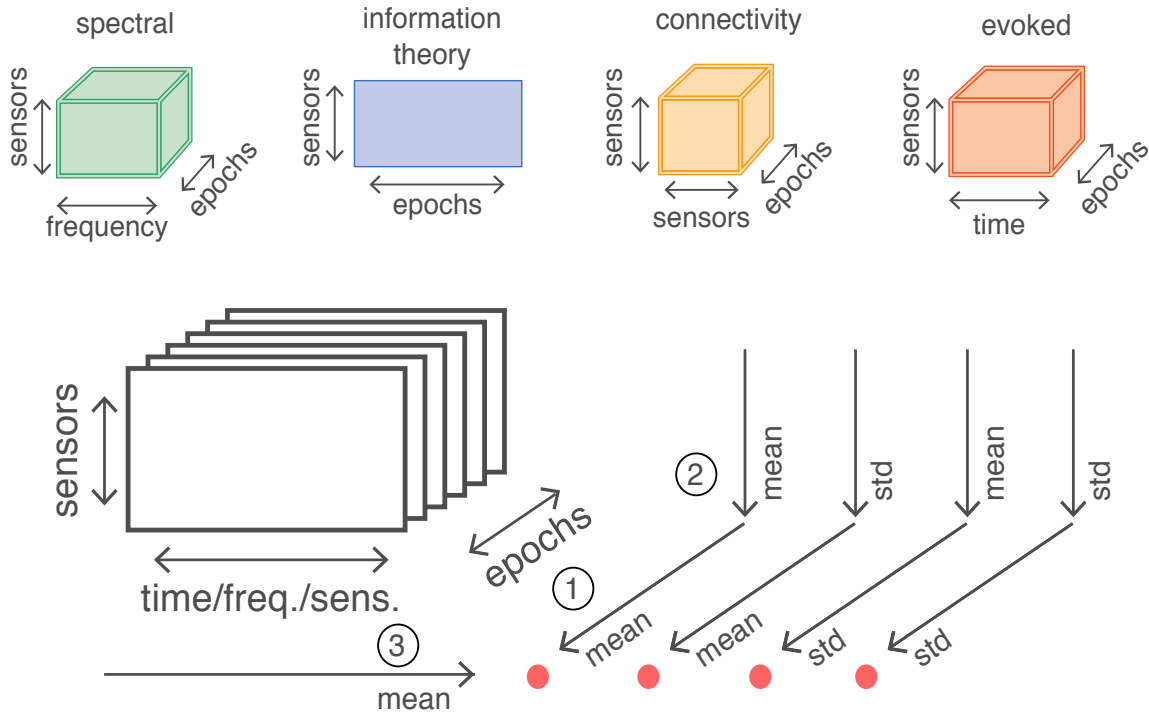


Figure 2.3: Diagram of the dimensions for each of the families of markers. To compute the scalar values, dimensions were first aggregated by epochs (1), then by sensors (2), and finally, if needed, by the remaining dimensions. (3)

“mean,std” and “std,std” and in figures, for brevity, “m,m”, “s,m”, “m,s”, “s,s”. A description on the dimensions and the procedure can be seen in Figure 2.3

These markers were then fitted into a classifier trained to distinguish between the VS/UWS and MCS patients. The classification algorithm used in the original publication consisted on a Support Vector Machine (SVM). The SVM-based classifier (SVC) aims at finding the optimal linear combination of features (w) that separates the training samples with distinct classes in the hyperspace of features. A penalisation parameter is used to find a solution which is likely to generalise to another dataset, and hence avoid over-fitting. Here, the penalisation parameter C , was chosen by nested cross-validation among the values = [.001 .01 .1 .2 .5 1 2 10] using a grid-search method (Pedregosa et al., 2012). The SVC can provide a continuous probability by fitting the distribution of the samples with regard to w (Platt, 1999).

Additionally, we used the Extremely Randomised Trees (ET) algorithm (Geurts et al.,

2006) to address a potential decrease of performance when generalising to new data. Unlike Support Vector Machines, Extremely Randomised Trees are non-parametric and robust by design, and are not sensitive to the measurement scale of the input data. This algorithm can handle so-called wide datasets in which more variables than samples are available. Moreover, it belongs to the family of adaptive algorithms capable of scaling the complexity of the learned model to the amount of data available. The algorithm achieves its efficiency by generalising the non-linear decision tree approach. Single decision trees are non-parametric rule-based models that automatise variable selection and can be thought of as learning a “regression surface” from the data by recursive orthogonal partitioning (Efron and Hastie, 2016). In other words, decision trees map joint value ranges of the input variables to values of the outcome variable. However, decision trees poorly generalise to new data. The Extremely Randomised Trees retains all benefits of decision trees while mitigating their excessive variance and poor generalisation capability. This is achieved by averaging over many randomly constructed, hence uncorrelated, decision trees. To avoid overfitting, we used 2000 trees, limited the tree depth to a value of four and to maximise randomisation and minimise masking effects in feature importances (Louppe et al., 2013), we constrained the maximum number of features used for finding split points to one.

For cross-validation, a group Monte Carlo sampling scheme was used with a training set size of 80 percent, a testing set size of 20 percent and 50 iterations. The Monte Carlo procedure is known to minimise estimation variance and has been shown to yield low positive cross-validation bias (Varoquaux et al., 2017). The group variant consisted in exclusively assigning subjects to either the test or the train sets in order further avoid positive bias due to intra-subject sample correlations that are known to inflate the performance and constitute a violation to the assumptions of generalisation inference.

2.4.2 Results

Using our automated implementation, we obtained an AUC of 78.32% with the SVM classifier and an AUC of 77.35% with the ET algorithm, consistent with the 78% AUC reported in Sitt et al. 2014.

2.5 Validation

Despite the successful replication of the results obtained in [Sitt et al. \(2014\)](#), there was still a methodological risk: with repeated analysis on the same data, one risks to overfit the classifier and overestimate its diagnostic accuracy. For this purpose, the recommended approach is to test the accuracy on unobserved data. We then analysed 107 recordings from 92 patients registered after 2014 (see Paris 2 in 2.2 on page 41).

2.5.1 Methods

To assess the diagnostic accuracy on new data, we contrasted the performance of the classifiers against empirically estimated chance levels. These values were obtained from dummy classifiers which generates random predictions based on simple rules that do not depend on the actual predictors but could nevertheless lead to correct guess. Common dummy classifiers consist in 1) predicting the most frequent class, and 2) stratified random guessing while respecting the class distributions. We then used the bootstrap method to analyse the AUC and differences of the means. Following the recommendations by [Efron and Tibshirani 1993](#), we generated 2000 samples by drawing with uniform probability and with replacement.

2.5.2 Results

The resulting performance of the SVM showed a mean AUC of 74.27% while the ET classifier presented a mean AUC of 72.91%. Both performances were significantly different from the chance level AUC of 50.01% as estimated by a dummy classifier (figure 2.4 on the facing page).

Even though the classifiers performed similarly, one key aspect is still unanswered: is the combination of markers better than any marker alone? In other words, the use of a multivariate classifier is still not tested against univariate solutions. The direct comparison between the univariate model-free AUC and multivariate models is not entirely correct. In the first case, we do not build a predictive model but test how ‘good’ each marker separates the MCS and VS/UWS patients. Indeed, the in-sample estimation of the univariate AUC might give positively distorted estimates of true classification performance. To use a directly compara-

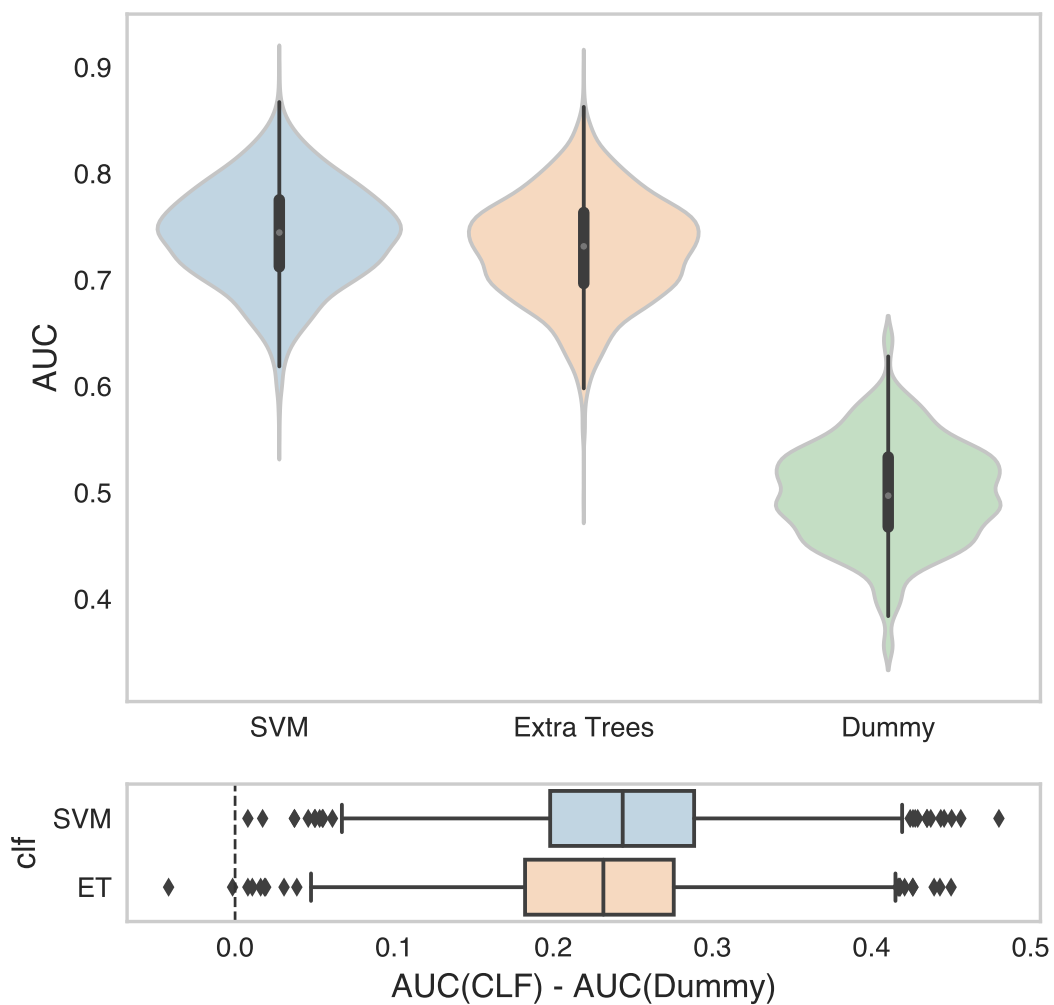
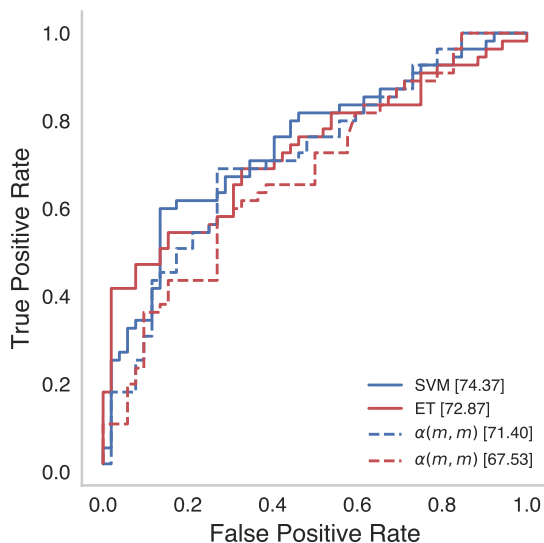


Figure 2.4: Our new implementation, tested on unobserved data, presents an AUC of 74.27% with an SVM classifier and 72.91% with an Extremely Randomised Trees algorithm (top). When compared to a dummy classifier to estimate the empirical chance level, the results of the classifiers are significantly different (bottom). The results were computed using 2000 bootstrap replicates.

Figure 2.5: Multivariate classifiers outperforms univariate counterparts. Both SVM (blue) and ET (red) multivariate classifiers presented a superior AUC than the respective univariate versions on $\alpha(m, m)$ (dashed)



ble measure, we trained univariate versions of SVM and ET classifiers. This allowed us to use the identical classification and prediction framework as for our multivariate analysis and obtain predicted probabilities of DOC diagnosis from single markers.

Interestingly, both univariate SVM and ET depicted alpha power (mean, mean) as the best univariate marker with an AUC of 71.40% and 67.53% respectively. Nevertheless, both of them were under their respective multivariate mean (figure 2.5).

2.6 Clinical application

2.6.1 Report

Once the markers were recomputed and validated, the next step was to use this procedure in the clinical settings. Having a trained classifier with an automated method could be useful to predict the diagnosis of patients based on the EEG-extracted markers. MNE-Python provides a useful reporting tool: a self-contained HTML file with images and text that can be easily transferred by mail and reviewed even without internet connection. This report provides quantitative information on the preprocessing results, individual markers values, ERP time-series and statistics, as well as results from the multivariate (SVM) and univariate (Logistic

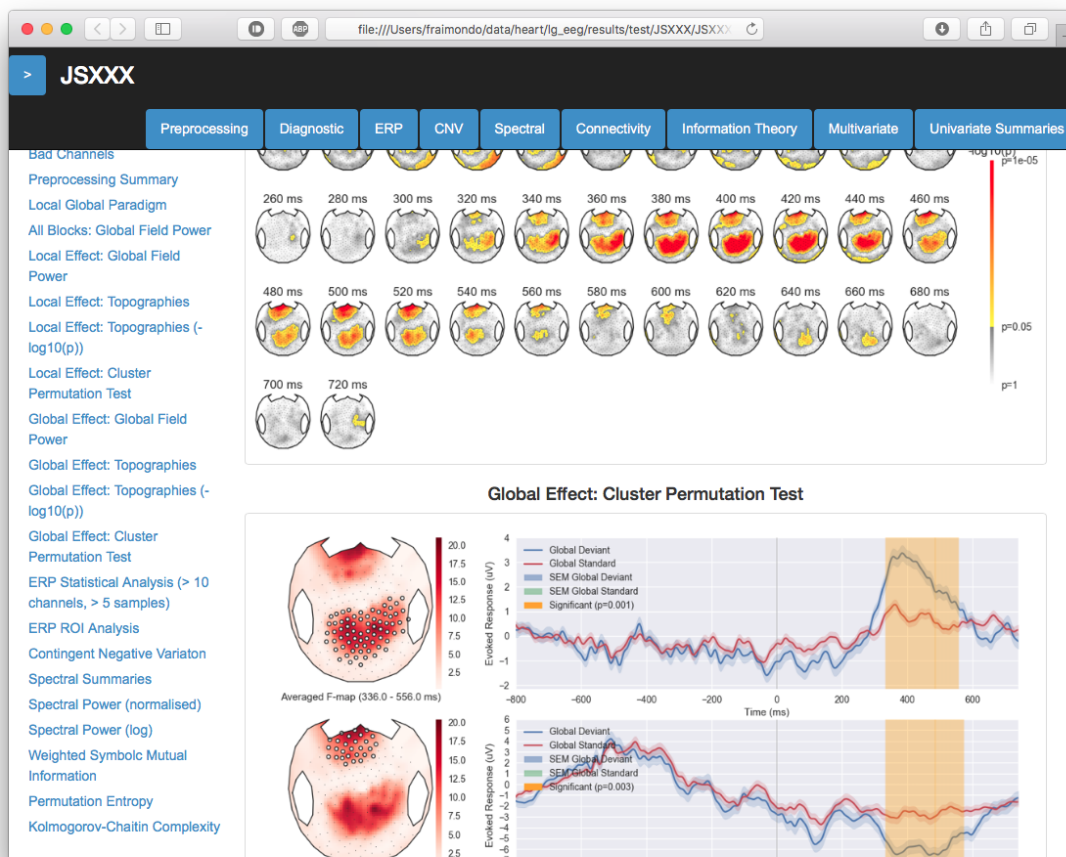


Figure 2.6: A self contained HTML-report presents all the results from the automated processing. This includes quantitative information regarding the preprocessing procedures, markers, statistics and predictions.

Regression) classifications (Figure 2.6).

2.7 Further steps: towards a universal tool

So far, we have provided strong evidence supporting our classification model for the automated diagnosis of DOC patients. Nevertheless, the domain of application is still restricted: all the data comes from the same clinical centre, acquired with the same EEG system and under the same conditions. If the purpose is to build a tool that can be used to assess disorders

of consciousness, it is important to assess the behaviour of such procedures under different conditions.

In clinical applications, we identified three main sources of variability related to EEG-based diagnosis of DOC. First, the behavioural assessment, despite the standardisation efforts and guidelines, are performed differently. Second, EEG systems configurations varies from clinical centres: the amount of electrodes and positions, the sampling rate and the recording quality changes depending on the brand and model of the acquisition systems. Finally, every clinical centre performs the EEG acquisitions under its own protocols: stimulation paradigms or resting state with varying parameters, including the recording length.

To assess the possibility of creating a universal tool for the EEG-based diagnosis of DOC, a generalisation analysis must be carried out to address the potential limitations. What is the optimal duration for individual EEG-recordings? Which stimuli and task should the patient be exposed to, if any? How many EEG sensors should be used, and where should they be located? Can the same machine learning algorithm operate on recordings acquired in different clinical centres?

To answer these questions, we probed the robustness and generality of EEG-signatures of consciousness under several simulated and real conditions. We first analysed the potential use of the tool across different EEG-systems using simulated electrodes montages and recording length from the EEG data recorded at the Pitié Salpêtrière hospital in Paris, France. Finally, we analysed a cross-clinical centre analysis and cross-protocol generalisation using resting state EEG data from the Liège University Hospital in Belgium. A description of the dataset can be found in table 2.2 on the next page.

2.7.1 Generalisation to difference EEG recording configurations

Methods To assess the potential use across incompatible EEG systems, we downsampled the data spatially and temporally after the preprocessing step. Spatially, we selected standard EEG configurations with 6 different number of electrodes (256, 128, 64, 32, 16, 8). Position were selected such that they approximated realistic EEG caps respecting the international 10-20 system. Temporally, we reduced the amount of epochs to 6 different percentages (1, 5, 25, 50, 75, 100), respecting the proportions of conditions within the Local Global paradigm. See figure 2.7 on page 42 for a graphical representation of the selected electrodes and temporal

Protocol	Auditory Local Global Task		Resting State
	Paris 1	Paris 2	Liège
Dataset	Paris 1	Paris 2	Liège
n(EEG)	142	107	78
n(patients)	98	92	78
n(UWS)	75	52	22
n(MCS)	66	56	57
Sex ratio (male/female)	2.0	1.9	1.2
Age (M [SD]), in years	46.5 [17.8]	45.4 [17.7]	38.0 [14.3]
Delay (M [SD]), in days	125.9 [372.9]	299.5 [823.6]	1040.5 [1227.6]
Delay (MD), in days	30.0	40.5	529.0
Delay (SD)	372.8	823.6	1227.6
Delay (min to max), in days	6 to 2611	8 to 6570	11 to 5380
Anoxia (%)	29.6	30.4	N/A
Stroke (%)	29.6	15.2	N/A
TBI (%)	23.5	28.2	48.1
Other (%)	18.4	29.4	N/A

Table 2.2: Description of the three datasets used throughout the analysis in this chapter. Paris 1 refers to the data used in [Sitt et al. 2014](#) and in section 2.4 on page 30, Paris 2 to the data used for the validation analysis in section 2.5 on page 36. Data provided by the Liège university hospital was used in section 2.7.2 on page 43.

subsampling.

Results When we compared the univariate in-sample performance of the markers from the cross-validated multivariate AUC using the SVM and ET classifiers, we observed that many individual markers exhibited dramatic variability of performance across different combinations of sensor and epochs configurations. Nevertheless, the multivariate classifiers fluctuated between 70.94% and 78.33% for the SVM and 72.08% and 77.76 % for the ET (figure 2.8 on the next page).

Although the overall performance of the multivariate classifiers were in similar ranges, the ET classifier seems to be more stable than the SVM with alternative spatial configurations (figure 2.9 on page 43). Both classifiers tended to improve as more epochs and sensors were used. For the ET classifier, optimal performance was achieved with 128 electrodes. Nevertheless, reasonable performance could still be obtained with only 16 electrodes and a minimum of epochs. On the other hand, the SVM classifier peak accuracy stands at 256 electrodes and 100% epochs, but stability is severely affected by the amount of epochs and

Figure 2.7: Alternative EEG configurations with 6 different number of electrodes (256, 128, 64, 32, 16, 8). Position were selected such that they approximated realistic EEG caps respecting the international 10-20 system. Temporally, we reduced the amount of epochs to 6 different percentages (1, 5, 25, 50, 75, 100), respecting the original proportion of trials.

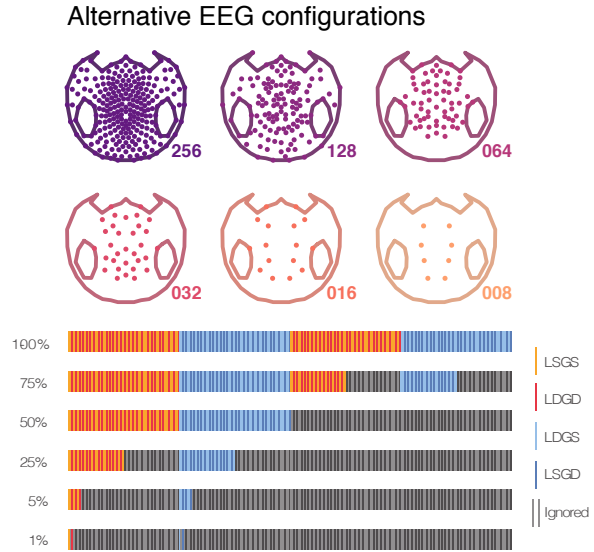
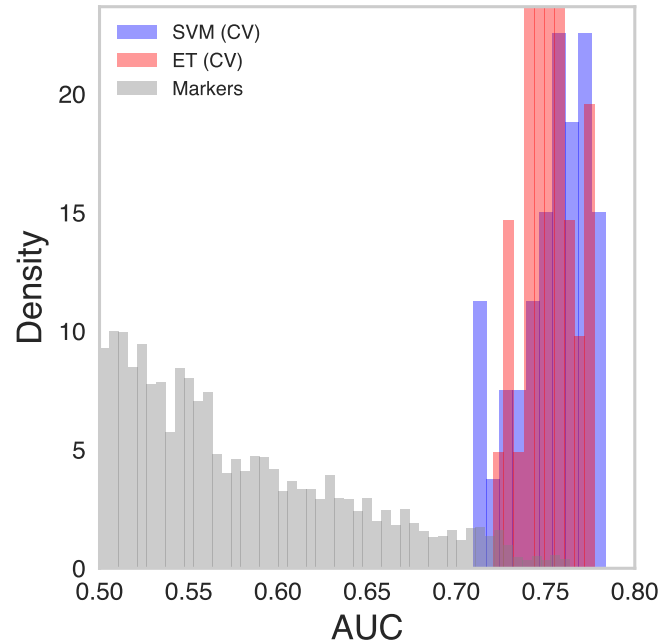


Figure 2.8: Multivariate classifiers perform robustly on alternative EEG spatial configurations and recording lengths. Across all 36 experiments (6 alternative sensors locations by 6 temporal subsamplings) in-sample markers AUC (gray) are less performant than multivariate models.



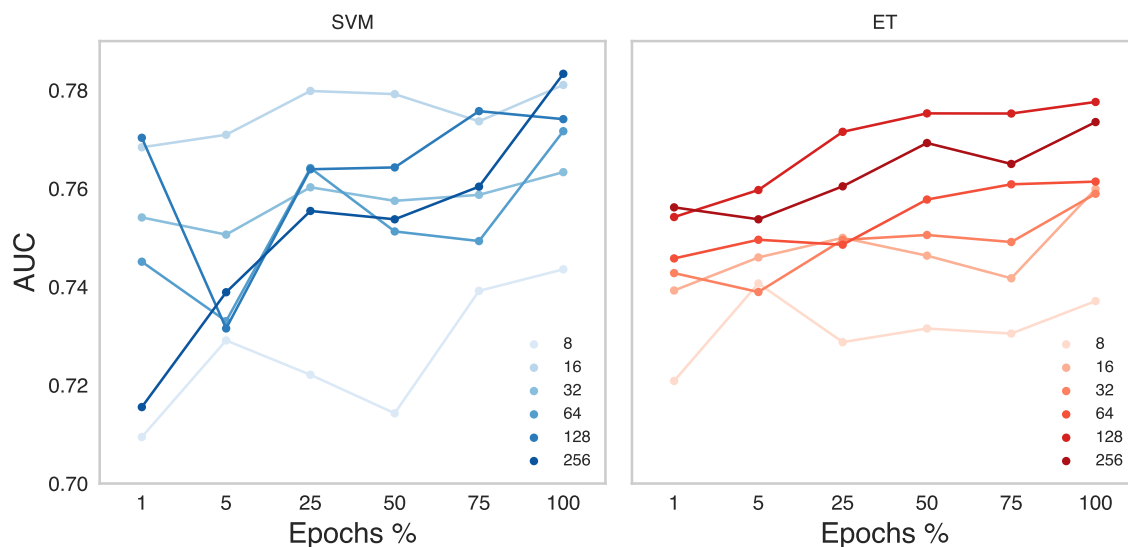


Figure 2.9: Performance of the ET is more stable across spatial and temporal configurations compared to the SVM. Both classifiers present a trend to better accuracy with more epochs and electrodes. Nevertheless, SVM presents higher variability when the number of epochs is reduced.

sensors.

2.7.2 Generalisation to Resting State

When training the classifiers on the all available data from Paris (Paris 1 and Paris 2) but ignoring the markers derived from evoked responses (table 2.1) the ET achieved an AUC of 78.28% on the Liège resting state data and the SVM an AUC of 81.62% (figure 2.10 on the next page). Both classifiers presented significant differences compared to a dummy classifier.

We then compared the univariate and multivariate generalisation performances. Interestingly, the best univariate performance was achieved with alpha power with the *(mean, mean)* variation in the ET and the *(mean, std)* variation in the SVM, with AUCs of 74.85% and 75.73% respectively (figure 2.11 on page 45).

Finally, and coming back to the EEG configuration generalisation analysis, we tested the performance of the models across the temporal and spatial subsamplings. We trained and tested our models using each one of the 36 EEG configurations (see 2.7 on the preceding page) independently, yielding a total of 1296 experiments (36×36). When trained on the

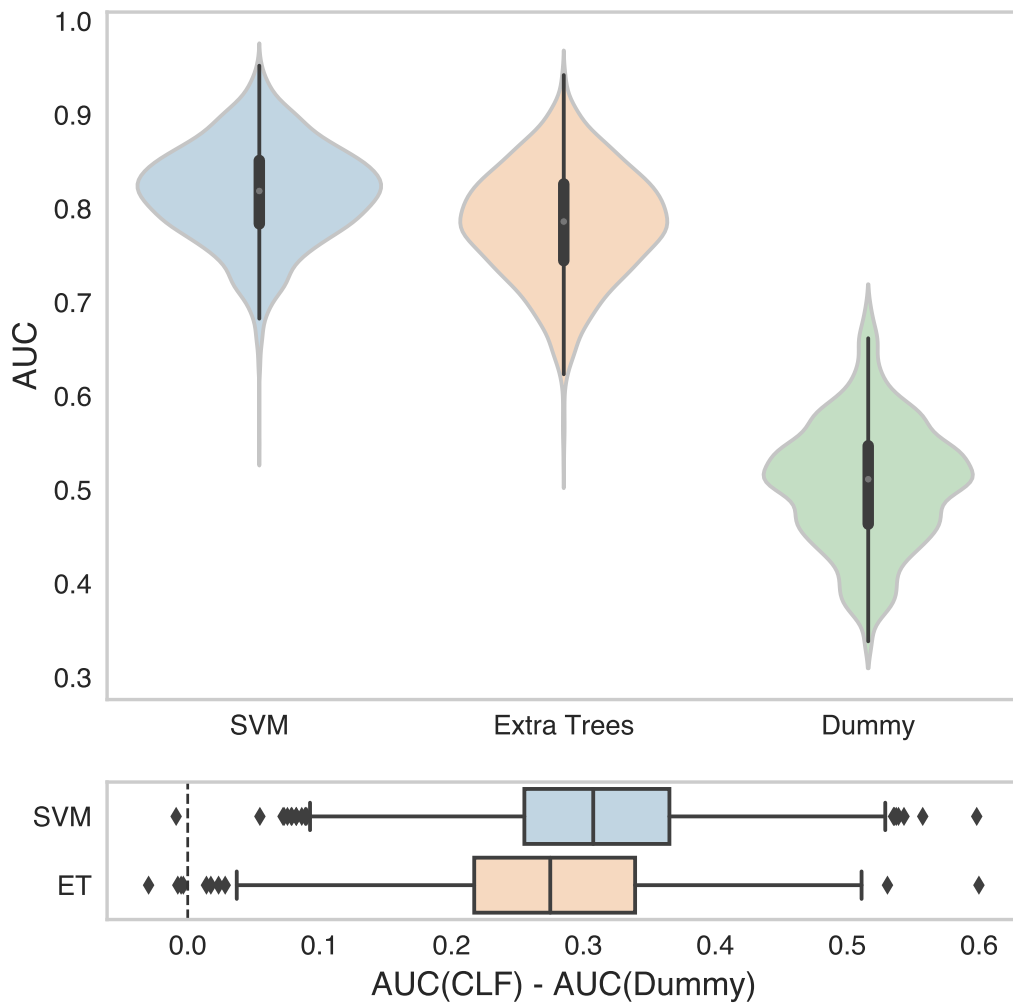


Figure 2.10: Both our models generalise to resting state. The ET classifier present an AUC of 78.28% and the SVM classifier an AUC of 81.62%. When compared to a dummy classifier to estimate the empirical chance level, the results of the classifiers are significantly different (bottom). The results where computed using 2000 bootstrap replicates.

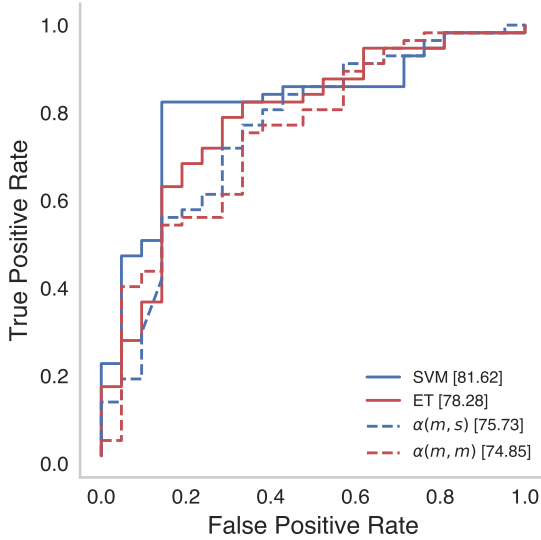


Figure 2.11: Multivariate classifiers outperforms univariate counterparts also when generalising to resting state data. Both SVM (blue) and ET (red) multivariate classifiers presented a superior AUC than its univariate versions on $\alpha(m, s)$ (dashed blue) and $\alpha(m, m)$ (dashed red).

Paris 1 dataset and tested on Paris 2, both multivariate models outperformed the best univariate ones. Mean AUCs were as follows: SVM AUC 72.30%, ET AUC 73.20%, SVM $|\alpha(s, m)|$ AUC 69.58% and ET $\alpha(m, m)$ AUC 70.99%. When trained on Paris and tested on Liège, the same effect was achieved: SVM AUC 75.97%, ET AUC 76.59%, SVM $\alpha(m, m)$ AUC 73.47% and ET $\alpha(m, m)$ AUC 73.04%. Nevertheless, as depicted before, best performances are achieved with the SVM classifier: 80.55% and 82.95% vs 78.77% and 81.20% obtained with the ET classifier for the Paris 2 and Liège test sets respectively. For a visual representation, see 2.12 on the following page.

2.7.3 Discussion

These findings show that robust generalisation can be achieved despite changes in the spatiotemporal configurations of the EEG and the recording protocols. We compared systematically two different multivariate models that always outperformed its univariate counterparts. While certain EEG-signatures, i.e., alpha band power and its fluctuations turned out to be useful as stand-alone classifiers we found that the advantage of multivariate over univariate classification was most striking when systematic differences between the training and testing sets were present. We showed that by relying on a robust classification algorithm, mean-

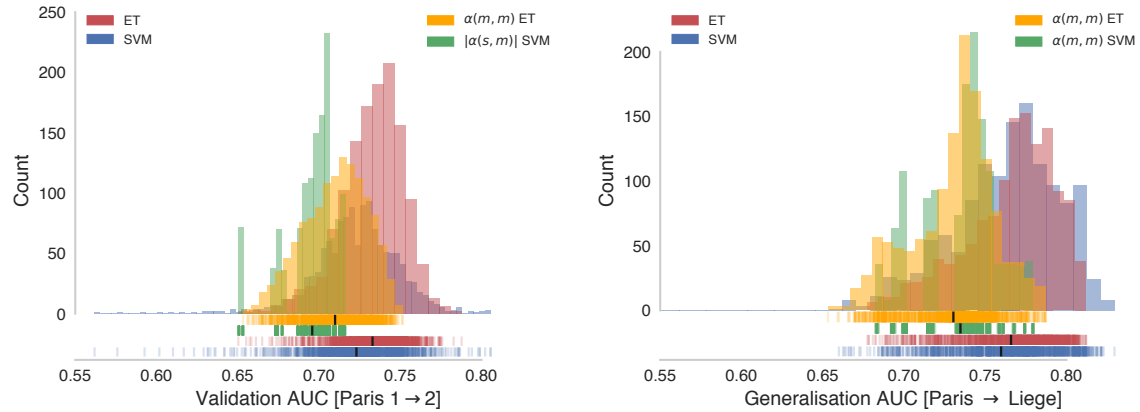


Figure 2.12: ET classifier presents less variability than SVM across spatiotemporal subsamplings. All the different spatial and temporal configurations were considered for training and testing (1296 combinations, 36 for each set). The corresponding best univariate models were also considered next to the multivariate ones. The distribution of AUC scores is indicated by the histograms for both validation (left) and generalisation (right) sets. Samples are depicted underneath the histograms, with black solid lines indicating the mean of the distributions. Both multivariate classifiers outperformed the corresponding best univariate ones. In both cases, the ET classifier presented less variance, although the highest accuracy was always obtained using the SVM model.

ingful generalisation could be achieved even if the performance of individual markers varied systematically between datasets.

Our results demonstrate that diagnosis of DOC patients can be robustly inferred from multivariate pattern classification using a wide array of EEG configurations. This was also the case with a minimum of sensors and epochs and even when EEG configurations differed on the training and testing data, e.g., when training on 10% of the epochs with 8 sensors and testing on all epochs with 256 sensors. We observed that many individual markers were highly variable. Nonetheless, our models fluctuated between AUC scores of 71% and 78% for the SVM and 72% and 77% for the ET.

It is important to note though, that the choice between the SVM and ET classifiers should be done based on the domain of application. While SVM reported higher AUCs for most cases, the variability across conditions was always lower with the ET classifier. In that sense, the ET is preferred as the model to *Fit Them All*, since it can absorb the heterogeneity of the datasets. On the other hand, if the priority is to maximise the AUC, then our recommendation is to maintain the data variability as low as possible and use an SVM classifier, since in

homogeneous data outperformed the ET in most of the cases.

2.8 Insights from Machine Learning

It is possible to analyse, post-hoc, which are the markers that the models are using to perform the classification. In 2.7 on page 39 we showed that the Extra Trees classifier was robust and could serve as a model to *Fit Them All* since it tolerates the variability on the individual markers due to heterogeneous EEG spatial and temporal configurations. Given that the ET classifier trained on one configuration generalises above chance for other configurations, one can argue that this classifier is capturing the common substrate of the EEG markers that allows the distinction between VS/UWS and MCS patients, disregarding the spatial and temporal resolutions of the recordings. Hence, analysing the groups of forests can depict if such common substrate is related to one or several particular markers, or it is the combination and interaction among all of them what allows the model to maintain its performance.

2.8.1 Methods

To obtain this insight, we extracted the *variable importance* metric from the Extra Trees classifiers. When entropy is used as impurity criterion, this multivariate metric can be shown to correspond to a weighted average of the mutual information between one variable and the outcome, conditionally over any possible configuration of any subset of the other variables (Louppe et al., 2013). Moreover, it has been shown that in fully randomised trees variable importance is only driven by relevant variables and not uninformative ones (Louppe et al., 2013). Also, the variable importance can deviate systematically from the univariate AUC whenever information is shared between markers or the model has identified non-linear interaction effects. To enforce this interpretation, we used entropy as impurity measure and only used one single marker for splitting, which maximised randomisation and made the tree-growing independent from the data (Geurts et al., 2006; Louppe et al., 2013).

2.8.2 Results

Inspecting all 36 DOC-Forest classifiers trained on the Paris 1 dataset using different EEG-configurations, we observed that markers contributing most strongly on average belonged to different conceptual families (Figure 2.13 on the facing page left). Specifically, permutation entropy and long-range connectivity also in the theta band as well as alpha frequency band power were top ranked, both, in terms of univariate discrimination and variable importance. In contrast, evoked markers, on average, often assumed values below 0.89%, which is less than would be expected if all markers were equally influential. We observed a positive but non-linear relationship between average AUC and average variable importance ($\rho_{Spearman} = 0.82, p < 0.001$). It can be seen that highly performing markers were disproportionately more important than expected for a linear association.

When we compared the models variable importance against each marker's out-of-sample performance for the validation and generalisation cases (Figure 2.13 on the next page middle and right), we also found positive non-linear correlations in Paris 1 \rightarrow 2 ($\rho_{Spearman} = 0.48, p < 0.001$) and Paris \rightarrow Liège ($\rho_{Spearman} = 0.521, p < 0.001$). The display reveals that several univariate models showed reasonable generalisation performance with AUC values beyond .70. Highly performing markers were disproportionately more important for the DOC-Forest than would have been expected assuming a linear relationship. Again, these findings suggest that the DOC-Forest achieves generalisation by preferentially enhancing the influence of reliable markers.

2.8.3 Discussion

Our findings suggested that protocol-general markers were, overall, more reliable. Strikingly, these markers belong to different conceptual families were all related to neuronal dynamics in the theta and alpha range (Figure 2.13 on the facing page). The robustness of these markers may be explained by the fact that no excessive averaging is needed for their extraction and their characteristic EEG-topographies are simple and easy to capture with few sensors. However, the tight relationship between variable importance and conditional mutual information (Louppe, 2014) suggests that these top-performing markers carry independent information. Indeed, recent research has suggested a rather complex picture of functional and pathophys-

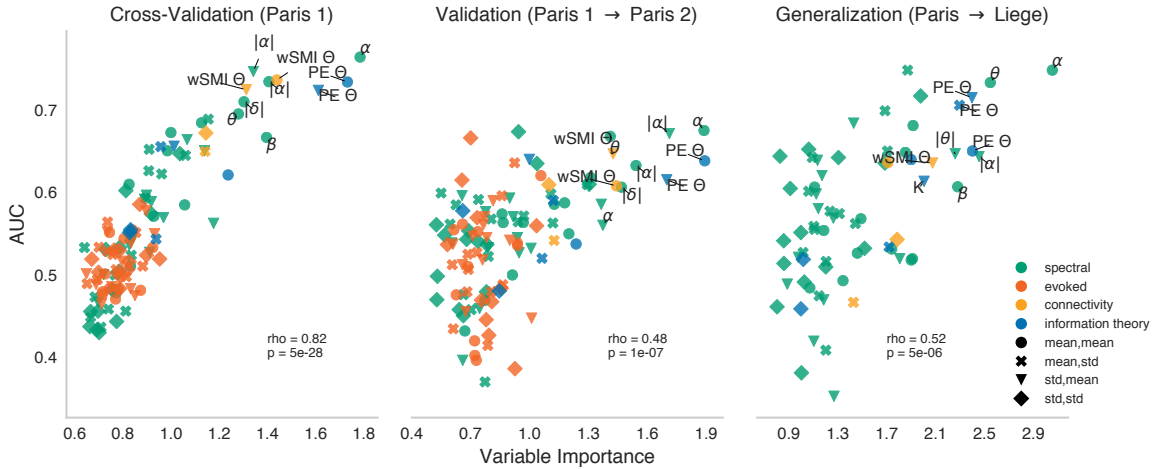


Figure 2.13: We observed a positive but non-linear relationship between univariate AUC and variable importance in the ET classifier. Left plot depicts the correlation between the univariate AUC and variable importance of the ET classifier when averaged across the 36 experiments. Middle and Right plots depicts the same correlation for the validation and generalisation cases. Colours indicate the family of the marker, while the shape depicts the variant. The three correlations were statistically tested using Spearman rank correlation coefficient.

iological landscapes. The complexity of theta-band signals and their long-range interactions could reflect distinct memory processes underlying consciousness, such as access and maintenance (Axmacher et al., 2010). Similarly, alpha band power may reflect global arousal and demands for dynamic inhibition required for functional encapsulation of cortical networks (For an overview see Sadaghiani and Kleinschmidt 2016). Moreover, intact consciousness has been related to the peak frequency of alpha and theta band oscillations originating from distinct cerebral generators (Schiff, 2010; Williams et al., 2013). This is further complicated by the fact that these generators can be selectively disrupted for different aetiologies and can show a variety of regional effects during anaesthesia (Purdon et al., 2013). While future experimental research is desirable to disentangle these facets, our findings suggest that the presence of independent physiological sources of information may enhance generalisation as it is unlikely that all of them are jointly corrupted on new data samples.

Markers of Evoked Potentials are subject to extensive neuroscientific validation and intuitively support clinical reasoning. The P3 markers, for example, belong to the most studied indices of consciousness in the EEG literature and are commonly used in brain computer interfaces settings (Lulé et al., 2013). They have been related to processing novelty in bottom-up information, the global neuronal workspace, access consciousness, and context-updating

(Dehaene et al., 2006; Donchin and Coles, 1988; Pins and Ffytche, 2003; Polich, 2007; Sergent et al., 2005). Considering such markers for multivariate analysis may, thus, improve interpretability. Additionally, evoked markers indexing auditory novelty have been shown to be rather specific than sensitive (King et al., 2013a). Like-wise, it could be the case that candidate signatures of conscious access, e.g., P3b, may be more relevant to distinguish MCS+ from MCS- patients (Naccache, 2017). Although being deemphasised by the ET classifier, evoked markers may still have contributed positively. Indeed, excluding all evoked markers from the Paris 1 to Paris 2 generalisation actually reduced the performance marginally (AUC = 71%). One could, therefore, argue that, evoked markers should be considered for multivariate analysis applied to DOC whenever available, alongside a few robust markers.

2.9 Summary

In this chapter, we analysed and compared two multivariate classifiers for the diagnosis of disorders of consciousness. We demonstrated that electrophysiological signatures of consciousness can be robustly exploited across contexts and protocols by relying on robust machine learning techniques. We validated on unseen data, analysed generalisation to resting state EEG and analysed the individual marker contribution to the multivariate model.

The significant generalisation from task to resting state EEG deserves separate consideration. It is well conceivable that EEG signatures related to the functional axis of consciousness (Sergent et al., 2017), are accessible during task and resting state EEG. Accordingly, changing states of consciousness should impact markers of global house-keeping functions such as alpha band power, global long-range connectivity or signal complexity, irrespective of the context. For instance, for a patient with locked-in syndrome we observed EEG-patterns similar to healthy persons during rest (Rohaut et al., 2017). And indeed, we observed significant generalisation from task to resting state EEG.

These findings imply that EEG signatures of consciousness can be reliably extracted from different contexts and combined into coherent predictive models, encouraging future efforts in large-scale data-driven clinical neuroscience.

Chapter 3

Towards cross-modal integration as a measure of consciousness

Contents

3.1	Background	52
3.2	Hypotheses	54
3.3	Methods	55
3.3.1	Cross-modal Local-Global	55
3.3.2	Subjects	58
3.3.3	EEG acquisition	58
3.3.4	Analysis	59
3.3.5	Group-Level analysis	59
3.3.6	Statistics	60
3.4	Results	60
3.4.1	ERP analysis	60
3.4.2	ERP characterisation through MVPA	61
3.5	Discussion	61

In the previous chapter, we analysed a solution to address one of the main problems of the Local-Global paradigm as a tool for the diagnosis of DOC: it is highly specific, but not sensitive. If the test is positive, the patient is clearly able to maintain conscious attention and thus in a higher state of consciousness. Nevertheless, conscious but inattentive healthy controls presented a negative outcome for the test ([Bekinschtein et al., 2009](#)).

The proposed solution using machine learning increases its sensitivity, nonetheless, it requires a dataset in which all the samples have already been labelled. Such cohort of patients required 6 years (from 2008 to 2014) of data acquisition. And even if one is able to acquire such data, there still no error-free and objective gold standard ([Schnakers et al., 2009](#); [Wannez et al., 2017](#)), and one risks to reason in a circular manner: i.e. building a tool to label patients that works as good as the experts.

Furthermore, it is often the case that patients presents sensorimotor impairments. The Local-Global test relies only on auditory stimulation, which could yield negative results in case of auditory impairments. In 2017, we reported a case in which the test failed, but the machine learning approach described in chapter 2 on page 25 detected signs of consciousness ([Rohaut et al., 2017](#)) on a patient with no responses to auditory stimulation.

In this chapter, we propose to address these issues by analysing neural correlates of multisensory integration in DOC patients, with the objective to create a more sensitive test, independent of a database of previously diagnosed patients, and able to be used in sensory impaired patients.

3.1 Background

The way we experience our environment is by ongoing interactions between our brains and our senses ([Ernst and Bühlhoff, 2004](#)). The brain is able to assemble impressions of the outside world and, in conjunction with intrinsic cognitive processes (memory, language, executive function), is able to “know” that these images and patterns are being viewed by and belong to the self ([Fabrega, 2000](#)). The senses provide the link between the body and the environment. The synergy or interaction among the senses, and the fusion of their information content, is described as multisensory integration ([Stein and Stanford, 2008](#)).

As regards external sources, evolution has provided us with a specialised set of sensory organs, each of which is linked to multiple specialised brain regions. There are obvious advantages associated with having multiple senses: each sense is of optimal usefulness in a different circumstance, and collectively they increase the likelihood of detecting and identifying events or objects of interest. However, the greater advantage comes with the ability to fuse the information content of different senses. In this case, the integrated product reveals

more about the nature of the external event and does so in a faster and more accurate manner than would be predicted from the sum of its individual contributors (Stein and Stanford, 2008).

Neuronal mechanisms of multisensory integration in the cortex have been studied and are nowadays well characterised from single neuron perspective to whole brain function (Stein and Stanford, 2008; Clavagnier et al., 2004; Lütkenhöner et al., 2002; Senkowski et al., 2008; Stekelenburg and Vroomen, 2007; Karns and Knight, 2009; Driver and Noesselt, 2008). On the relation between multisensory integration and consciousness, previous studies focused on attention and conscious content (Hartcher-O'Brien et al., 2017; Talsma and Woldorff, 2005), and bodily self-consciousness (Blanke, 2012). At any given moment, only a limited amount of information is consciously accessed and defines the current conscious content, which is reportable by the perceiving subject. At the same time, many other processing streams co-occur but remain nonconscious (Dehaene and Changeux, 2011), such as subliminal stimuli, motor reflex or sensory analysis (Kouider and Dehaene, 2007). By manipulating visual perception and creating a disruption with somatosensory input, a previous study recreated the neurological condition of out-of-body experiences, a disturbance of bodily self-consciousness (Lenggenhager et al., 2007). A recent work studied the effects of multisensory integration when stimuli were presented below the threshold of perception, concluding that multisensory inputs, even outside of awareness, are integrated and affect the phenomenological content of bodily self-consciousness (Salomon et al., 2017). Collectively, these studies show that multisensory integration can be studied either by manipulating the way sensory stimuli are combined or how intense these stimuli are. Importantly, they indicate that multisensory integration is realised beyond reportability. Interestingly, though, no much is known about how the conscious state affects multisensory integration. This knowledge is important if we were to tackle the necessary conditions for subjective experience (or self) to happen. Essentially, an unsolved issue is whether our ongoing sense of self, which presents itself so clearly in typical wakefulness but seems to demolish in sleep and anaesthesia, is preserved even when we are unable to report upon it (Windt and Metzinger, 2007). Importantly for clinics, could patients in vegetative/unresponsive conditions be considered as retaining basic subjective experiences?

Past research on ERPs depicts enhanced neural responses to multimodal stimulation when

compared to unimodal stimuli (Giard and Peronnet, 2006; Talsma and Woldorff, 2005; Teder-Sälejärvi et al., 2002; Fort et al., 2002). In a recent publication, Chennu et al. 2013 uses a variant of the auditory Local-Global paradigm adding laterality mismatches. The effect of contralateral deviants depicted stronger MMN responses, reflecting the integrative processing of patterns across both auditory cortices to detect laterality shifts, and larger P300s waves, indexing the greater amount of cortical activation generated by the rare shifts in laterality of tones.

Taken together, these results suggest the existence of a variety of distinct neural responses that can be measured using EEG. While they have been linked to conscious content and attention, the relation between the neural components of multisensory integration and state of consciousness remains unexplored. It is hereby proposed to add cross-modal stimuli as an extra layer to the Local-Global paradigm which is expected to promote multisensory integration, and therefore increase the sensitivity to detect consciousness in various states.

3.2 Hypotheses

For the purpose of this study, we propose an extension of the Local-Global paradigm to include three stimulation modalities (auditory, somatosensory and visual) that contains unimodal (same stimuli) and cross-modal (two modalities) trials.

The following are the working hypotheses:

1. Unimodal within-trial effects will differ between stimulation modalities, as a result of the different cortical sensory pathways.
2. Unimodal Global effects (associated with conscious processing) will be present and indistinctively of the stimulation modality, as a result of higher cognitive function not attributed to sensory pathways. All stimulation modalities will induce the same ERP.
3. Cross-modal and unimodal within-trial effects will differ, depicting the differential neural responses to cross-modal stimulation.
4. Within-trial effects will be detected in some DOC patients. Not all MCS patients will show the effect, with less proportion for VS/UWS patients, as a result of restricted cerebral integrity.

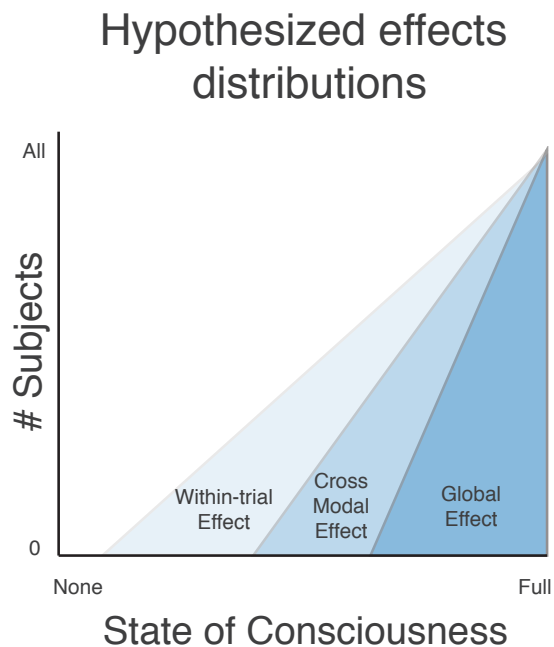


Figure 3.1: Illustration of the hypotheses, depicting the number of subjects presenting within-trial, cross-modal and global effects in relation to the state of consciousness. In short, we expect that conscious subjects will show global effects while unconscious subjects will be able to show some local effects. The cross-modal effects will fall in between, because they require the interaction between sensory-specific cortical areas.

5. Global effects will be detected only in patients with preserved levels of awareness, implying the presence of multisensory integration induced by cross-modal stimulation.
6. Effects to cross-modal stimulation are expected to lay in an intermediate level. They will be present in fewer patients as compared to the within-trial effect and in more patients as compared to the global effect. Importantly, the presence of this response will not imply the presence of global effects (conscious attention).

At a first stage, the study will focus on the additional stimulation modalities, i.e. the *local* and *global* effects in the unimodal conditions (hypotheses 1 and 2).

3.3 Methods

3.3.1 Cross-modal Local-Global

In contrast to the original paradigm presented in [Bekinschtein et al. 2009](#) in which the two different stimuli are presented as different tones, and in order to keep the conditions equal

across stimulation modalities, this new version of the stimulation paradigm uses laterality as the rule, as introduced in [Chennu et al. 2013](#). In other words, local standard trials presents all five stimuli either on the left or right sides, while local deviant trials presents the fifth stimulus on the opposite side to the first four. Side is chosen randomly with 50% chance each and timings between stimulus and trials were as in the original version. As described in 1.5.2 on page 18, two types of blocks are defined. In the XX blocks, the frequent trials (80% of trials) correspond to five ipsilateral stimuli (local standard and global standard [LSGS]). In contrast, the infrequent stimulus (20% of trials) corresponds to four ipsilateral stimuli followed by a fifth contralateral stimulus (local deviant and global deviant [LDGD]). In the XY blocks, the frequent and rare stimulus are reversed: four ipsilateral stimuli followed by a contralateral one defines the global regularity (local deviant and global standard [LDGS]) which is violated by five ipsilateral stimuli (local standard and global deviant [LSGD]).

In order to differentiate the effects of this paradigm from the previously described in 1.5.2 on page 18, we will define two main effects: the *Laterality Mismatch* and the *Rule Mismatch* effects. The *Laterality Mismatch* effect is quantified by contrasting the trials with a fifth contralateral stimuli (all local deviant trials; LDGS+LDGD) versus the trials with all ipsilateral stimuli (all local standard; LSGS+LSGD). The *Rule Mismatch* effect is quantified by contrasting the rare trials (all global deviant; LSGD+LDGD) versus the rare ones (all global standard; LSGS+LDGS).

In each recording (20 minutes), subjects were presented with these four conditions, twice for each block type (XX, XY, XX, XY). Each block started with 24 global standard trials to establish the regularity. Subjects were instructed to count the GD trials and asked to report this number after each stimulation block (4.5 minutes).

Stimulations were presented as sounds, vibrations or visual stimuli. Sounds were presented using insert earphones either to the left or right ears. Vibrations were generated by two Eccentric Rotating Mass motors attached to the wrists (one in each wrist) and controlled by two Texas Instruments DRV2605 haptic driver for independent behaviour. Visual stimuli was delivered using two independent 8x8 LED matrix placed within virtual reality goggles that isolated the left and right visual fields. All devices were controlled by an Arduino Zero microcontroller that executed the stimulation as previously described.

For each recording, two stimulation modalities were selected: one for the first four stimuli

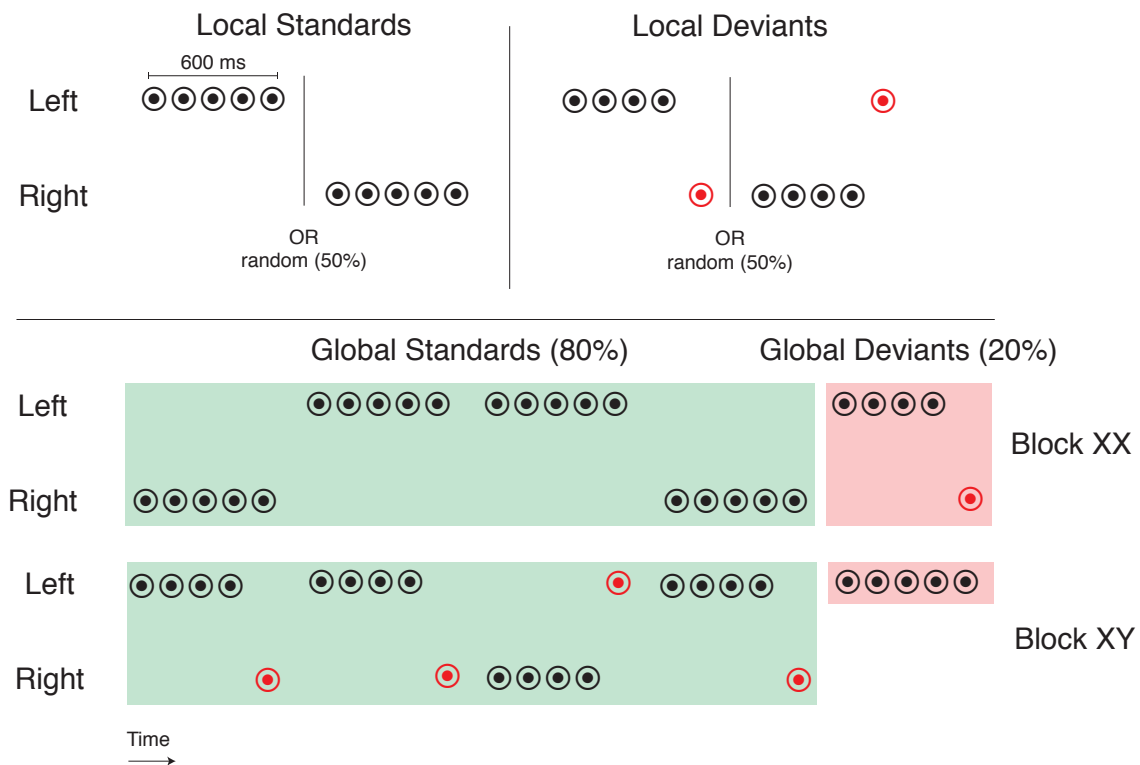
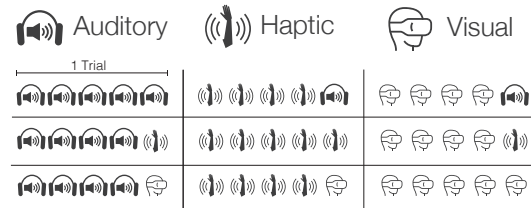


Figure 3.2: Illustration of the modification of the Local-Global paradigm that uses laterality as the difference between stimuli instead of modality-specific differences. Each trial is composed by 5 stimuli over a 600 ms interval as in the original paradigm (see 1.5 on page 19). The first four stimuli are delivered to the same side defining the local regularity. The fifth stimulus can be ipsilateral or contralateral, defining a local standard or deviant trial respectively. At the global (or across trial) level, the regularities are defined by frequent trials (80%, green shaded area) and violated by rare trials (20%, red shaded area). The choice of side for each trial is done pseudorandomly, keeping a balance of 50% for each side.

Figure 3.3: Illustration of the types of trials used in the Cross-modal Local-Global paradigm. Three different stimulation modalities were possible. For each recording, two modalities were selected, defining 9 types of recordings. The matrix illustrates all the possible combinations, with the trials corresponding to unimodal recordings in the diagonal.



of each trial, and the second for the last stimulus of each trial. Depending on the selection of the stimulation modalities, recordings were either *unimodal* (equal modalities) or *crossmodal* (different modalities). A total of 9 different types or recordings were possible (figure 3.3).

3.3.2 Subjects

A group of 44 right-handed healthy volunteers (35/9 female/male, mean \pm STD age is 25.20 ± 4.1) participated in the study. Inclusion criteria was set to individuals aged 18-80 with normal binaural hearing, no tactile or visual impairment and no history of neurological or psychiatric disease. Participants were recruited via the RISC system from the Centre Nationale de la Recherche Scientifique (CNRS) in France. Subjects gave written and consent to participate in the study and received a remuneration of €40. Each participant was subject to three recordings which shared the same stimulation modality for the last stimulus (one row of figure 3.3) during a one hour session.

3.3.3 EEG acquisition

Data were acquired using 256-channel high density EEG net and a Net Amps 300 amplifier developed by Electrical Geodesics. Data were preprocessed in Python using MNE-Python (Gramfort et al., 2013, 2014) and a self-developed python library. EEG data were filtered between 0.5 and 45Hz and epoched 200ms before and 1356ms after trial onset. Artefacts were rejected by visual inspection of all channels. Channels which did not record activity were excluded from further analysis and interpolated at a later stage. Artefacts originating from eye blinks, muscle movements and electrical interference were visually identified and removed using independent component analysis (Lee et al., 1999). Following the interpolation of missing channels, data were re-referenced to the average and baseline-corrected relative to a

200ms interval before the presentation of the last stimulus in the five-stimulus trial sequence. We then removed channels from the face and neck, retaining a total of 224 channels for further analysis.

3.3.4 Analysis

Evoked Responses (ERP) were computed by averaging all trials for each condition described in 3.3.1 on page 55. Additionally, to characterise the temporal dynamics of the observed effects, Time Generalisation decoding was performed as described in [King and Dehaene 2014](#).

Time Decoding consists of training a MVPA classifier to separate between the trials conditions using the values in each electrode as features and trials as samples. At each time point t , a linear SVM estimator is trained and tested using Stratified 5-Fold cross validation and the performance is measured using the ROC-AUC metric. The Time Generalisation decoding consists on testing each one of the previously described estimators at all the different times points. That is, train an estimator on time t and test the ability to classify trials at a different time point t' , so as to estimate whether the scalp pattern is similar between t and t' .

Similarity of patterns across stimulation modalities were tested using Time Generalisation with different training and testing conditions. That is, each estimator is trained to differentiate trials A from B when using a modality X , and its discrimination accuracy is evaluated on the same type of trials but with the stimulation modality Y . In this case, the results reveals the similarities between scalp patterns that are transferred from modality X to Y .

3.3.5 Group-Level analysis

In order to perform decoding at the group level, it is not enough to use the averaged epochs of each subject, as the amount of samples for the decoding will be equal to the number of subjects ($N \leq 15$). To overcome this issue, trials were averaged in groups (meta-epochs) of 10 epochs for each subject. Each group of epochs was randomly sampled 50 times, creating 50 different meta-epochs per subject. Decoding performance was estimated on each one of the meta-epochs sets.

3.3.6 Statistics

Evoked Responses (ERP) contrasts and Time Generalisation decodings were statistically tested using nonparametric permutation cluster test (Maris and Oostenveld, 2007). The statistical function was set to paired t-tests for the ERPs and independent samples t-test for the decoding. The clustering t-threshold was set equivalent to $p < 0.05$ for the give number of subjects or samples respectively.

3.4 Results

3.4.1 ERP analysis

We first analysed the Laterality Mismatch effect, by contrasting the trials with ipsilateral stimuli against the ones with contralateral stimuli. For the auditory modality, the time series differ with a central negative deflection around 100 ms, and a centro-posterior positive peak with a maximum at 200 ms after the onset of the 5th stimuli (Figure 3.4 on page 62 top). Somatosensory contralateral stimuli, on the other hand, depicted an earlier frontal negative deflection (50ms to 150 ms after the onset of the 5th stimuli) and longer central positivity with a maximum around 300 ms after the onset (Figure 3.4 middle). For the visual modality, a negative deflection was detected from 50ms to 200ms after the onset of the 5th stimuli and a positive centro-posterior positive activation from 200ms to 400ms after the onset of the 5th stimuli (Figure 3.4 bottom). Nonparametric permutation cluster test indicated that 2 of the 3 contrasts were significantly different with $p = 0.0002$ for the auditory modality, $p = 0.06$ for the somatosensory modality and $p = 0.01$ for the visual modality.

Correspondingly, we performed the same analysis on the Rule Mismatch effect, by contrasting the frequent and rare trials. For the auditory stimulation, the contrast depicted a long-lasting posterior positivity starting 300ms after the onset of the 5th sound, till the end of the trial (Figure 3.5 on page 63 top). The somatosensory modality presented the same long lasting positivity, with an additional early frontal positivity around 200-250ms, which presents the characteristics of time-locked eye blinks (Figure 3.5 on page 63 middle). Finally, the visual modality presented the posterior positivity starting 400 ms after the onset of the 5th sound, and an additional frontal positivity from 0 to 300ms, also consistent with the pattern of

eye-blinks (Figure 3.5 on page 63 center). Nonparametric permutation cluster test indicated that the 3 contrasts were significantly different with $p = 0.0002$ for the auditory modality, $p = 0.0012$ for the somatosensory modality and $p = 0.0006$ for the visual modality.

3.4.2 ERP characterisation through MVPA

As a first step, we characterised the spatiotemporal patterns of the laterality and rule mismatches for each one of the stimulation modalities. Using Time Decoding, we found that Laterality Mismatches presented short patterns between 175ms to 250ms after the onset of the stimuli when stimulated with sounds, from 100ms to 375ms when stimulated with vibrations and from 200ms to 400ms when stimulated visually (Figure 3.6 on page 64) left). For the Rule Mismatches, the patterns appeared later and were more sustained in time. From 250ms to 600ms for auditory stimulation, 350 to 700 ms for somatosensory stimulation and 400ms to 700ms for visual stimulation.

To compare the spatiotemporal patterns, we applied the Time Generalisation decoding using different training and testing modalities. When we tested the Laterality Mismatches, we found a decrease in the decoding accuracy to almost the chance level (Figure 3.7 on page 65). That is, spatial patterns that separate with high AUC the ipsilateral and contralateral trials differ across modalities. In contrast, for the Rule Mismatches, the spatiotemporal patterns of the decoding accuracy are preserved, with some temporal shifts (Figure 3.8 on page 66).

3.5 Discussion

In this chapter, we aimed at analysing the viability of creating a multisensory Local-Global test with the objective of increasing its sensitivity while providing an alternative for auditory impaired patients. We proposed a novel stimulation paradigm in which stimuli is presented with sounds, vibrations and lights, while keeping the two-level oddball structure of the original Local-Global paradigm. We then analysed the neural responses to the effects for each oddball level as measured on healthy controls. We found that the effect of the Laterality Mismatch (short-term within trial mismatch) presented distinct spatiotemporal patterns across stimulation modalities. On the other hand, the Rule Mismatch effect (across-trial mismatch) were similar and shared spatiotemporal patterns across the three stimulation modalities.

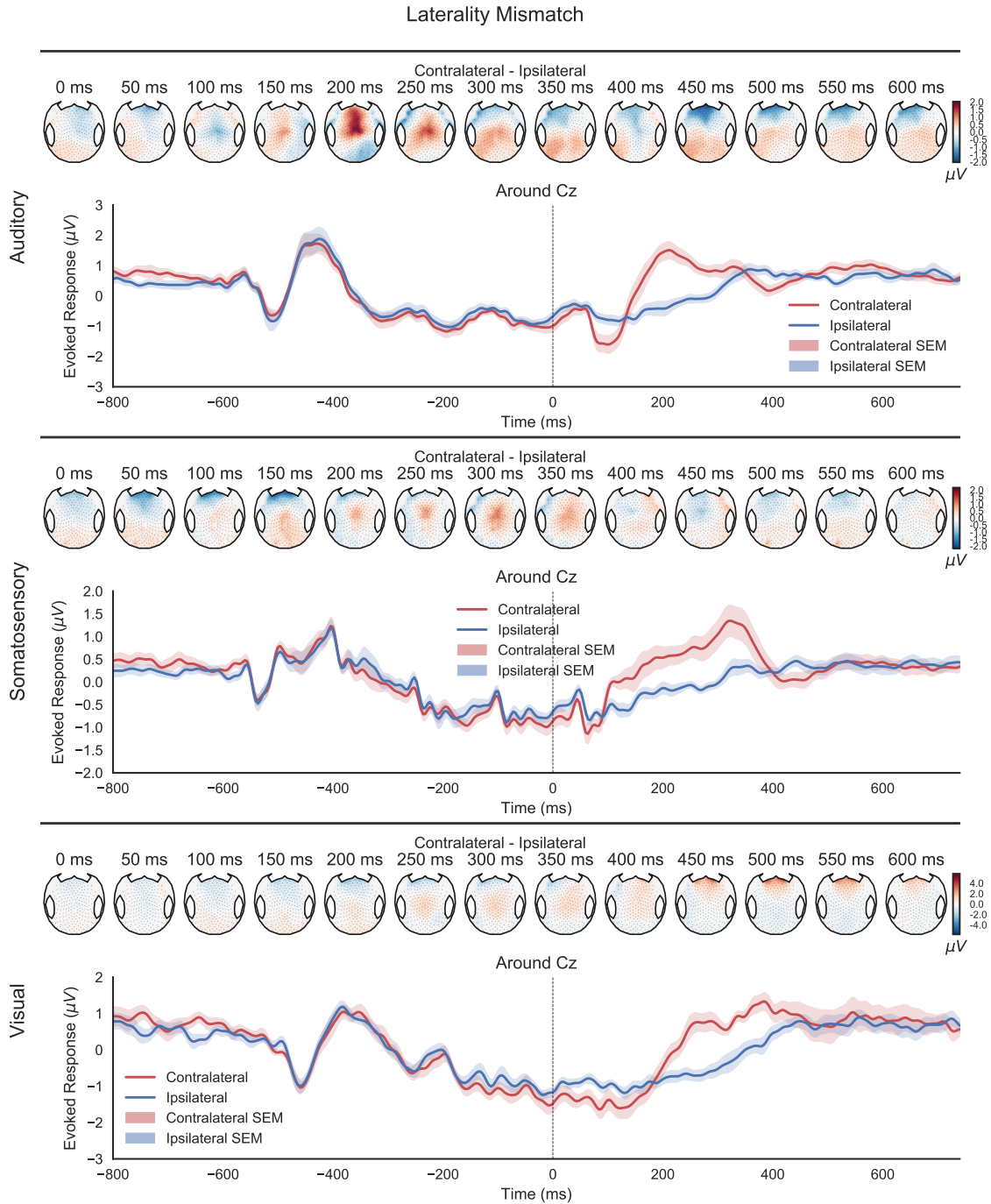


Figure 3.4: Topographies and ROI plots for the Laterality Mismatches comparing ipsilateral and contralateral stimuli for auditory (top), somatosensory (middle) and visual (bottom) modalities. Topographies depict the values of the contrast (subtraction) between conditions for the 224 scalp electrodes. Time series represents the average values around Cz for each condition. The $t = 0$ for the x-axis corresponds to the onset of the 5th stimuli.

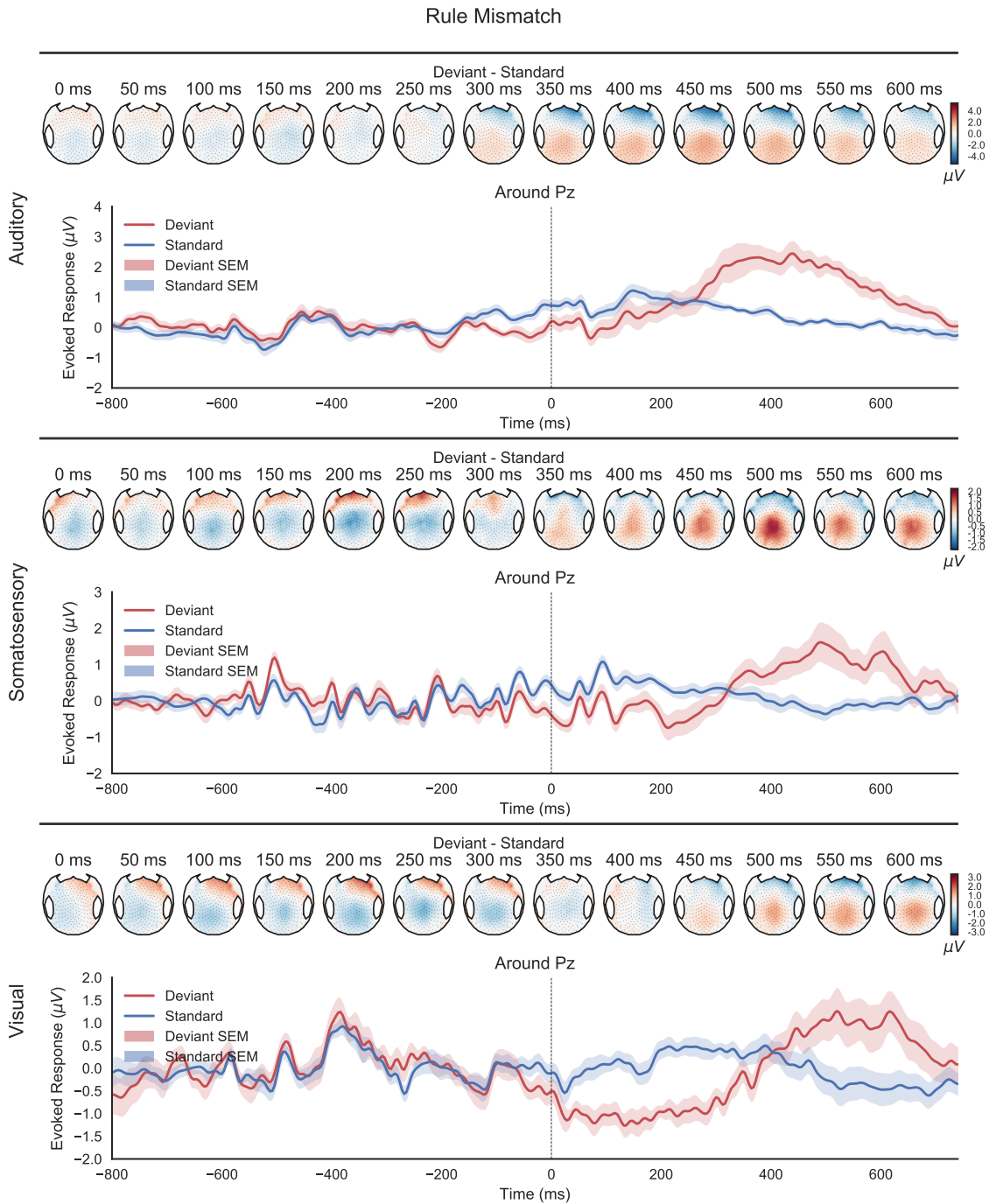


Figure 3.5: Topographies and ROI plots for the Rule Mismatches comparing standard and deviant stimuli for auditory (top), somatosensory (middle) and visual (bottom) modalities. Topographies depict the values of the contrast (subtraction) between conditions for the 224 scalp electrodes. Time series represents the average values around Pz for each condition. The $t = 0$ for the x-axis corresponds to the onset of the 5th stimuli

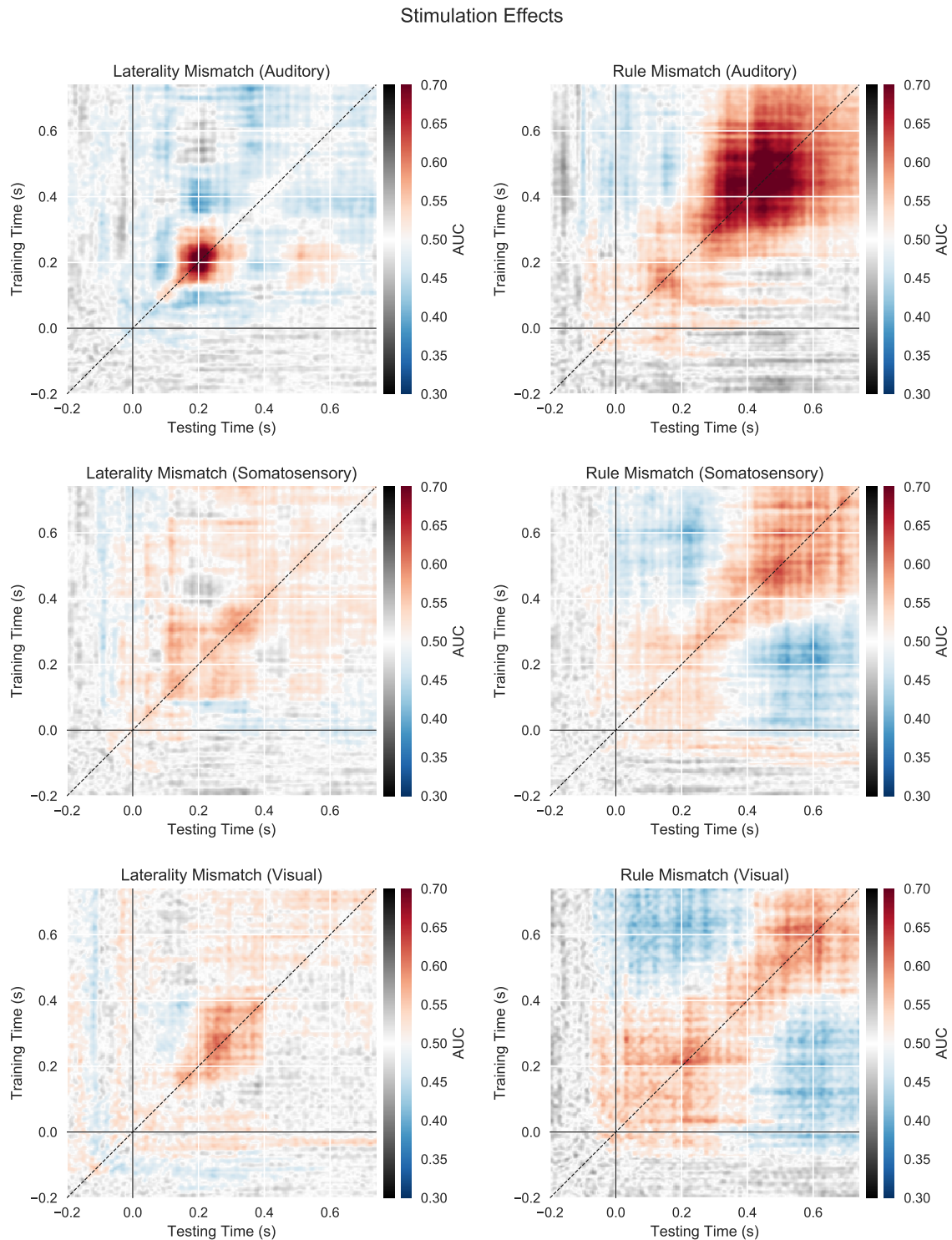


Figure 3.6: While Laterality Mismatch decoding patterns differ across stimulation modalities, Rule Mismatch decoding patterns do not present differences. Each one of the 6 images depicts the decoding AUC for each training and testing time. Decoding patterns of Laterality Mismatch (left) present a significant high AUC between 100ms and 400ms after the onset of the stimuli with some differences between auditory (top), somatosensory (middle) and visual (bottom) stimulation modalities. In contrast, Rule Mismatches (right) present later and

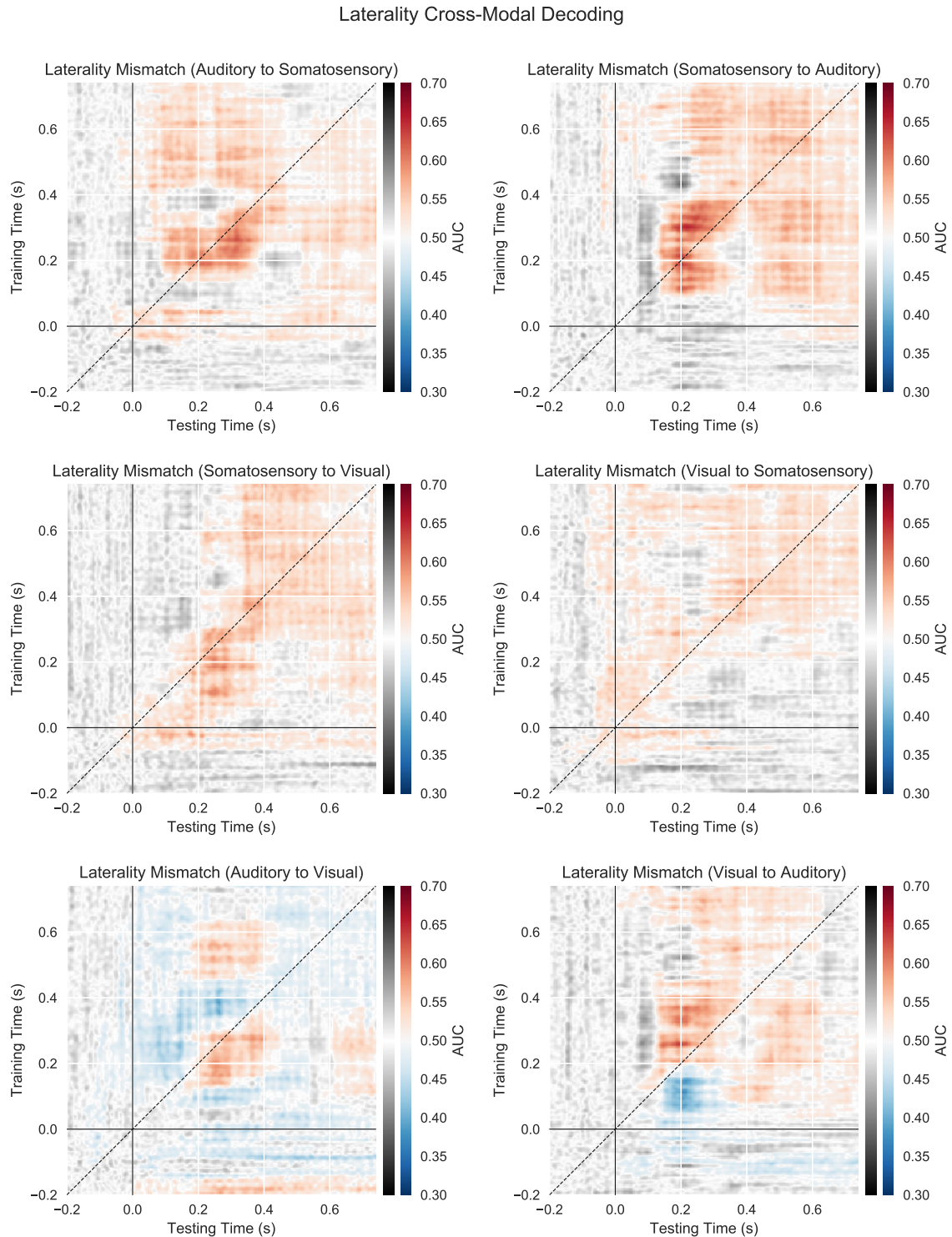


Figure 3.7: Spatiotemporal patterns of neural activity in response to Laterality Mismatches are not transferable across stimulation modalities. Each row of images depict the decoding AUC when training and testing using different pairs of modalities. Significant clusters ($p < 0.05$) are depicted in colour.

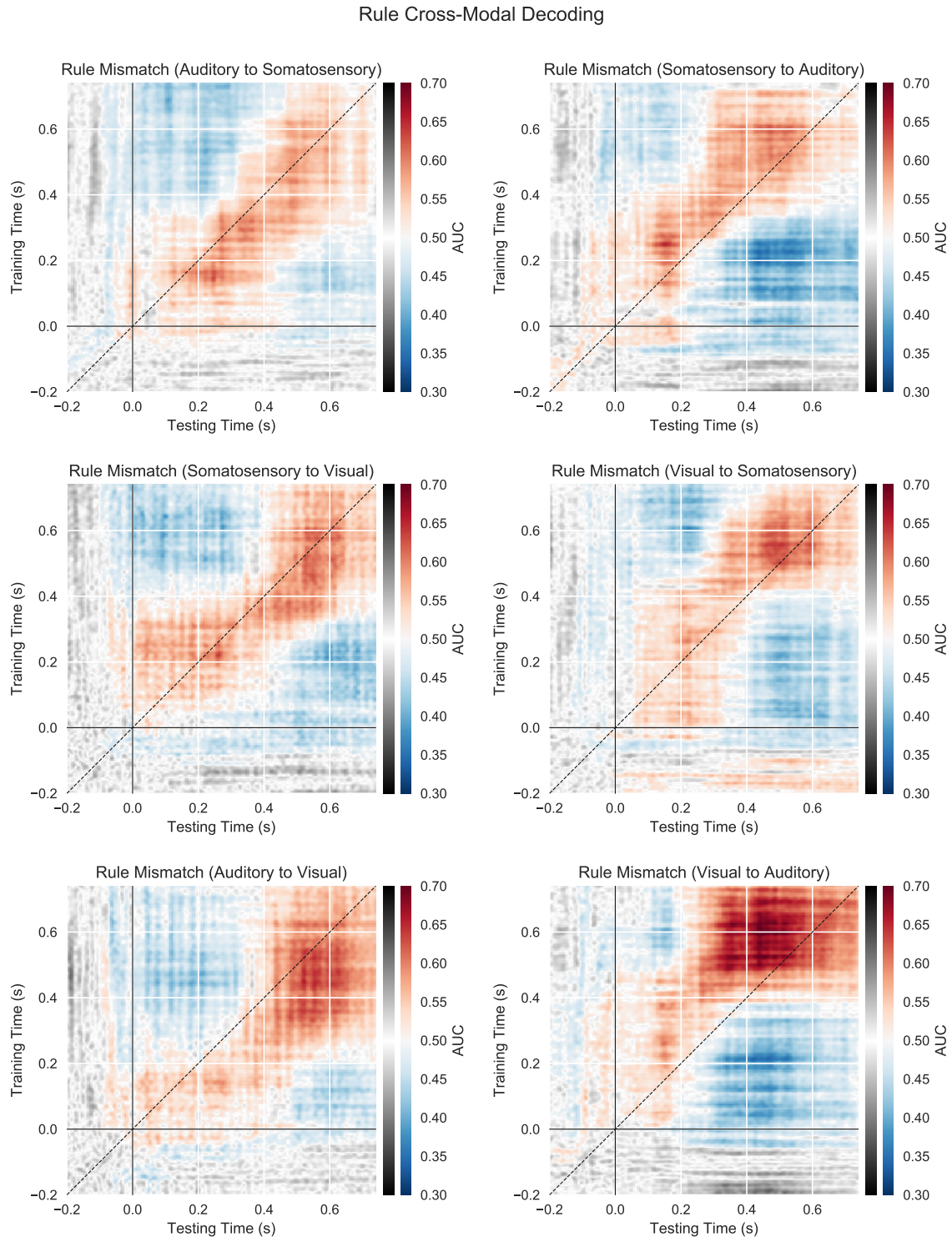


Figure 3.8: Spatiotemporal patterns of neural activity in response to Rule Mismatches are similar across stimulation modalities, with specific temporal shifts. Each row of images depict the decoding AUC when training and testing using different pairs of modalities. Significant clusters ($p < 0.05$) are depicted in colour.

Our results are consistent with previous reports on ERPs. Despite the fact that the original auditory Local-Global used tones as a varying factor instead of laterality, the obtained results with auditory stimulation are consistent with [Bekinschtein et al. 2009](#), [Chennu et al. 2013](#) (classic ERP analysis) and [King et al. 2014](#) (Time Generalisation decoding). Regarding visual ERPs, we also found later responses to stimuli when compared to auditory responses, as reported in [Giard and Peronnet 2006](#); [Talsma and Woldorff 2005](#); [Teder-Sälejärvi et al. 2002](#).

The Time Generalisation decoding across modalities depicted distinct spatiotemporal patterns for the Laterality Mismatch effect. This can be explained by the fact that the different responses are generated by the sensory-specific cortices, resulting in modality-specific components, as described in [Giard and Peronnet 2006](#).

On the other hand, the Time Generalisation decoding across modalities did not show differences for the Rule Mismatch effect, besides the delay in the visual response. This results can be attributed to the fact that the obtained response, a P3b potential, reflects higher-order violation of the subjects expectation, which are not directly linked to the stimulation modality and the sensory pathways, but to the task being performed. This results are coherent with previous work on the P3b component, which associates the P3b to working memory ([Goldstein et al., 2002](#); [Polich, 2007](#)) and conscious access ([Dehaene et al., 2006](#)).

Taken together, this preliminary results suggest that at a first step, the sensory-specific cortical areas are activated, while the task is then resolved in a common manner, independently of the modalities involved. This results settles the basis for the study of cross-modal interactions in relation to states of consciousness. Future work applied under different states of consciousness is needed to determine whether somatosensory and visual Laterality Mismatches responses are also nonconscious as the auditory Local Effect ([Faugeras et al., 2012](#); [Bekinschtein et al., 2009](#)). Interestingly, this paradigm also contemplates using more than one modality in order to perform the task. This raises the questions on how and when is the information of these two modalities merged, and how this processing is affected by the different states of consciousness.

All in all, we believe that these results settles the bases for a deeper study with scientific and clinical implications. Scientifically, it paves the way for the study of the relation between multisensory integration and consciousness. Clinically, it is a start in the development of novel clinical tool which can help overcome the limitations of the current auditory Local-

Global paradigm when applied to auditory impaired patients ([Rohaut et al., 2017](#)).

Chapter 4

Brain-Body interactions as a diagnostic marker for DOC

The work described in this chapter has been published as “Brain–heart interactions reveal consciousness in noncommunicating patients”. Raimondo F, Rohaut B., Demertzi A., Valente M., Engemann DA., Salti M., Fernandez Slezak D., Naccache L., Sitt JD. Annals of Neurology, Volume 82, Issue 4, October 2017.

Contents

4.1	Background	70
4.2	Hypotheses	71
4.3	Baseline cardiac activity	72
4.3.1	Methods	72
4.3.2	Results	75
4.4	Cardiac markers of cognitive processing	78
4.4.1	Methods	78
4.4.2	Results	82
4.5	EEG and EKG Multivariate Pattern Analysis	82
4.5.1	Methods	82
4.5.2	Results	84
4.6	Discussion	86

4.1 Background

A common aspect of the assisting technologies currently used to evaluate DOC patients is that all of them adapted a strict neuro-centric approach. However, classic (Critchley et al., 2001; Craig, 2002) and more recent studies (Critchley et al., 2001; Gray et al., 2007; Park et al., 2014; Seth et al., 2012; Park and Tallon-Baudry, 2014) in healthy subjects demonstrate that brain modulation of peripheral body functions are affected by concomitant cognitive processes. This evidence make the ‘brain-body’ interaction a relevant and promising space to evaluate consciousness level in patients. Cardiac activity is one of such peripheral body signals that has been linked to cognitive processes. For example, ‘bradycardia of attention’ refers to the effect of heartbeat frequency deceleration when the subject is engaged in an active cognitive task (such as target detection or auditory odd-ball counting) (Lacey and Lacey, 1978). Depending on the stimulation inter-trial interval, this cardiac cycle slowing is reversed when, or after, the target is detected (Van Der Molen et al., 1983; Jennings and Wood, 1977). More recently, it was also shown that by quantifying the neural events locked to heartbeats, one could predict whether a subject would report a fast flashing visual stimulus as perceived or not (Park et al., 2014). In addition, during complex cognitive processing, such as when playing chess, the heartrate dynamics, as measured before players made a move, could predict the likelihood of them eventually committing an error (Leone et al., 2012). Heartbeat-evoked cortical responses were further shown to differ in auditory interoceptive learning tasks (Canales-Johnson et al., 2015). Taken together, these studies suggest a bi-directional interaction between brain and heart that can be modulated by cognitive processes.

As regards patients with DOC, previous work has shown that cardiac autonomic markers, such as Heart Rate (HR) and Heart Rate Variability (HRV), were markers of autonomic system malfunction (dysautonomia) in traumatic brain injuries (Baguley et al., 1999). Specifically, patients with low scores on the Glasgow Coma Scale had altered autonomic functions including tachycardia and low HRV (Baguley et al., 2006). More recently, the same markers have been used to differentiate between VS/UWS and MCS when patients’ cardiac activity was recorded during sleep or after noxious stimulation (Leo et al., 2016). However, the link between these autonomic markers and conscious stimuli processing in DOC patients remains unknown.

In this chapter, we aimed at (1) evaluating if the heart-brain interactions could characterise the state-of-consciousness of DOC patients and (2) determining if the EKG-extracted information could complement the EEG evaluations of the patients. For the first objective, we quantified the modulation of cardiac cycle during the Local-Global paradigm ([Bekinschtein et al., 2009](#)) (see 1.5.2 on page 18). For the second objective, we contrasted the performance of multivariate patient classification of the state-of-consciousness at the single patient level using either only the EEG markers or using the combination of EEG and cardiac cycle modulation markers.

4.2 Hypotheses

We hereby defined two working hypotheses:

1. Patients overall cardiac activity (HR and HRV) will be as described in previous works ([Leo et al., 2016](#)).
2. Markers of cardiac modulation by cognitive function, tested with the Local Global paradigm (see 1.5.2 on page 18), are expected to be present under the same conditions as the neural responses measured with the EEG. That is, the local effect should not discriminate between the patients group ([Faugeras et al., 2011](#)) and the global effect should be present only in patients with preserved levels of consciousness ([Faugeras et al., 2012](#); [King et al., 2013a](#)).

Additionally, in order to test whether EKG has additional information to the EEG, we will test if the combination of EEG and EKG-extracted features modifies the accuracy of an automatic diagnosis by machine learning. If the accuracy is higher, this will mean that the EKG-extracted information is partially independent and complements the EEG-extracted information.

4.3 Baseline cardiac activity

4.3.1 Methods

Subjects and Patients Patients admitted for consciousness evaluation at the Neurological Department of the Pitié-Salpêtrière Hospital, Paris between February 2008 and April 2015 were included. The neurological evaluation of the patients' disorders of consciousness was performed by trained clinicians using the Coma Recovery Scale–Revised (CRS-R) as described in 1.5.1. Behavioural evaluations were performed systematically before each EEG recording.

In the present chapter, we aimed at characterising the cardiac cycle in relation to the state of consciousness as a post-hoc analysis. Since no EKG was available during the EEG evaluations, EKG time series were obtained using independent component analysis (ICA) on the EEG recordings for each patient. The current analysis only used the temporal location of the R wave peaks.

From the 259 patients originally assessed with EEG (130 VS/UWS, 129 MCS), 132 patients (51%; 60 VS/UWS, 72 MCS) were rejected due to the lack of a clear EEG recording or EKG reconstructed source that produced at least 40 samples for each stimulation block type. There were no differences between the included and excluded patients in terms of diagnostic state ($\chi^2[1, n = 259] = 2.07, p = 0.15$) and sex ($\chi^2[1, n = 259] = 0.21, p = 0.64$). Included patients were older than excluded patients (48 ± 18 vs 44 ± 17 years; $W = 6701, p = 0.04$), and more patients suffered from anoxic as compared to traumatic injuries in the included group compared to the excluded group ($\chi^2[4, n = 259] = 12.84, p = 0.01$).

A final cohort of 127 (49%) patients remained: 70 VS/UWS (20 females, mean age = 45 ± 19 years, range 17 – 80, 12 traumatic, 21 assessed in a chronic setting [ie, >2 months postinsult]), and 57 MCS (17 females, mean age = 52 ± 16 years, range 21 – 79, 13 traumatic, 17 assessed in a chronic setting). Patient groups did not differ in terms of gender ($\chi^2[1, n = 127] = 6.2e^{-31}, p = 1$), etiologies ($\chi^2[4, n = 127] = 9.4, p = 0.051$), and chronicity ($\chi^2[1, n = 127] = 2e^{-30}, p = 1$). MCS patients were older than VS/UWS patients (52 ± 16 vs 45 ± 19 ; $W = 2435, p = 0.03$). No patient had any history of cervical spinal cord injury or symptoms of autonomic dysfunction (eg, hemodynamic instability, abnormal HRV) at the time of EEG recording.

EKG Extraction from EEG In the absence of direct recordings of cardiac activity, EKG was extracted from the EEG using Independent Component Analysis. The independent components (IC) corresponding to the EKG were selected by visual inspection based on the spatial and temporal representation of the QRS complex. Raw EEG data was first filtered using an 8th order low-pass Butterworth filter at 45Hz and a 4th order high-pass filter at 0.5Hz (Figure 4.1 on the following page; top). Secondly, we computed three different ICA decompositions:

1. FastICA ([Hyvärinen and Oja, 2000](#)) parametrised to obtain the components that explain 99% of the variance and computed from raw filtered data.
2. INFOMAX ([Bell and Sejnowski, 1995](#); [Lee et al., 1999](#)) parametrised to obtain 256 components from raw filtered data and
3. INFOMAX in combination to artifact channels rejection. Individual channels were removed when the temporal variance was more than 3 standard deviations away from the mean of the variance of the rest of the channels.

The independent component with the EKG information was selected based on the time series and the weights' topographies by visual inspection (Figure 4.1 on the next page; bottom). The selected time series had to clearly contain the R-peak corresponding to the QRS complex. The R-peak had to be easily detected by using a simple threshold. The corresponding topography had to concentrate the mixing weights on the frontal right and posterior left electrodes. These electrodes are located in the right cheek, left maxillary junction and underneath the left mastoid, as depicted by previous studies on cardiac electrical fields ([Dirlich et al., 1997](#)).

We then picked the algorithm that presented the clearest decomposition, usually the one with the highest rank in descending order of explained variance. Finally, R-peaks onsets were obtained automatically by the algorithm described in [Elgendi 2013](#). Subjects for which the EKG component was unclear were excluded from the analysis. Exclusion criteria was set to any of: EKG reconstructed signal with no clear R-peaks, detection failure by the automatic algorithm, or a topography of corresponding weights with a mix of peripheral and central electrodes.

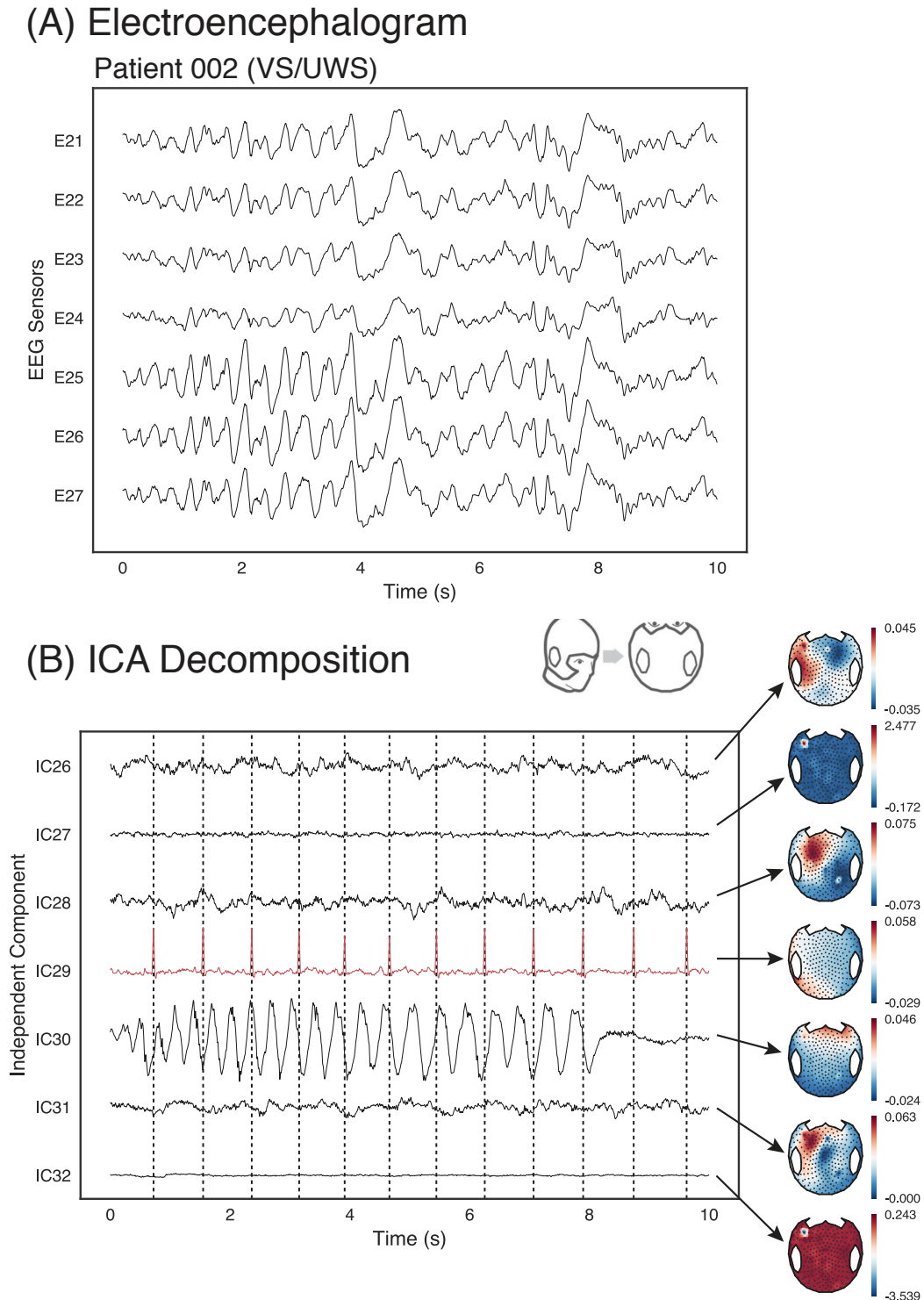


Figure 4.1: (A) Filtered EEG time series from 7 EEG sensors from one VS/UWS patient. (B) Corresponding time series of 7 ICA components extracted from the previous EEG recording and the respective weights to topographies. The independent component with cardiac information is shown in red. Dotted lines represents the automatically detected R-peak.

Baseline cardiac activity The overall heart rate (HR) was computed by averaging the differences between consecutive R-peaks (RR Intervals) during the whole recording. Following the method described in [Deboer et al. 1984](#), heart rate variability (HRV) spectral variables were obtained by computing the power spectrum decomposition on the point events time series from the detected R-peaks. Power Spectral Density was estimated in whole recording using Welch's method with 32768 samples (131.072s) per segment and 28672 samples (114.688s) overlap using a Hanning window. HRV variables were extracted from the sum of the spectral power in three frequency bands: 1) very low frequencies (VLF, range 0–0.04Hz), 2) low frequencies (LF, range 0.04–0.15Hz) and 3) high frequencies (HF, range 0.15–0.4Hz).

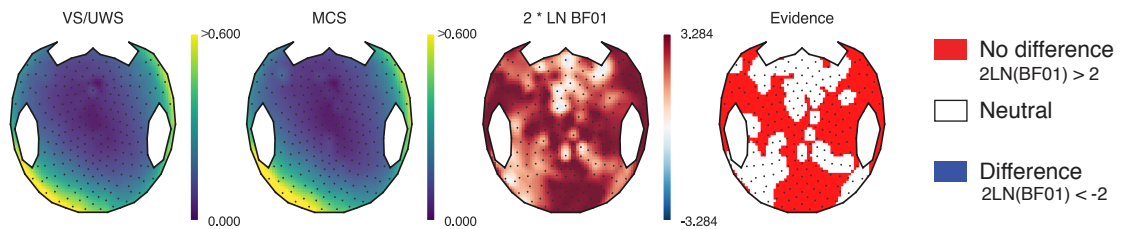
R-peak locked EEG evoked responses EEG recordings were filtered as previously described, segmented from -200ms to 600ms relative to the onset of the R-peak and baseline corrected using the 200ms long window before R-peak. Bad channels and trials were rejected based on peak to peak amplitude exceeding $100\mu V$. Bad channels were interpolated. The remaining trials were averaged. We performed a group analysis and obtained the mean evoked response for each group, and contrasted the VS/UWS mean evoked activity to the MCS one. Statistics on EEG responses were done using non-parametric cluster corrected permutation test ([Maris and Oostenveld, 2007](#)).

4.3.2 Results

EKG extraction method validation To test the homogeneity of the EKG-related ICA decompositions between groups, we computed the mean IC weights across subjects for the selected components. A sensor-wise Bayesian t-test showed evidence for no difference in the weights between the MCS and VS/UWS groups (Figure 4.2 on the following page; top). We then averaged the cardiac cycle locked to the QRS complex at the group level and the contrasted the obtained time series between clinical groups (Figure 4.2; bottom). A single channel cluster permutation test found only one significant difference ($p = 0.017$) between 184 and 344 ms after the R-peak, consistent with the location of the T wave. No difference was found in the QRS complex.

Finally, we aimed at ensuring that the results obtained in terms of cardiac cycle induced by the processing of the auditory stimulation paradigm were not a side-effect of the EKG

(A) Group IC Topographies



(B) Group EKG

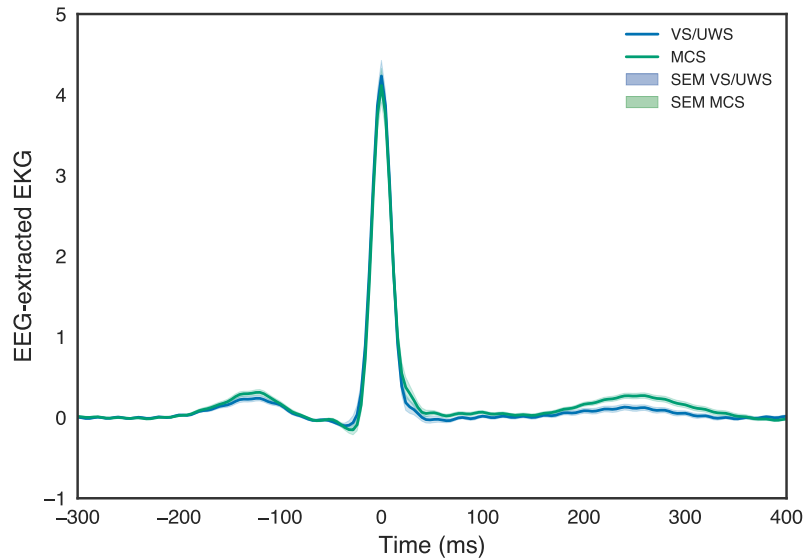


Figure 4.2: (A) Mean weights topographies for each clinical group (left). A sensor-wise Bayesian t -test shows evidence for no difference in the topographies between groups (right). (B) Mean and standard error of the mean for each clinical group QRS complex from the ICA-extracted EKG. A single channel cluster permutation test indicated significant differences ($p = 0.017$) only between 184 and 344ms after the R-peak, consistent with the location of the T wave.

extraction methodology. In other words, we focused on testing that EEG-ICA extraction methodology was not injecting relevant EEG related activity to the EKG extracted signal. For this objective, we compared pure EKG to EEG extracted EKG. We performed simultaneous EEG-EKG recordings in an independent group of 24 healthy subjects and 32 patients (14 VS/UWS, 18 MCS). We applied the same EKG extraction method previously described and obtained 12 (50%) healthy subjects and 12 (37.5%; 3 VS/UWS; 9 MCS) patients with both direct EKG and indirect EEG-extracted EKG. We contrasted the two corresponding EKG time series in each trial, by subtracting the timing of the R-peaks in the direct EKG signal from EEG-extracted signal (Figure 4.3). A repeated measures Bayesian ANOVA was computed using the REKG-REEG time differences as the study variable; trial types (LSGS, LDGD, LDGS and LSGD) and clinical state as factors. All the models including the trial type as a factor presented positive evidence in favour of no difference ($BF_{01} \geq 4.27$). Furthermore, the model that tested the interaction between clinical state and trial type presented even stronger evidence of no difference ($BF_{01} \geq 15$). Given that the only information used in this study was the timing of the R-peaks (automatically extracted and analysed within subjects), the here presented validation results strongly suggest that no effect was induced by the adopted EKG extraction methodology.

Heart Rate and Heart Rate Variability Overall Heart Rate was similar in patients across the two diagnostic groups ($BF_{10} = 0.73$; Figure 4.4 on the facing page A). When patients with overlapping behavioural CRS-R scores (CRS-R=6 or 7; 10 MCS; 20 VS/UWS) were excluded from the analysis to match the population in previous works (Leo et al., 2016) there was evidence for faster heart frequencies in the VS/UWS group ($BF_{10} = 8.80$). In the VS/UWS group, a positive correlation was identified between the HR and the CRS-R scores ($\rho = 0.27, p = 0.02$). No such correlation was found for the MCS patients. Similarly, HRV markers were comparable in both diagnostic groups (Figures 4.4 on the next page B-D), HRV high frequencies $BF_{10} = 0.62$; HRV low frequencies $BF_{10} = 0.36$, HRV very low frequencies $BF_{10} = 0.21$). In the VS/UWS group a positive correlation was identified between the CRS-R and the HRV markers in high frequencies ($\rho = 0.40, p = 0.0007$) and in low frequencies ($\rho = 0.27, p = 0.02$). No such correlations were identified for the MCS group in either frequency.

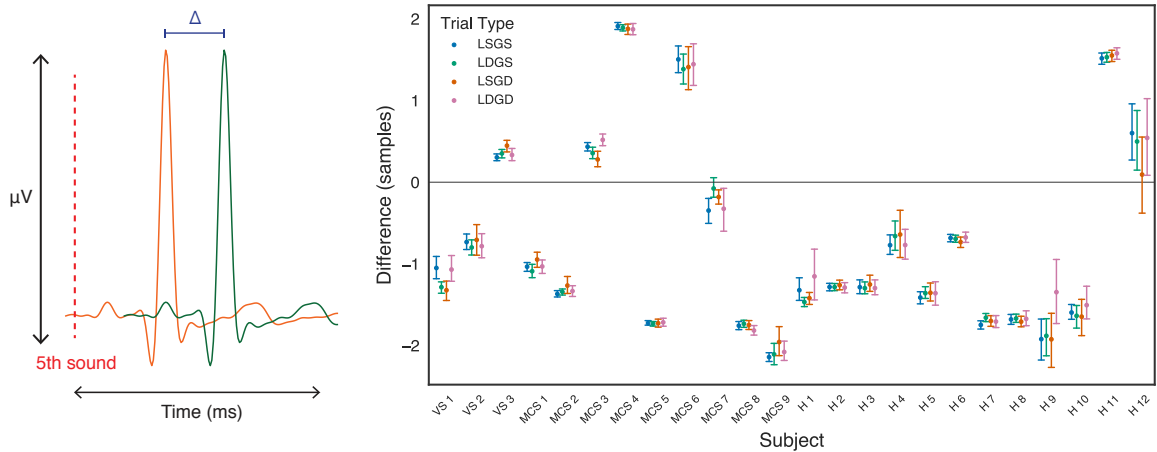


Figure 4.3: EKG and ECG extraction methods comparison. We evaluated two independent groups of healthy controls ($n=12$) and patients ($n=12$) using simultaneous EEG and EKG recordings. For each subject, EKG was also extracted using the described ICA method. We then computed the differences between each R-peak onset detected in the direct EKG and the corresponding R-peak detected using ICA (left). Right panel shows the mean difference and 95% CI for each type of trial and subject as measured in samples (1 sample = 4 ms). Using Bayesian ANOVA, we found no evidence for a difference as an effect of the trial type ($BF_{01} \geq 4.27$) and strong evidence for no difference for the interaction between the type of trial and the clinical state ($BF_{01} \geq 15$)

R-peak locked EEG evoked responses In terms of evoked responses to the cardiac activity as measured by EEG, a sharp peripheral bipolar topography was observed at the R-peak for both clinical groups (Figure 4.5 A and B). Between 0 and 250ms after the R-peak, both groups presented topographies following the pattern of the cardiac field artifact (CFA; Dirlich et al. (1997)). A cluster-level permutation test revealed a single significant cluster ($p = 0.034$; Figure 4.5 on page 80 C) located between 144 and 540ms after the R-peak, with two spatial patterns, one similar to the CFA associated to the T-wave between 144 and 340ms, and second central spatial pattern after 340ms.

4.4 Cardiac markers of cognitive processing

4.4.1 Methods

To evaluate potential phase shifts in the cardiac cycle associated to the processing of different types of auditory stimuli, two intervals temporally locked to the onset of the fifth sound were

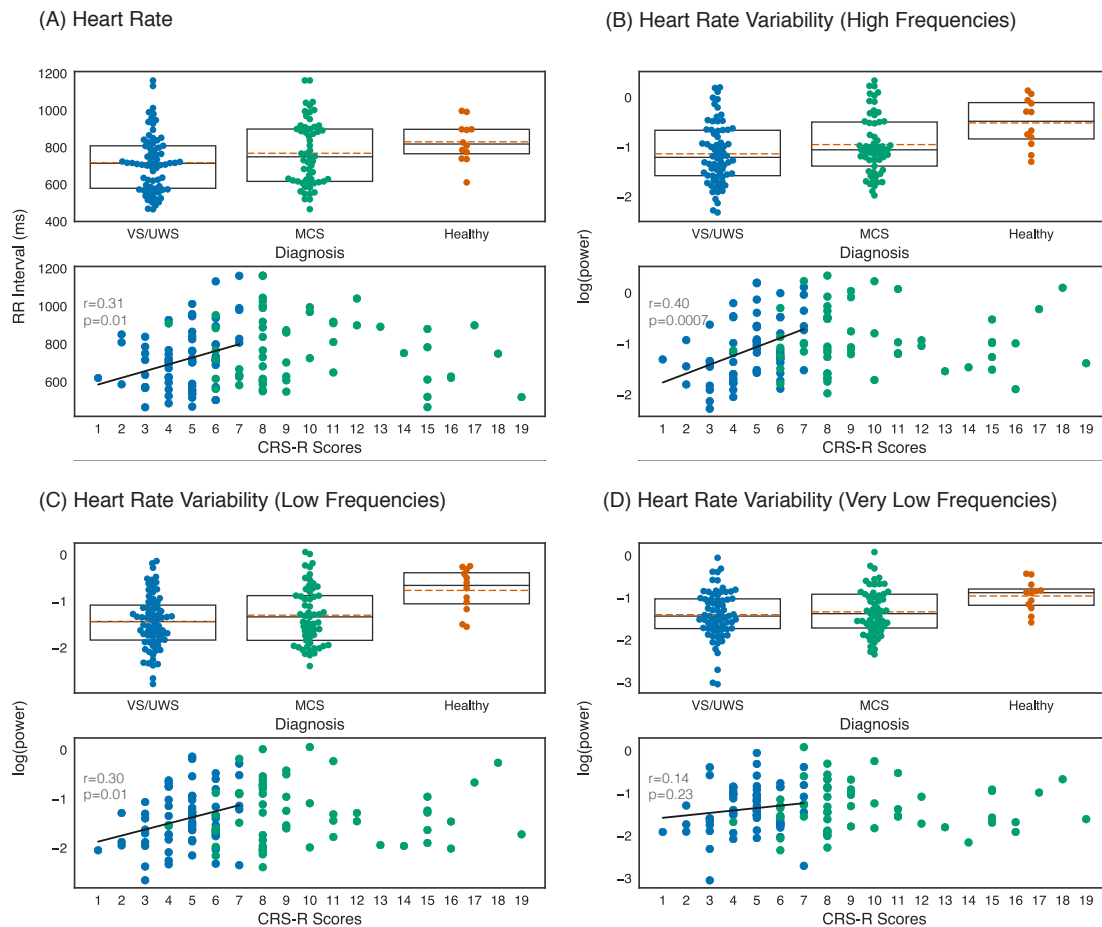
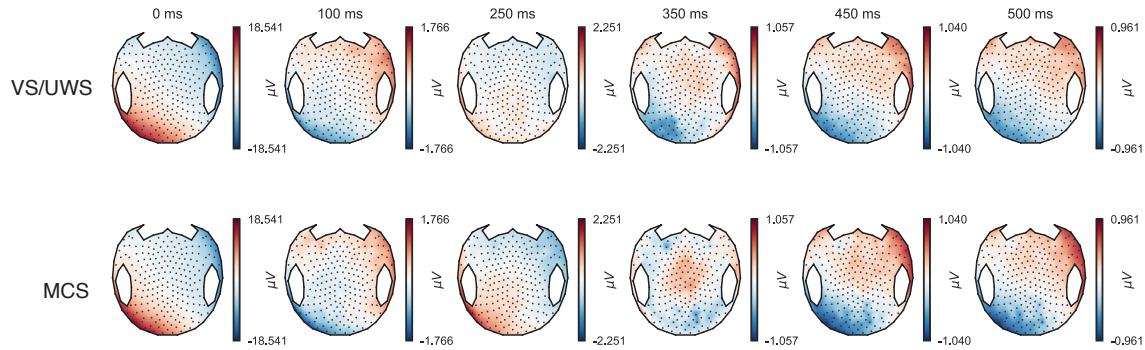
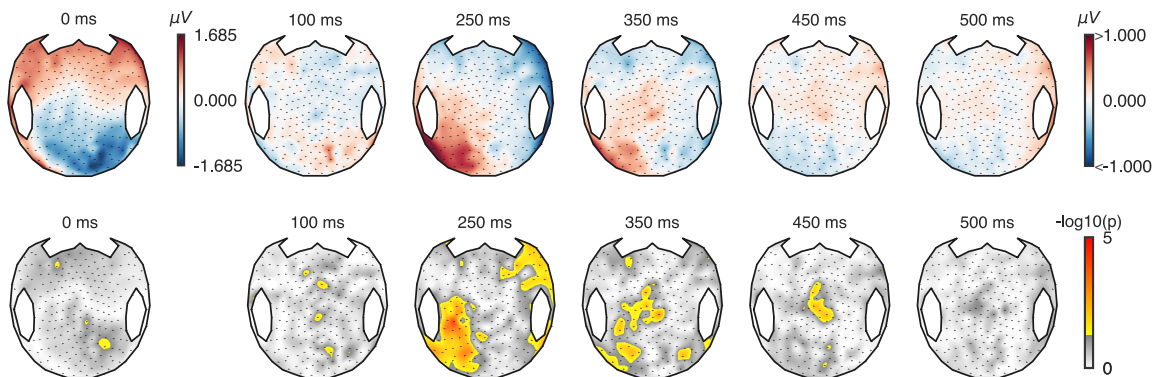


Figure 4.4: Cardiac autonomic markers show no difference between clinical groups. Lower CRS-R scores in VS/UWS patients correlates with a faster and less variable cardiac cycle as a manifestation of the overall deterioration of the clinical condition. Each panel depicts the cardiac marker values (y-axis, Heart rate (A), Heart rate variability in high frequencies (B), in low frequencies (C), and in very low frequencies (D)) for each patient (dot), categorised by clinical group (top, 70 VS/UWS, 57 MCS, 12 Healthy) and by Coma Recovery Scale-Revised scores (CRS-R, bottom - only for patients). The Spearman's regression line between the scores and the EKG-related markers for the VS/UWS patients, indicates a significant positive correlation between the CRS-R score and RR interval (A), Heart Rate Variability in high frequencies (B), and in low frequencies (C). Boxplots with interquartile range, median (black line) and mean (dashed line) represent the distribution of data in both clinical groups.

(A) R-Peak locked Evoked Responses



(B) MCS - VS/UWS Contrast



(C) Cluster analysis

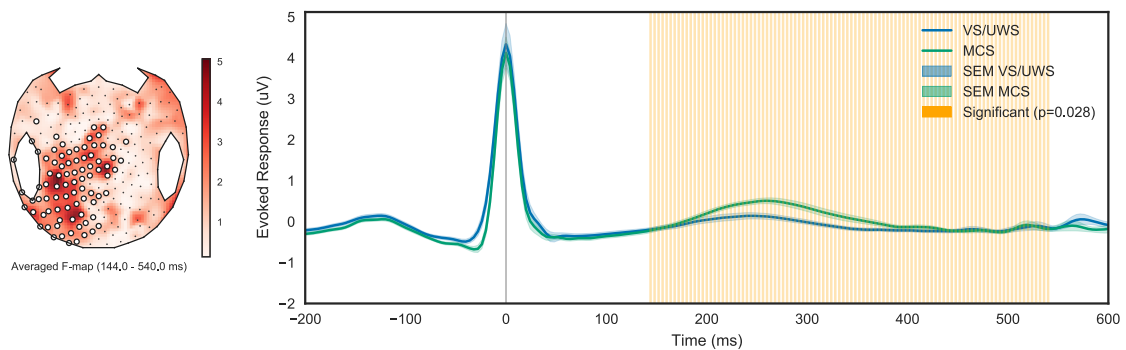


Figure 4.5: R-peak locked EEG evoked responses shows differences between clinical groups. (A) Mean EEG topographies for each clinical group time locked to the R-peak at 0, 100, 250, 350, 450 and 500 ms. (B) Contrast and statistical comparison of the R-peak evoked potentials between clinical groups. (C) The left panel shows the only significant cluster of a permutation analysis ($p = 0.034$), the electrodes composing the cluster are shown with white circles (left). The right panel shows the time series of the corresponding cluster (mean and standard deviation across subjects). Two main modulations are observed, (1) in the time window corresponding to the T wave, a left-posterior positivity and a right-frontal negativity; and, (2) a central electrode spatial pattern positivity after the T-wave (>350ms), suggesting differences in the brain processing of the heart activity between VS/UWS and MCS patients.

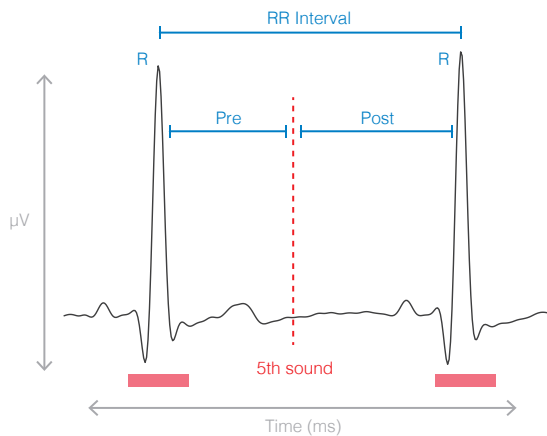


Figure 4.6: Two consecutive EKG QRS complexes defined an RR interval. Overall heart rate was computed from the robust average of the RR intervals. Conscious response to the stimulation was analysed based on the definition of two intervals: (1) the PRE interval, measured between the R-peak previous to the 5th sound and the onset of that sound and (2) the POST interval, measured between the onset of the 5th sound and the following R-peak. In order to avoid coupling with the heartbeats, trials in which the sound was less than 20 ms or more than 600 ms apart from the R-peak were discarded.

defined (Figure 4.6 on page 81): (1) the PRE interval: the interval between the heartbeat (defined by the location of the R-peak) preceding the onset of the auditory stimulation, and (2) the POST interval: the interval between the stimulus onset and the following heartbeat. All time intervals were then labelled according to the contained auditory stimulation following the Local-Global paradigm (XX block: LSGS or LDGD; XY block: LDGS or LSGD; see 1.5.2 on page 18).

Finally, In order to avoid using peaks without a clearly defined temporal association to a given heartbeat (and not the previous or following one), we restricted the analysis to the trials in which both the PRE and POST intervals were between 20 and 600 milliseconds. A mean of 520 ± 150 trials per subject were included while 135 ± 100 trials were rejected ($20 \pm 13\%$). A repeated measures Bayesian ANOVA was computed for each interval using the ratio of rejected trials as the study variable and the trial label and clinical state as factors. All the models including the clinical state factor presented evidence for no difference (PRE $BF_{01} \geq 2.35$; POST $BF_{01} \geq 2.61$). When the models included the trial type factor, the test showed strong evidence for no difference (PRE $BF_{01} \geq 39.19$; POST $BF_{01} \geq 45.17$).

To test if conscious processing of auditory regularities affects the ongoing cardiac activity, we analysed the PRE and POST stimulus intervals for each group of subjects in relation with the type of trials. For the Local effect, each subject mean of the PRE and POST intervals corresponding to LD trials were subtracted from the mean of the LS ones. Similarly, for the Global effect, the mean of the PRE and POST intervals corresponding to GD trials were subtracted from the mean of GS ones.

4.4.2 Results

There was no evidence for difference in cardiac cycle modulation between groups due to the processing of the Local regularities in either the PRE ($BF_{10} = 0.19$) or the POST ($BF_{10} = 0.19$) intervals (Figure 4.7 on the next page). Within the groups, neither the VS/UWS nor the MCS patients presented significant differences between LS and LD trials (sign-test LD-LS trials, VS/UWS $p > 0.7$, MCS $p > 0.2$). In the case of the Global effect (GS vs GD trials), there was no evidence of modulation difference between groups due to the global auditory processing in the PRE interval ($BF_{10} = 0.21$). On the contrary, in the POST interval, there was a strong evidence for a difference between the MCS and VS/UWS groups ($BF_{10} = 43.07$). This result is explained by a shortening of the POST intervals in the GD trials compared to the GS trials in the MCS patients (sign-test GD-GS trials, $p = 0.007$) and no difference between GD and GS in the VS/UWS patients (sign-test GD-GS trials, $p = 0.55$). The small sample of healthy controls (N=12) included in this study presented a pattern of results similar to the MCS subjects (although not statistically significant).

4.5 EEG and EKG Multivariate Pattern Analysis

4.5.1 Methods

In order to analyse the relevance and independence of the markers to the diagnosis of DOC, we used Multivariate Pattern Analysis in combination with wrappers algorithms for feature selection (Kohavi and John, 1997). This method consists on training classifiers with different set of features and comparing the obtained performance. Based on the performance comparisons, a set of features can be defined as (1) strongly or weakly relevant when they are partially independent and contribute to an optimal classification or (2) irrelevant, when they do not contribute to the classification.

Multivariate pattern analyses were done using 120 EEG-extracted markers (corresponding to quantification of power spectrum and complexity in individual EEG sensors and information sharing between EEG sensors) as described in Sitt et al. 2014 (see chapter 2 on page 25) and 8 EKG extracted markers: HR, HRV (high, low and very low frequency), Local PRE, Local POST, Global PRE and Global POST. We trained a Support Vector Classifier

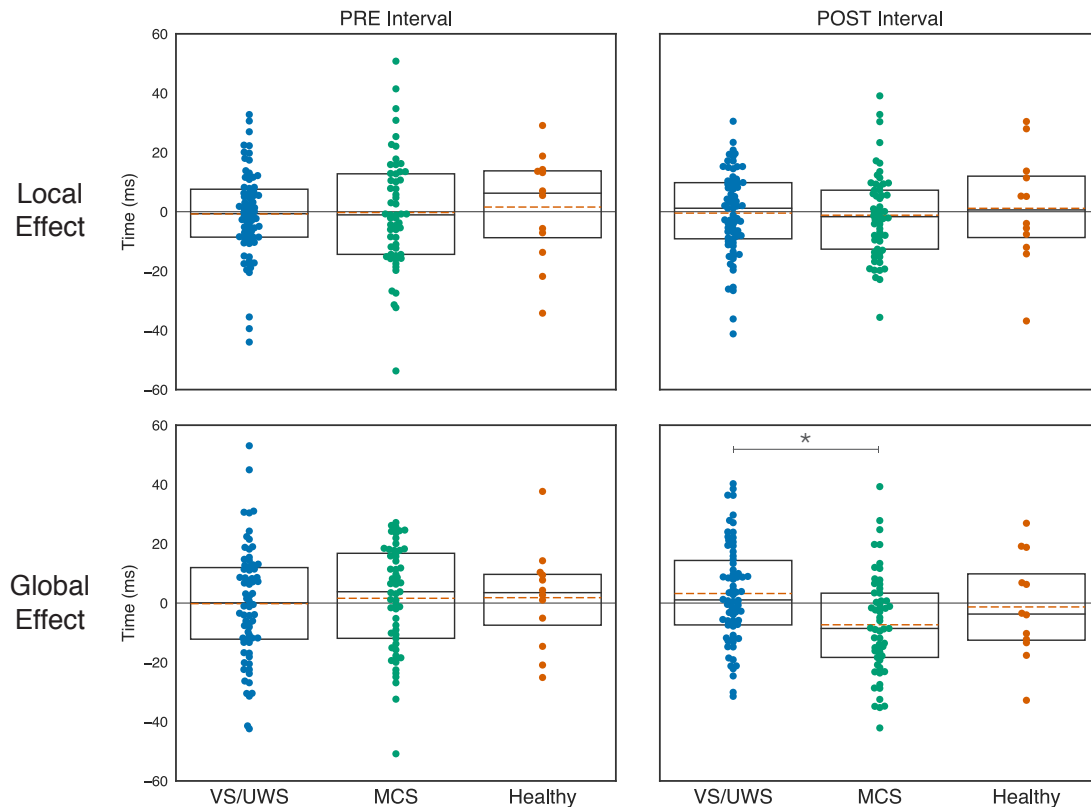


Figure 4.7: Violations of global regularities induce cardiac cycle phase acceleration only in minimally conscious patients. Local violations did not affect the ongoing cardiac activity for the intervals between the stimulation onset and the preceding R-peak (PRE, top left) nor the following R-peak (POST, top right). Similarly, global violations did not affect the ongoing cardiac activity at the PRE interval (bottom left). In clear contrast, they induced shortened POST intervals (bottom right) only in the minimally conscious state (MCS) group (between-group contrast $BF_{10} = 43.07$; within-group sign-test $p = 0.007$). The small sample of healthy controls included in this study presented a pattern of results similar to the MCS subjects (although not statistically significant). Each dot represents a patient in vegetative state/unresponsive wakefulness syndrome (VS/UWS, $N=70$), in minimally consciousness state (MCS, $N=57$) or a healthy control (Healthy, $n=12$). Boxplots with interquartile range, median (black line) and mean (dashed line) represent the distribution of data in the clinical groups.

(SVC) to distinguish between the VS/UWS and the MCS patients with a penalisation parameter (C) equal to 1. The SVC was repeatedly cross-validated with randomised stratified k-folding (k=8). Previously to the training of the classifier, relevant features were automatically selected keeping the highest 20% of the ANOVA F-value scores. Performance of the classifier was measured using AUC scores.

We defined 3 sets of features: (1) EKG markers of cognitive processes, corresponding to the PRE and POST intervals for the Local and Global contrasts (termed EKG_{cog}), (2) EKG markers of baseline vegetative function (termed EKG_{veg}) corresponding to the HR and HRV in the three frequencies previously defined and (3) EEG markers. We estimated the accuracy of the classification algorithm with 6 different combinations of these sets of markers: (1) $EEG+EKG_{cog}+EKG_{veg}$, (2) $EEG+EKG_{cog}$, (3) $EEG+EKG_{veg}$, (4) EEG markers only, (5) EEG with both EKG_{cog} and EKG_{veg} markers shuffled and (6) $EKG_{cog}+EKG_{veg}$ markers only. To minimise the effect of the random selection of folds, the AUC scores were averaged across 250 repetitions.

4.5.2 Results

Correlation between EEG and EKG markers of consciousness We first tested the relationship between cardiac cycle modulation markers and EEG markers that previously were reported to distinguishing VS/UWS and MCS patients in [Sitt et al. 2014](#). The modulation of the POST interval due to the Global Effect significantly correlated with EEG Kolmogorov Complexity (K; $r = -2.31, p = 0.02$), Permutation Entropy (PE; $r = -2.63, p = 0.01$), Spectral Entropy (SE; $r = -2.3, p = 0.02$), Weighted Symbolic Mutual Information (wSMI; $r = -0.19, p = 0.02$) and normalised Delta Power ($r = 0.2, p = 0.02$). No correlation was found between EEG evoked responses to the Global Effect and the phase shifts computed in the EKG (See 4.1 on the next page 1 for all markers). Nevertheless, none of the computed correlations survived a false discovery rate correction from multiple comparisons.

Multivariate patient classification by means of EKG and EEG markers To determine if the EKG extracted information is partially independent to the consciousness related information extracted from the EEG, we trained classifiers to distinguish clinical groups and compared the performance of using as features EEG makers alone or combinations of EEG

Marker	R Statistic	p value	p value (FDR)
PE Θ	-2.63	0.009 *	0.138
K	-2.31	0.022 *	0.138
wSMI Θ	-2.34	0.020 *	0.138
α	-1.30	0.192	0.412
$\ \alpha\ $	-1.31	0.190	0.412
β	-1.91	0.058	0.251
$\ \beta\ $	-1.53	0.128	0.349
δ	0.85	0.393	0.562
$\ \delta\ $	2.40	0.017 *	0.138
γ	-1.67	0.096	0.321
$\ \gamma\ $	-1.43	0.154	0.385
θ	-0.50	0.616	0.744
$\ \theta\ $	-0.94	0.345	0.562
MSF	-1.61	0.108	0.324
SE90	-1.87	0.062	0.251
SE95	-1.84	0.067	0.251
SE	-2.30	0.023 *	0.138
CNV	0.45	0.649	0.744
P1	-0.22	0.820	0.848
P3A	-0.86	0.387	0.562
P3B	-1.11	0.265	0.501
GD-GS	0.54	0.589	0.744
LD-LS	0.43	0.662	0.744
LSGD-LDGS	-0.31	0.756	0.810
LSGS-LDGD	-0.99	0.320	0.562
Δ P3A	-0.02	0.979	0.979
Δ P3B	-0.42	0.669	0.744
Δ MMN	-0.86	0.387	0.562

Table 4.1: Correlations between the Global Effect values as measured by the EKG POST interval and EEG markers used to diagnose the state of consciousness in DOC patients.

and EKG markers. Multivariate analysis combining *EEG* and *EKG_{cog}* showed better performance compared to *EEG* and *EKG_{veg}* markers and *EEG* markers alone (Figure 4.8 on the facing page). Combining the *EKG_{cog}* and *EEG* markers led to an improvement of the performance (*EEG+EKG_{cog}*, AUC=76.1%; *EEG+EKG_{cog}+EKG_{veg}*, AUC=75.7%). On the other hand, when *EKG_{cog}* markers were not included in the MVPA the performance did not differ from EEG alone (*EEG* only, AUC=73.7%; *EEG+EKG_{veg}*, AUC=73.3%). As a control test for the effect of the number of features, classification was also computed combining *EEG* and label-shuffled *EKG* markers; in this case, the AUC was estimated at 73.6%. Using solely cardiac markers, the classifier performed above chance with a mean AUC of 60.1%. When we compared the performance of MVPAs that included EEG features, we only found significant differences when the MVPAs also included *EKG_{cog}* versus when the MVPAs did not include these cardiac features ($p < 1e^{-9}$, Kruskal-Willis test, corrected for multiple comparisons). The inclusion of *EKG_{veg}* features didn't significantly changed the performance of the tested MVPA classifiers ($p > 0.1$).

4.6 Discussion

We here aimed at characterising consciousness state in patients with DOC by means of baseline heart activity and heart-brain interactions. We tested if cardiac-extracted information can complement single-patient EEG-based classification performance. When we contrasted behaviourally non-overlapping VS/UWS and MCS patients we found higher HR and HRV in the VS/UWS than MCS group, in accordance to [Leo et al. \(2016\)](#). This comparison included MCS patients who were in the higher end of the CRS-R scale versus the VS/UWS patients who were in the lower end of the CRS-R. When all DOC patients were included in order to retain clinical reality we did not find group differences of overall cardiac autonomic markers between the groups. This suggests a common underlying baseline cardiac function across patients. Interestingly, we found a positive correlation between CRS-R total scores and three autonomic markers (HR, HRV HF and HRF LF) only in the VS/UWS patients.

Our results are consistent with previous findings showing a relationship between the level of consciousness and dysautonomia in DOC after traumatic brain injuries. Specifically, low CRS-R scores were related to tachycardia in patients with low scores on the Glasgow Coma

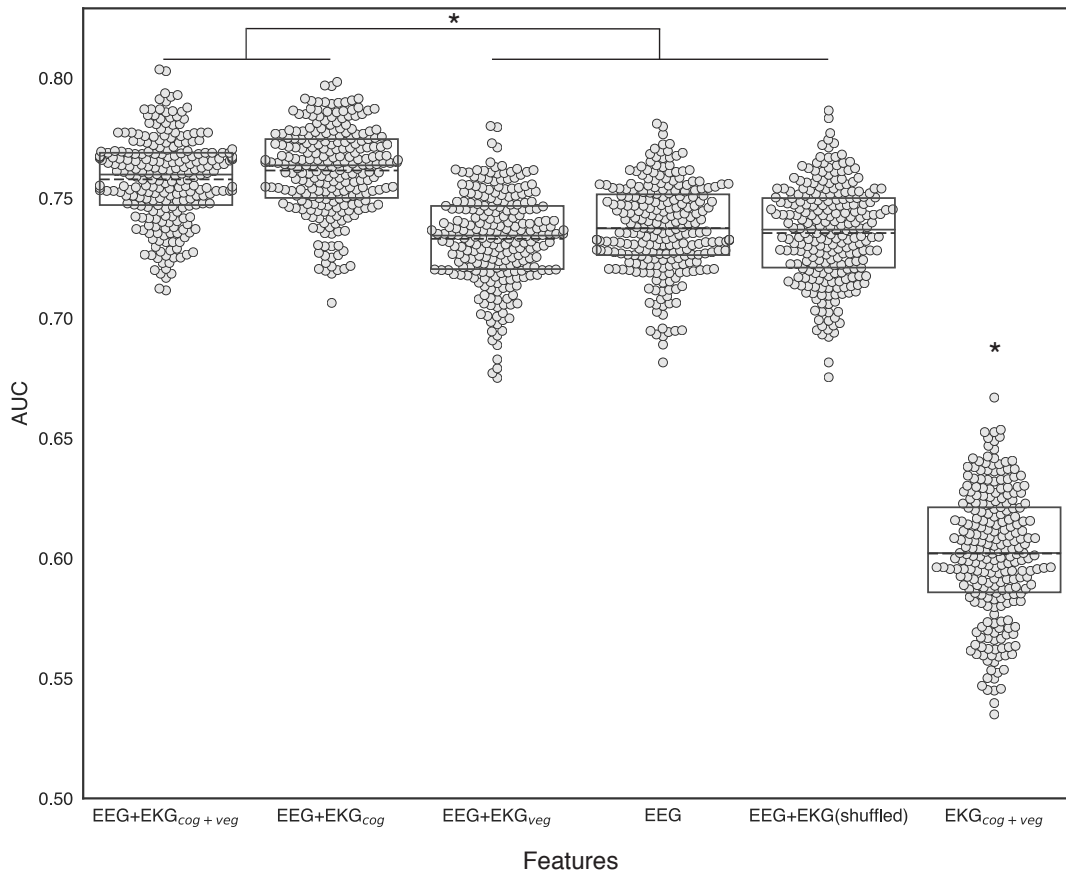


Figure 4.8: Cognitive EKG markers carries partially independent information from EEG. Six distinct multivariate classifiers were trained to distinguish between VS/UWS and MCS patients using different combinations of EKG and EEG markers. We used as features combinations of 120 EEG markers, cognitive EKG markers (EKG_{cog} ; PRE and POST intervals, Local and Global effects contrasts) and the vegetative function markers (EKG_{veg} ; Heart Rate and Variability). All the models that summed EEG markers and EKG_{cog} , presented a significant increase in the classification accuracy (compared to MVPA of EEG without EKG_{cog} , $p < 1e^{-9}$). Using only EEG markers (mean AUC 73.7%) showed no significant difference with EEG in combination with EKG_{veg} markers (mean AUC 73.3%). As a control to equalise the number of features, the combination of EEG and all of the EKG markers with shuffled labels reported a mean AUC of 73.3%. When we used only EKG markers, the classifier performed above chance, obtaining a mean AUC of 60.1%. Means were estimated using 250 repetitions of stratified 8-fold cross validation. Each dot represents the mean value across folds for each repetition. Boxplots with interquartile range, median and mean (dotted line) represent the distribution of values for each set of features.

Scale (Baguley et al., 1999) and to lower HRV (in both high and low frequencies), which was considered as a symptom of a neurological disconnection syndrome (Baguley et al., 2006). Taken together, these results suggest that the diversity of behaviours characterising conscious states (associated with cortical processing) does not necessarily translate into strong correlations with autonomic markers, such as HR and HRV. Therefore, the observed differences in these markers in VS/UWS patients on the lower end of the CRS-R scale seems to be associated with an overall deterioration of clinical condition, rather than to cognitive processing.

Our analysis of the heart evoked potentials revealed two results. First, we observed a statistical difference between VS/UWS and MCS in the CFA corresponding to the T wave but no difference in association to the QRS wave. The differences observed in the T-wave between VS/UWS and MCS patients, in the shape of a dipole with a left-posterior positivity and a right-frontal negativity, are similar to the reported cardiac repolarisation changes induced by mental stress (Gray et al., 2007) and neurodegeneration or stroke (García-Cordero et al., 2016). Although previous works depict a main modulation during the time window corresponding to the T-wave with frontal negativities, in our study the differences between the groups of DOC patients are highlighted by the cluster statistic in the posterior positive side of the dipole. Second, we found differences between VS/UWS and MCS patients in a time window after the T-wave. Crucially, this difference had a different topography to the previously described CFA. The maximal differences in the EEG were obtained in the central electrodes. Taken together these results further suggest differences in heart-brain interaction between VS/UWS and MCS patients.

In terms of cognitive processing, we analysed the cardiac activity while patients were evaluated with the *Local Global* paradigm aiming to probe cognitive-related responses on cardiac markers. Such brain-heart interactions have been previously shown in protocols where, by quantifying neural events locked to heartbeats, one could predict whether a subject would report a fast flashing visual stimulus as perceived or not (Park et al., 2014). In addition, during complex cognitive processing, such as when playing chess, the heartrate dynamics, as measured before players made a move, could predict the likelihood of them eventually committing an error (Leone et al., 2012). Heartbeat-evoked cortical responses were further shown to differ in auditory interoceptive learning tasks (Canales-Johnson et al., 2015) and emotional states (Couto et al., 2015). Taken together, these studies suggest a bi-directional

interaction between brain and heart that can be modulated by cognitive processes.

In our protocol, we found that the cardiac cycle was modulated by the processing of global auditory regularities only in the MCS group. Specifically, MCS patients showed an acceleration of the timing of the heartbeat following the auditory stimulus (shortening of the POST interval) which disrupted the global regularity. No such modulation of cardiac cycle was found in the VS/UWS patients, nor any effect was found in either group for the local irregularities. No modulations of the PRE intervals were found, this suggests that the only observed modulation is a direct effect of the cognitive process of the stimulation. It is important to compare this results with previous works that analysed the evoked responses in the EEG using the same protocol. These studies show that the violations of local regularities (in the form of a mismatch negativity response) can be detected in healthy and awake controls but also unconscious conditions such as subjects during sleep, coma and VS/UWS (Faugeras et al., 2011; Strauss et al., 2015; Morlet and Fischer, 2013). In contrast, disruptions of the global regularities (eliciting a P3b response) are only present in conscious and attentive subjects (although see Tzovara et al. (2015) and Naccache et al. (2015) for ongoing discussions). The fact that cardiac cycle modulation effect was present only associated to global irregularities (which requires maintaining conscious attention) and only in the MCS patients (who are generally characterized by more complex brain function compared to VS/UWS patients; Giacino et al. 2014) suggests that the source of this effect is a brain-driven indirect modulation due to the conscious processing of information.

A recent study demonstrated a link between conscious perception and cardiac activity in normal subjects (Park et al., 2014). Specifically, in visual detection task, subjects' heart rate decreased during a warning cue and increased immediately after reporting the perception or not of the stimuli following the cue. When subjects responded correctly, following RR intervals were significantly shorter than the ones corresponding to an incorrect response. This indicates an interaction between conscious perception and the modulation of cardiac activity. Interestingly, previous studies showed that the characterisation of the modulation depends on the stimulation inter-trial interval. With short intervals, this cardiac slowing is reversed within the same cycle that the target is detected (Van Der Molen et al., 1983; Jennings and Wood, 1977). In our work we depict a shortening of the RR interval containing the stimuli. Nevertheless, only when the stimulus is known to produce neural modulations and only in

patients with higher level of consciousness. Our attention-driven effect is consistent with these previous results and characterises the modulation in relation to the subjects' overall level of consciousness.

Having a proficient test at the single-subject level is a clinical necessity in order to reduce the diagnostic uncertainty each case. The modulation of the heart cycle within each subject was not powerful enough to have a significant effect to distinguish the clinical state of individual subject. With the aim of improving the single case performance of diagnostics tests, and particularly in terms of EEG, we have shown that multivariate classification performance of the combination of 120 EEG markers (such as quantifications comprising connectivity analysis, information complexity, spectral analysis and evoked related potentials) outperformed the univariate classification accuracy, when markers were considered individually. This combination of EEG markers allowed an enhanced classification of conscious state at single-patient level (Sitt et al., 2014). Although the cardiac measures alone did not allow a single subject diagnosis, combining information from both neural and cardiac sources increased significantly the accuracy of the classification of these patients. This indicates that the information extracted from the modulations of cardiac activity due to cognitive processing is partially independent from the neural correlates of consciousness as measured by EEG. To our knowledge, this is the first time that body-related signals are considered as contributing factors in data-driven diagnosis in patient with DOC. We think that such an embodied approach to cognition (Clark, 1999) paves the way for further investigations of body-brain interactions in DOC which might be informative not only for clinics but also for tracing the neural correlates of consciousness. In the future, and with the aim of improving the single case performance of this test, we will introduce novel versions of stimulation paradigm (with stimulations contextually locked to the ongoing cardiac cycle).

In conclusion, we show a relation between autonomic nervous system function and a stimulation paradigm exposing subjects to violations of auditory regularities in MCS patients. Our results suggest that cardiac cycle modulation is relevant for the assessment of patients with DOC because it potentially carries partially independent information when taken together with neural correlates of consciousness. We think that our work opens a window to the study of DOC via the embodied paradigm, according to which body-brain functions contribute to a holistic approach to conscious processing.

Chapter 5

Summary and final remarks

In chapter one, we described the fundamentals of EEG, the problematic of DOC, and the current state-of-the-art tools for the diagnosis of DOC. In chapter two, we analysed the validity and robustness of an automatic processing and DOC diagnostic method based on EEG-extracted markers. We tested this method under distinct simulated and real conditions from different clinical centres, concluding that the model extracts reliable signatures of consciousness, maintaining the diagnostic accuracy across conditions. In chapter three, we aimed at extending our knowledge on multisensory integration and states of consciousness. For this purpose, we introduced a modification of an auditory paradigm, currently used to assess the diagnosis of DOC patients, to include somatosensory and visual stimulation. We tested this paradigm on healthy controls, obtaining results consistent with previous works on multisensory integration. In chapter four, we moved away from a strict neurocentric approach for the study of consciousness and included bodily signals in our analysis. We found that the already known brain-heart interactions are mediated by the state of consciousness. Interestingly, this modulation of cardiac activity by cognitive processes is present only in the group of DOC patients showing high-order behavioural responses.

The present work exceed the current state of knowledge at two dimensions. Clinically, our work on automated EEG-based diagnosis confirms and expands the utility of machine learning as an assisting technology for the clinical management of DOC. On the one hand, the here proposed automated diagnostic tool validates previous findings. On the other, it generalises to other experimental setups and recording conditions. Therefore, our results provide support for the use of EEG-extracted markers and machine learning in clinical settings, in a

flexible and reliable way. At the same time, it permits the extrapolation to other experimental application, such as the multisensory cross-modal investigation as a supplementary marker of conscious state. In that case, the here proposed methods can be used synergically with other physiologically-extracted information.

Scientifically, it sheds light on the relationship between states of consciousness and the embodied paradigm to cognition. To date, consciousness is directly inferred by means of subjective reports, task performance and by observing nonreflex behaviours. In the absence of subjective reportability, like in DOC patients, it is challenging to know whether patients retain any form of subjective experiences. According to cognitive science, subjectivity is a construct which can be approached hierarchically, from the experience of a "me" shaped by perceptions of others and their perceptions of me (social self), to being a continuous person over time (narrative self), to the experience of a sense of reality of the world and of me within it (minimal self) (Seth, 2013). Especially the case of the minimal self can be understood as the conscious experience of being someone, which is pre-reflective in nature, i.e. independent from explicit cognition and linguistic properties (Gallagher, 2000). Contemporary neurocognitive approaches, which are formulated based on reportable experiences, imply that undifferentiated brain activity might account for the inability to retain subjective experience. Therefore, the self in unconscious conditions is severely compromised and therefore absent. Alternatively, embodiment, a position in cognitive neuroscience and philosophy of mind, provides a more specific framework for the study of minimal selfhood by emphasising the role of body in shaping cognition (Varela et al., 1991). According to the theory, an organism is considered to be a self when the following conditions are jointly met: a) it possesses volume in space (localised within bodily boundaries), b) it recognises a global body representation (the body is perceived as a whole as opposed to localised body parts and isolated movements), and c) it possesses a visuospatial frame of reference/ egocentric model of reality. In other words, subjectivity in its fundamental form is the process of the conscious experience of being a distinct, holistic entity, embodied and embedded in space and time (Blanke and Metzinger, 2009). Consequently, to infer the presence of a minimal self "it is sufficient to show a passive, multisensory and globalised availability of an integrated, transparent and global representation of the spatiotemporally situated body"(Blanke and Metzinger, 2009). The here presented work on brain-heart interaction bridges the empirical gap of the relationship be-

tween subjective experience and altered states of consciousness in DOC because it extends from a merely neurocentric approach. It shows that human cognition is realised holistically adding to growing evidence that the mind is a dynamic process between the organism and the world.

List of Figures

1.1	Simplified illustration of the two major components of consciousness: the level (wakefulness) and the content of consciousness (awareness). Normal physiological states (purple) present a positive correlation. Patients in coma or anaesthesia (gray) are unconscious and they cannot be awakened. DOC patients are awake but do not present signs of awareness (VS/UWS patients; blue) or show inconsistent but discernible signs of behavioural activity (MCS patients; green). Adapted from Laureys 2005b	4
1.2	FDG-PET images for representative group samples as extracted from Stender et al. 2016	7
1.3	Regions showing higher functional connectivity in MCS patients as compared to VS/UWS patients (extracted from Demertzi et al. 2015).	8
1.4	Timeseries of two auditory evoked responses corresponding to an oddball paradigm. Rare trials (blue) present distinct evoked responses when compared to frequent trials (red). This classic paradigm elicits a P300 wave. The two main components of the wave are a negative deflection 100 ms after the stimuli (N100) and a positivity 300ms after the stimuli (P300).	13
1.5	Illustration of the Local-Global paradigm. Each trial of the auditory paradigm was composed by 5 consecutive sounds. Four equal sounds define a local regularity (music notes). The fifth sound could be equal or different, defining a local standard or deviant trial, respectively. At a second level, frequent trials (80%, green shaded area) defined a global regularity and rare trials (20%, red shaded area) violated this regularity.	19

1.6	Local and Global effects as measured with EEG in one of the directors of this thesis. Timeseries of the Local Effect around the Fz electrode (top left) present the MMN around 140 ms after the onset of the 5th sound only when it is different from the first four. The associated scalp map (top right) shows a frontal/central negativity and a posterior positivity. Timeseris of the Global Effect around the Pz electrode (bottom left) depict the P3b component starting around 350ms after the onset of the 5th sound. The associated scalp map (bottom right) presents a central/posterior positivity.	20
2.1	Scalp topographies of the most discriminatory measures. The fifth column indicates whether the VS and MCS patients were significantly different (Black: $p = 0.01$, light grey: $p = 0.05$, white: not significant, uncorrected). The sixth column shows the statistics of a regression analysis of the measure across the four states of consciousness (VS < MCS < CS (EMCS) < healthy controls (H). Black: $p = 0.01$, light grey: $p = 0.05$, white: not significant, uncorrected). Extracted from Sitt et al. 2014	31
2.2	Reproduction of the figure from Sitt et al. 2014 using our Python implementation.	32
2.3	Diagram of the dimensions for each of the families of markers. To compute the scalar values, dimensions were first aggregated by epochs (1), then by sensors (2), and finally, if needed, by the remaining dimensions. (3)	34
2.4	Our new implementation, tested on unobserved data, presents an AUC of 74.27% with an SVM classifier and 72.91% with an Extremely Randomised Trees algorithm (top). When compared to a dummy classifier to estimate the empirical chance level, the results of the classifiers are significantly different (bottom). The results where computed using 2000 bootstrap replicates.	37
2.5	Multivariate classifiers outperforms univariate counterparts. Both SVM (blue) and ET (red) multivariate classifiers presented a superior AUC than the respective univariate versions on $\alpha(m, m)$ (dashed)	38
2.6	A self contained HTML-report presents all the results from the automated processing. This includes quantitative information regarding the preprocessing procedures, markers, statistics and predictions.	39
2.7	Alternative EEG configurations with 6 different number of electrodes (256, 128, 64, 32, 16, 8). Position were selected such that they approximated realistic EEG caps respecting the international 10-20 system. Temporally, we reduced the amount of epochs to 6 different percentages (1, 5, 25, 50, 75, 100), respecting the original proportion of trials.	42

2.8 Multivariate classifiers perform robustly on alternative EEG spatial configurations and recording lengths. Across all 36 experiments (6 alternative sensors locations by 6 temporal subsamplings) in-sample markers AUC (gray) are less performant than multivariate models. 42

2.9 Performance of the ET is more stable across spatial and temporal configurations compared to the SVM. Both classifiers present a trend to better accuracy with more epochs and electrodes. Nevertheless, SVM presents higher variability when the number of epochs is reduced. 43

2.10 Both our models generalise to resting state. The ET classifier present an AUC of 78.28% and the SVM classifier an AUC of 81.62%. When compared to a dummy classifier to estimate the empirical chance level, the results of the classifiers are significantly different (bottom). The results where computed using 2000 bootstrap replicates. 44

2.11 Multivariate classifiers outperforms univariate counterparts also when generalising to resting state data. Both SVM (blue) and ET (red) multivariate classifiers presented a superior AUC than its univariate versions on $\alpha(m, s)$ (dashed blue) and $\alpha(m, m)$ (dashed red). 45

2.12 ET classifier presents less variability than SVM across spatiotemporal subsamplings. All the different spatial and temporal configurations were considered for training and testing (1296 combinations, 36 for each set). The corresponding best univariate models were also considered next to the multivariate ones. The distribution of AUC scores is indicated by the histograms for both validation (left) and generalisation (right) sets. Samples are depicted underneath the histograms, with black solid lines indicating the mean of the distributions. Both multivariate classifiers outperformed the corresponding best univariate ones. In both cases, the ET classifier presented less variance, although the highest accuracy was always obtained using the SVM model. 46

2.13 We observed a positive but non-linear relationship between univariate AUC and variable importance in the ET classifier. Left plot depicts the correlation between the univariate AUC and variable importance of the ET classifier when averaged across the 36 experiments. Middle and Right plots depicts the same correlation for the validation and generalisation cases. Colours indicate the family of the marker, while the shape depicts the variant. The three correlations were statistically tested using Spearman rank correlation coefficient. 49

- 3.1 Illustration of the hypotheses, depicting the number of subjects presenting within-trial, cross-modal and global effects in relation to the state of consciousness. In short, we expect that conscious subjects will show global effects while unconscious subjects will be able to show some local effects. The cross-modal effects will fall in between, because they require the interaction between sensory-specific cortical areas. 55
- 3.2 Illustration of the modification of the Local-Global paradigm that uses laterality as the difference between stimuli instead of modality-specific differences. Each trial is composed by 5 stimuli over a 600 ms interval as in the original paradigm (see 1.5 on page 19). The first four stimuli are delivered to the same side defining the local regularity. The fifth stimulus can be ipsilateral or contralateral, defining a local standard or deviant trial respectively. At the global (or across trial) level, the regularities are defined by frequent trials (80%, green shaded area) and violated by rare trials (20%, red shaded area). The choice of side for each trial is done pseudorandomly, keeping a balance of 50% for each side. 57
- 3.3 Illustration of the types of trials used in the *Cross-modal Local-Global* paradigm. Three different stimulation modalities were possible. For each recording, two modalities were selected, defining 9 types of recordings. The matrix illustrates all the possible combinations, with the trials corresponding to unimodal recordings in the diagonal. 58
- 3.4 Topographies and ROI plots for the Laterality Mismatches comparing ipsilateral and contralateral stimuli for auditory (top), somatosensory (middle) and visual (bottom) modalities. Topographies depict the values of the contrast (subtraction) between conditions for the 224 scalp electrodes. Time series represents the average values around Cz for each condition. The $t = 0$ for the x-axis corresponds to the onset of the 5th stimuli. 62
- 3.5 Topographies and ROI plots for the Rule Mismatches comparing standard and deviant stimuli for auditory (top), somatosensory (middle) and visual (bottom) modalities. Topographies depict the values of the contrast (subtraction) between conditions for the 224 scalp electrodes. Time series represents the average values around Pz for each condition. The $t = 0$ for the x-axis corresponds to the onset of the 5th stimuli 63

- 3.6 While Laterality Mismatch decoding patterns differ across stimulation modalities, Rule Mismatch decoding patterns do not present differences. Each one of the 6 images depicts the decoding AUC for each training and testing time. Decoding patterns of Laterality Mismatch (left) present a significant high AUC between 100ms and 400ms after the onset of the stimuli with some differences between auditory (top), somatosensory (middle) and visual (bottom) stimulation modalities. In contrast, Rule Mismatches (right) present later and longer decoding patterns. Significant clusters ($p < 0.05$) are depicted in color. 64
- 3.7 Spatiotemporal patterns of neural activity in response to Laterality Mismatches are not transferable across stimulation modalities. Each row of images depict the decoding AUC when training and testing using different pairs of modalities. Significant clusters ($p < 0.05$) are depicted in colour. 65
- 3.8 Spatiotemporal patterns of neural activity in response to Rule Mismatches are similar across stimulation modalities, with specific temporal shifts. Each row of images depict the decoding AUC when training and testing using different pairs of modalities. Significant clusters ($p < 0.05$) are depicted in colour. . . 66
- 4.1 (A) Filtered EEG time series from 7 EEG sensors from one VS/UWS patient. (B) Corresponding time series of 7 ICA components extracted from the previous EEG recording and the respective weights topographies. The independent component with cardiac information is shown in red. Dotted lines represents the automatically detected R-peak. 74
- 4.2 (A) Mean weights topographies for each clinical group (left). A sensor-wise Bayesian t-test shows evidence for no difference in the topographies between groups (right). (B) Mean and standard error of the mean for each clinical group QRS complex from the ICA-extracted EKG. A single channel cluster permutation test indicated significant differences ($p = 0.017$) only between 184 and 344ms after the R-peak, consistent with the location of the T wave. . 76
- 4.3 EKG and ECG extraction methods comparison. We evaluated two independent groups of healthy controls (n=12) and patients (n=12) using simultaneous EEG and EKG recordings. For each subject, EKG was also extracted using the described ICA method. We then computed the differences between each R-peak onset detected in the direct EKG and the corresponding R-peak detected using ICA (left). Right panel shows the mean difference and 95% CI for each type of trial and subject as measured in samples (1 sample = 4 ms). Using Bayesian ANOVA, we found no evidence for a difference as an effect of the trial type ($BF_{01} \geq 4.27$) and strong evidence for no difference for the interaction between the type of trial and the clinical state ($BF_{01} \geq 15$) 77

- 4.4 Cardiac autonomic markers show no difference between clinical groups. Lower CRS-R scores in VS/UWS patients correlates with a faster and less variable cardiac cycle as a manifestation of the overall deterioration of the clinical condition. Each panel depicts the cardiac marker values (y-axis, Heart rate (A), Heart rate variability in high frequencies (B), in low frequencies (C), and in very low frequencies (D)) for each patient (dot), categorised by clinical group (top, 70 VS/UWS, 57 MCS, 12 Healthy) and by Coma Recovery Scale-Revised scores (CRS-R, bottom - only for patients). The Spearman's regression line between the scores and the EKG-related markers for the VS/UWS patients, indicates a significant positive correlation between the CRS-R score and RR interval (A), Heart Rate Variability in high frequencies (B), and in low frequencies (C). Boxplots with interquartile range, median (black line) and mean (dashed line) represent the distribution of data in both clinical groups. 79
- 4.5 R-peak locked EEG evoked responses shows differences between clinical groups. (A) Mean EEG topographies for each clinical group time locked to the R-peak at 0, 100, 250, 350, 450 and 500 ms. (B) Contrast and statistical comparison of the R-peak evoked potentials between clinical groups. (C) The left panel shows the only significant cluster of a permutation analysis ($p = 0.034$), the electrodes composing the cluster are shown with white circles (left). The right panel shows the time series of the corresponding cluster (mean and standard deviation across subjects). Two main modulations are observed, (1) in the time window corresponding to the T wave, a left-posterior positivity and a right-frontal negativity ; and, (2) a central electrode spatial pattern positivity after the T-wave (>350ms), suggesting differences in the brain processing of the heart activity between VS/UWS and MCS patients. . . 80
- 4.6 Two consecutive EKG QRS complexes defined an RR interval. Overall heart rate was computed from the robust average of the RR intervals. Conscious response to the stimulation was analysed based on the definition of two intervals: (1) the PRE interval, measured between the R-peak previous to the 5th sound and the onset of that sound and (2) the POST interval, measured between the onset of the 5th sound and the following R-peak. In order to avoid coupling with the heartbeats, trials in which the sound was less than 20 ms or more than 600 ms apart from the R-peak were discarded. 81

- 4.7 Violations of global regularities induce cardiac cycle phase acceleration only in minimally conscious patients. Local violations did not affect the ongoing cardiac activity for the intervals between the stimulation onset and the preceding R-peak (PRE, top left) nor the following R-peak (POST, top right). Similarly, global violations did not affect the ongoing cardiac activity at the PRE interval (bottom left). In clear contrast, they induced shortened POST intervals (bottom right) only in the minimally conscious state (MCS) group (between-group contrast $BF_{10} = 43.07$; within-group sign-test $p = 0.007$). The small sample of healthy controls included in this study presented a pattern of results similar to the MCS subjects (although not statistically significant). Each dot represents a patient in vegetative state/unresponsive wakefulness syndrome (VS/UWS, N=70), in minimally consciousness state (MCS, N=57) or a healthy control (Healthy, n=12). Boxplots with interquartile range, median (black line) and mean (dashed line) represent the distribution of data in the clinical groups. 83
- 4.8 Cognitive EKG markers carries partially independent information from EEG. Six distinct multivariate classifiers were trained to distinguish between VS/UWS and MCS patients using different combinations of EKG and EEG markers. We used as features combinations of 120 EEG markers, cognitive EKG markers (EKG_{cog} ; PRE and POST intervals, Local and Global effects contrasts) and the vegetative function markers (EKG_{veg} ; Heart Rate and Variability). All the models that summed EEG markers and EKG_{cog} , presented a significant increase in the classification accuracy (compared to MVPA of EEG without EKG_{cog} , $p < 1e^{-9}$). Using only EEG markers (mean AUC 73.7%) showed no significant difference with EEG in combination with EKG_{veg} markers (mean AUC 73.3%). As a control to equalise the number of features, the combination of EEG and all of the EKG markers with shuffled labels reported a mean AUC of 73.3%. When we used only EKG markers, the classifier performed above chance, obtaining a mean AUC of 60.1%. Means were estimated using 250 repetitions of stratified 8-fold cross validation. Each dot represents the mean value across folds for each repetition. Boxplots with interquartile range, median and mean (dotted line) represent the distribution of values for each set of features. 87

List of Tables

2.1	Acronyms used for EEG-measures	33
2.2	Description of the three datasets used throughout the analysis in this chapter. Paris 1 refers to the data used in Sitt et al. 2014 and in section 2.4 on page 30, Paris 2 to the data used for the validation analysis in section 2.5 on page 36. Data provided by the Liège university hospital was used in section 2.7.2 on page 43.	41
4.1	Correlations between the Global Effect values as measured by the EKG POST interval and EEG markers used to diagnose the state of consciousness in DOC patients.	85

Bibliography

- B J Ansell and J E Keenan. The Western Neuro Sensory Stimulation Profile: A tool for assessing slow-to-recover head-injured patients. *Archives of Physical Medicine and Rehabilitation*, 70(2):104–108, 1989. ISSN 0003-9993. 6
- N. Axmacher, M. M. Henseler, O. Jensen, I. Weinreich, C. E. Elger, and J. Fell. Cross-frequency coupling supports multi-item working memory in the human hippocampus. *Proceedings of the National Academy of Sciences*, 107(7):3228–3233, 2010. ISSN 0027-8424. doi: 10.1073/pnas.0911531107. 49
- B. J Baars. Consciousness. *Scholarpedia*, 10(8):2207, 2015. doi: 10.4249/scholarpedia.2207. revision #150323. 2
- Ian J Baguley, J L Nicholls, Kim L Felmingham, J Crooks, J A Gurka, and L D Wade. Dysautonomia after traumatic brain injury: a forgotten syndrome? *Journal of neurology, neurosurgery, and psychiatry*, 67(1):39–43, 1999. ISSN 0022-3050. doi: 10.1136/jnnp.67.1.39. 70, 88
- Ian J Baguley, Roxana E Heriseanu, Kim L Felmingham, and Ian D Cameron. Dysautonomia and heart rate variability following severe traumatic brain injury. *Brain injury*, 20(4):437–444, 2006. ISSN 0269-9052. doi: 10.1080/02699050600664715. 70, 88
- Yang Bai, Xiaoyu Xia, and Xiaoli Li. A review of resting-state electroencephalography analysis in disorders of consciousness. *Frontiers in Neurology*, 8(SEP), 2017. ISSN 16642295. doi: 10.3389/fneur.2017.00471. 17
- Christoph Bandt and Bernd Pompe. Permutation Entropy: A Natural Complexity Measure for Time Series. *Physical Review Letters*, 88(17):174102, 2002. ISSN 0031-9007. doi: 10.1103/PhysRevLett.88.174102. 29
- Tim Bayne, Jakob Hohwy, and Adrian M. Owen. Are There Levels of Consciousness?, 2016. ISSN 1879307X. 2

Henry Beecher, Raymond Adams, A Clifford Barger, William Curran, Derek Denny-Brown, Dana Farnsworth, Jordi Folch-Pi, Everett Mendelsohn, John Merrill, Joseph Murray, Ralph Potter, Robert Schwab, and William Sweet. A definition of irreversible coma: report of the ad hoc committee of the Harvard Medical School to examine the definition of brain death, 1968. ISSN 0041-1337. 3

Tristan A Bekinschtein, Stanislas Dehaene, Benjamin Rohaut, François Tadel, Laurent Cohen, and Lionel Naccache. Neural signature of the conscious processing of auditory regularities. *Proceedings of the National Academy of Sciences*, 106(5):1672–1677, 2009. ISSN 0027-8424. doi: 10.1073/pnas.0809667106. 16, 18, 51, 55, 67, 71

Anthony J. Bell and Terrence J. Sejnowski. An information-maximization approach to blind separation and blind deconvolution. *Neural Computation*, 7(6):1129–1159, 1995. ISSN 0899-7667. doi: 10.1162/neco.1995.7.6.1129. 73

James L. Bernat. Clinical ethics and the law. In *Ethical issues in neurology*, pages 79–107. 2002. ISBN 9780781790604. 3

James L. Bernat. Ethical issues in the perioperative management of neurologic patients, 2004. ISSN 07338619. 3

Olaf Blanke. Multisensory brain mechanisms of bodily self-consciousness. *Nature reviews. Neuroscience*, 13(8):556–71, jul 2012. ISSN 1471-0048. doi: 10.1038/nrn3292. 53

Olaf Blanke and Thomas Metzinger. Full-body illusions and minimal phenomenal selfhood. *Trends in Cognitive Sciences*, 13(1):7–13, 2009. ISSN 13646613. doi: 10.1016/j.tics.2008.10.003. 92

Marie Aurélie Bruno, Didier Ledoux, Bernard Lambermont, François Damas, Caroline Schnakers, Audrey Vanhauzenhuyse, Olivia Gosseries, and Steven Laureys. Comparison of the full outline of unresponsiveness and Glasgow Liege Scale/Glasgow Coma Scale in an intensive care unit population. *Neurocritical Care*, 15(3):447–453, 2011. ISSN 15416933. doi: 10.1007/s12028-011-9547-2. 5

György Buzsáki. *Rhythms of the Brain*. 2009. ISBN 9780199863716. doi: 10.1093/acprof:oso/9780195301069.001.0001. 11, 12

György Buzsáki and Andreas Draguhn. Neuronal oscillations in cortical networks. *Science (New York, N.Y.)*, 304(5679):1926–9, 2004. ISSN 1095-9203. doi: 10.1126/science.1099745. 12

György Buzsáki, Costas A. Anastassiou, and Christof Koch. The origin of extracellular fields and currents — EEG, ECoG, LFP and spikes. *Nature Reviews Neuroscience*, 13(6):407–420, 2012. ISSN 1471-003X. doi: 10.1038/nrn3241. 11

Andrés Canales-Johnson, Carolina Silva, David Huepe, Álvaro Rivera-Rei, Valdas Noreika, María Del Carmen Garcia, Walter Silva, Carlos Ciralo, Esteban Vaucheret, Lucas Sedeño, Blas Couto, Lucila Kargieman, Fabricio Baglivo, Mariano Sigman, Srivas Chennu, Agustín Ibáñez, Eugenio Rodríguez, and Tristan A. Bekinschtein. Auditory feedback differentially modulates behavioral and neural markers of objective and subjective performance when tapping to your heartbeat. *Cerebral Cortex*, 25(11):4490–4503, 2015. ISSN 14602199. doi: 10.1093/cercor/bhv076. 70, 88

A. G. Casali, O. Gosseries, M. Rosanova, M. Boly, S. Sarasso, K. R. Casali, S. Casarotto, M.-A. Bruno, S. Laureys, G. Tononi, and M. Massimini. A Theoretically Based Index of Consciousness Independent of Sensory Processing and Behavior. *Science Translational Medicine*, 5(198):198ra105–198ra105, 2013. ISSN 1946-6234. doi: 10.1126/scitranslmed.3006294. 17

Silvia Casarotto, Angela Comanducci, Mario Rosanova, Simone Sarasso, Matteo Fecchio, Martino Napolitani, Andrea Pigorini, Adenauer G. Casali, Pietro D. Trimarchi, Melanie Boly, Olivia Gosseries, Olivier Bodart, Francesco Curto, Cristina Landi, Maurizio Mariotti, Guya Devalle, Steven Laureys, Giulio Tononi, and Marcello Massimini. Stratification of unresponsive patients by an independently validated index of brain complexity. *Annals of Neurology*, sep 2016. ISSN 03645134. doi: 10.1002/ana.24779. 17

S. Chennu, V. Noreika, D. Gueorguiev, A. Blenkmann, S. Kochen, A. Ibanez, A. M. Owen, and T. A. Bekinschtein. Expectation and attention in hierarchical auditory prediction. *Journal of Neuroscience*, 33(27):11194–11205, Jul 2013. ISSN 0270-6474, 1529-2401. doi: 10.1523/JNEUROSCI.0114-13.2013. 54, 56, 67

Andy Clark. An embodied cognitive science? *Trends in Cognitive Sciences*, 3(9):345–351, 1999. ISSN 13646613. doi: 10.1016/S1364-6613(99)01361-3. 90

Simon Clavagnier, Arnaud Falchier, and Henry Kennedy. Long-distance feedback projections to area V1: implications for multisensory integration, spatial awareness, and visual consciousness. *Cognitive, affective & behavioral neuroscience*, 4(2):117–126, 2004. ISSN 1530-7026. doi: 10.3758/CABN.4.2.117. 53

Mike X Cohen. *Analyzing Neural Time Series Data: Theory and Practice*. 2014. ISBN 0262019876. doi: 10.1017/CBO9781107415324.004. 11, 12

- Marco D. Comerchero and John Polich. P3a and P3b from typical auditory and visual stimuli. *Clinical Neurophysiology*, 110(1):24–30, 1999. ISSN 13882457. doi: 10.1016/S0168-5597(98)00033-1. 14
- Blas Couto, Federico Adolphi, María Velasquez, Marie Mesow, Justin Feinstein, Andres Canales-Johnson, Ezequiel Mikulan, David Martínez-Pérez, Tristan Bekinschtein, Mariano Sigman, Facundo Manes, and Agustin Ibanez. Heart evoked potential triggers brain responses to natural affective scenes: A preliminary study. *Autonomic Neuroscience: Basic and Clinical*, 193:132–137, 2015. ISSN 18727484. doi: 10.1016/j.autneu.2015.06.006. 88
- A. D. Craig. How do you feel? Interoception: the sense of the physiological condition of the body. *Nature Reviews Neuroscience*, 3(8):655–666, aug 2002. ISSN 1471-003X. doi: 10.1038/nrn894. 70
- Hugo D Critchley, Christopher J Mathias, and Raymond J Dolan. Neural Activity in the Human Brain Relating to Uncertainty and Arousal during Anticipation. *Neuron*, 29(2): 537–545, feb 2001. ISSN 08966273. doi: 10.1016/S0896-6273(01)00225-2. 70
- Damian Cruse, Srivas Chennu, Camille Chatelle, Tristan A. Bekinschtein, Davinia Fernández-Espejo, John D. Pickard, Steven Laureys, and Adrian M. Owen. Bedside detection of awareness in the vegetative state: A cohort study. *The Lancet*, 378(9809):2088–2094, 2011. ISSN 01406736. doi: 10.1016/S0140-6736(11)61224-5. 15
- Damian Cruse, Srivas Chennu, Davinia Fernández-Espejo, William L. Payne, G. Bryan Young, and Adrian M. Owen. Detecting Awareness in the Vegetative State: Electroencephalographic Evidence for Attempted Movements to Command. *PLoS ONE*, 7(11):1–9, 2012. ISSN 19326203. doi: 10.1371/journal.pone.0049933. 15
- Roel W. Deboer, John M. Karemaker, and Jan Strackee. Comparing Spectra of a Series of Point Events Particularly for Heart Rate Variability Data. *IEEE Transactions on Biomedical Engineering*, BME-31(4):384–387, 1984. ISSN 15582531. doi: 10.1109/TBME.1984.325351. 75
- Stanislas Dehaene and Jean Pierre Changeux. Experimental and Theoretical Approaches to Conscious Processing. *Neuron*, 70(2):200–227, 2011. ISSN 08966273. doi: 10.1016/j.neuron.2011.03.018. 2, 14, 17, 53
- Stanislas Dehaene, Jean Pierre Changeux, Lionel Naccache, Jérôme Sackur, and Claire Sergent. Conscious, preconscious, and subliminal processing: a testable taxonomy. *Trends in Cognitive Sciences*, 10(5):204–211, may 2006. ISSN 13646613. doi: 10.1016/j.tics.2006.03.007. 14, 50, 67

- A. Demertzi, C. Schnakers, D. Ledoux, C. Chatelle, M. A. Bruno, A. Vanhaudenhuyse, M. Boly, G. Moonen, and S. Laureys. Different beliefs about pain perception in the vegetative and minimally conscious states: a European survey of medical and paramedical professionals, 2009. ISSN 00796123. 3
- A. Demertzi, D. Ledoux, M. A. Bruno, A. Vanhaudenhuyse, O. Gosseries, A. Soddu, C. Schnakers, G. Moonen, and S. Laureys. Attitudes towards end-of-life issues in disorders of consciousness: A European survey. *Journal of Neurology*, 258(6):1058–1065, 2011. ISSN 03405354. doi: 10.1007/s00415-010-5882-z. 3
- Athena Demertzi, Georgios Antonopoulos, Lizette Heine, Henning U. Voss, Julia Sophia Crone, Carlo De Los Angeles, Mohamed Ali Bahri, Carol Di Perri, Audrey Vanhaudenhuyse, Vanessa Charland-Verville, Martin Kronbichler, Eugen Trinkka, Christophe Phillips, Francisco Gomez, Luaba Tshibanda, Andrea Soddu, Nicholas D. Schiff, Susan Whitfield-Gabrieli, and Steven Laureys. Intrinsic functional connectivity differentiates minimally conscious from unresponsive patients. *Brain*, 138(9):2619–2631, 2015. ISSN 14602156. doi: 10.1093/brain/awv169. 8, 95
- Joseph Dien, Kevin M. Spencer, and Emanuel Donchin. Localization of the event-related potential novelty response as defined by principal components analysis. *Cognitive Brain Research*, 17(3):637–650, 2003. ISSN 09266410. doi: 10.1016/S0926-6410(03)00188-5. 14
- G Dirlich, L Vogl, M Plaschke, and F Strian. Cardiac field effects on the EEG. 102:307–315, 1997. 73, 78
- Emanuel Donchin. Discriminant analysis in average evoked response studies: The study of single trial data. *Electroencephalography and Clinical Neurophysiology*, 27(3):311–314, 1969. ISSN 00134694. doi: 10.1016/0013-4694(69)90061-3. 15
- Emanuel Donchin and Michael G.H. Coles. Is the P300 component a manifestation of context updating? *Behavioral and Brain Sciences*, 11(3):357–374, 1988. ISSN 14691825. doi: 10.1017/S0140525X00058027. 50
- Jon Driver and Toemme Noesselt. Multisensory Interplay Reveals Crossmodal Influences on 'Sensory-Specific' Brain Regions, Neural Responses, and Judgments. *Neuron*, 57(1): 11–23, 2008. ISSN 08966273. doi: 10.1016/j.neuron.2007.12.013. 53
- B Efron and R J Tibshirani. An introduction to the bootstrap. *Refrigeration And Air Conditioning*, 57(57):436, 1993. ISSN 04120423. doi: 10.1111/1467-9639.00050. 36
- Bradley Efron and Trevor Hastie. *Computer Age Statistical Inference*. Cambridge University Press, Cambridge, 2016. ISBN 9781316576533. doi: 10.1017/CBO9781316576533. 35

- Bradley. Efron and Robert. Tibshirani. *An introduction to the bootstrap*. Chapman & Hall, 1994. ISBN 9780412042317. 23
- Mohamed Elgendi. Fast QRS Detection with an Optimized Knowledge-Based Method: Evaluation on 11 Standard ECG Databases. *PLoS ONE*, 8(9), 2013. ISSN 19326203. doi: 10.1371/journal.pone.0073557. 73
- Andreas K. Engel, Pascal Fries, and Wolf Singer. Dynamic predictions: Oscillations and synchrony in top-down processing. *Nature Reviews Neuroscience*, 2(10):704–716, 2001. ISSN 1471-003X. doi: 10.1038/35094565. 11
- Marc O. Ernst and Heinrich H. Bühlhoff. Merging the senses into a robust percept. *Trends in Cognitive Sciences*, 8(4):162–169, 2004. ISSN 13646613. doi: 10.1016/j.tics.2004.02.002. 52
- Horacio Fabrega. The Feeling of What Happens: Body and Emotion in the Making of Consciousness. *Psychiatric Services*, 51(12):1579–1579, dec 2000. ISSN 1075-2730. doi: 10.1176/appi.ps.51.12.1579. 52
- F. Faugeras, B. Rohaut, N. Weiss, T. A. Bekinschtein, D. Galanaud, L. Puybasset, F. Bolgert, C. Sergent, L. Cohen, S. Dehaene, and L. Naccache. Probing consciousness with event-related potentials in the vegetative state. *Neurology*, 77(3):264–268, jul 2011. ISSN 00283878. doi: 10.1212/WNL.0b013e3182217ee8. 16, 71, 89
- Frédéric Faugeras, Benjamin Rohaut, Nicolas Weiss, Tristan Bekinschtein, Damien Galanaud, Louis Puybasset, Francis Bolgert, Claire Sergent, Laurent Cohen, Stanislas Dehaene, and Lionel Naccache. Event related potentials elicited by violations of auditory regularities in patients with impaired consciousness. *Neuropsychologia*, 50(3):403–418, feb 2012. ISSN 00283932. doi: 10.1016/j.neuropsychologia.2011.12.015. 16, 67, 71
- Frédéric Faugeras, Benjamin Rohaut, Mélanie Valente, Jacobo Sitt, Sophie Demeret, Francis Bolgert, Nicolas Weiss, Alexandra Grinea, Clémence Marois, Marion Quirins, Athena Demertzi, Federico Raimondo, Damien Galanaud, Marie-Odile Habert, Denis Engemann, Louis Puybasset, and Lionel Naccache. Survival and consciousness recovery are better in the minimally conscious state than in the vegetative state. *Brain Injury*, pages 1–6, nov 2017. ISSN 0269-9052. doi: 10.1080/02699052.2017.1364421. 5
- Joseph J. Fins. Constructing an ethical stereotaxy for severe brain injury: Balancing risks, benefits and access. *Nature Reviews Neuroscience*, 4(4):323–327, 2003. ISSN 14710048. doi: 10.1038/nrn1079. 3

Catherine Fischer, Jacques Luauté, Patrice Adeleine, and Dominique Morlet. Predictive value of sensory and cognitive evoked potentials for awakening from coma. *Neurology*, 63(4): 669–673, 2004. ISSN 00283878. doi: 10.1212/01.WNL.0000134670.10384.E2. 16

Catherine Fischer, Jacques Luauté, and Dominique Morlet. Event-related potentials (MMN and novelty P3) in permanent vegetative or minimally conscious states. *Clinical Neurophysiology*, 121(7):1032–1042, 2010. ISSN 13882457. doi: 10.1016/j.clinph.2010.02.005. 16

Alexandra Fort, Claude Delpuech, Jacques Pernier, and M. H. Giard. Early auditory-visual interactions in human cortex during nonredundant target identification. *Cognitive Brain Research*, 14(1):20–30, 2002. ISSN 09266410. doi: 10.1016/S0926-6410(02)00058-7. 54

David Friedman and YM Cycowicz. The novelty P3: an event-related brain potential (ERP) sign of the brain's evaluation of novelty. *Neuroscience & Biobehavioral*, 25(4):355–373, 2001. 14

Karl Friston. Beyond Phrenology: What Can Neuroimaging Tell Us About Distributed Circuitry? *Annual Review of Neuroscience*, 25(1):221–250, 2002. ISSN 0147-006X. doi: 10.1146/annurev.neuro.25.112701.142846. 17

Thomas Frodl-Bauch, Ronald Bottlender, and Ulrich Hegerl. Neurochemical substrates and neuroanatomical generators of the event-related P300, 1999. ISSN 0302282X. 14

Damien Galanaud, Vincent Perlberg, Rajiv Gupta, Robert D Stevens, Paola Sanchez, Eléonore Tollard, Nicolas Menjot de Champfleury, Julien Dinkel, Sébastien Faivre, Gustavo Soto-Ares, Benoit Veber, Vincent Cottenceau, Françoise Masson, Thomas Tourdias, Edith André, Gérard Audibert, Emmanuelle Schmitt, Danielle Ibarrola, Frédéric Dailley, Audrey Vanhauzenhuyse, Luaba Tshibanda, Jean-François Payen, Jean-François Le Bas, Alexandre Krainik, Nicolas Bruder, Nadine Girard, Steven Laureys, Habib Benali, and Louis Puybasset. Assessment of white matter injury and outcome in severe brain trauma: a prospective multicenter cohort. *Anesthesiology*, 117(6):1300–10, 2012. ISSN 1528-1175. doi: 10.1097/ALN.0b013e3182755558. 6

Shaun Gallagher. Philosophical conceptions of the self: implications for cognitive science. *Trends in Cognitive Sciences*, 4(1):14–21, Jan 2000. ISSN 13646613. doi: 10.1016/S1364-6613(99)01417-5. 92

Indira García-Cordero, Lucas Sedeño, Laura De La Fuente, Andrea Slachevsky, Gonzalo Forno, Francisco Klein, Patricia Lillo, Jessica Ferrari, Clara Rodriguez, Julian Bustin,

- Teresa Torralva, Sandra Baez, Adrian Yoris, Sol Esteves, Margherita Melloni, Paula Salamone, David Huepe, Facundo Manes, Adolfo M García, and Agustín Ibañez. Feeling, learning from, and being aware of inner states: Interoceptive dimensions in neurodegeneration and stroke. *Philosophical Transactions of the Royal Society of London B: Biological Sciences*, (Accepted):0–34, 2016. ISSN 1972952943. doi: 10.1098/rstb.2016-0006. Accepted. 88
- Luis Garcia-Larrea, François Mauguier, François Artru, Olivier Bertrand, and Jacques Pernier. The combined monitoring of brain stem auditory evoked potentials and intracranial pressure in coma. A study of 57 patients. *Journal of Neurology, Neurosurgery and Psychiatry*, 55(9):792–798, 1992. ISSN 00223050. doi: 10.1136/jnnp.55.9.792. 15
- Pierre Geurts, Damien Ernst, and Louis Wehenkel. Extremely randomized trees. *Machine Learning*, 63(1):3–42, 2006. ISSN 08856125. doi: 10.1007/s10994-006-6226-1. 34, 47
- Joseph T. Giacino, Mary Ann Kezarsky, John DeLuca, and Keith D. Cicerone. Monitoring rate of recovery to predict outcome in minimally responsive patients. *Archives of Physical Medicine and Rehabilitation*, 72(11):897–901, 1991. ISSN 00039993. doi: 10.1016/0003-9993(91)90008-7. 17
- Joseph T Giacino, S Ashwal, N Childs, R Cranford, B Jennett, D I Katz, J P Kelly, J H Rosenberg, J Whyte, R D Zafonte, and N D Zasler. The minimally conscious state: definition and diagnostic criteria. *Neurology*, 58(3):349–53, 2002. ISSN 0028-3878. doi: 10.1212/WNL.58.3.349. 3, 5
- Joseph T. Giacino, Kathleen Kalmar, and John Whyte. The JFK Coma Recovery Scale-Revised: Measurement characteristics and diagnostic utility, 2004. ISSN 00039993. 5, 18
- Joseph T. Giacino, Joseph J. Fins, Steven Laureys, and Nicholas D. Schiff. Disorders of consciousness after acquired brain injury: The state of the science. *Nature Reviews Neurology*, 10(2):99–114, 2014. ISSN 17594758. doi: 10.1038/nrneurol.2013.279. 6, 89
- M H Giard and F Peronnet. Auditory-Visual Integration during Multimodal Object Recognition in Humans: A Behavioral and Electrophysiological Study. *Dx.Doi.Org*, 11(5):473–490, 2006. ISSN 0898-929X. doi: 10.1162/089892999563544. 54, 67
- Andrew M. Goldfine, Jonathan D. Victor, Mary M. Conte, Jonathan C. Bardin, and Nicholas D. Schiff. Determination of awareness in patients with severe brain injury using EEG power spectral analysis. *Clinical Neurophysiology*, 122(11):2157–2168, 2011. ISSN 13882457. doi: 10.1016/j.clinph.2011.03.022. 15

- Andrew M Goldfine, Jonathan C Bardin, Quentin Noirhomme, Joseph J Fins, Nicholas D Schiff, and Jonathan D Victor. Reanalysis of "Bedside detection of awareness in the vegetative state: a cohort study". *Lancet (London, England)*, 381(9863):289–91, jan 2013. ISSN 1474-547X. doi: 10.1016/S0140-6736(13)60125-7. 16
- Abraham Goldstein, Kevin M. Spencer, and Emanuel Donchin. The influence of stimulus deviance and novelty on the P300 and Novelty P3. *Psychophysiology*, 39(06):781–790, 2002. ISSN 1469-8986. doi: 10.1017/S004857720201048X. 14, 67
- Alexandre Gramfort, Martin Luessi, Eric Larson, Denis A. Engemann, Daniel Strohmeier, Christian Brodbeck, Roman Goj, Mainak Jas, Teon Brooks, Lauri Parkkonen, and Matti S. Hämäläinen. MEG and EEG data analysis with MNE-Python. *Frontiers in Neuroscience*, 7(7 DEC):267, 2013. ISSN 1662453X. doi: 10.3389/fnins.2013.00267. 28, 58
- Alexandre Gramfort, Martin Luessi, Eric Larson, Denis A. Engemann, Daniel Strohmeier, Christian Brodbeck, Lauri Parkkonen, and Matti S. Hämäläinen. MNE software for processing MEG and EEG data. *NeuroImage*, 86:446–460, 2014. ISSN 10959572. doi: 10.1016/j.neuroimage.2013.10.027. 28, 58
- Marcus A Gray, Peter Taggart, Peter M Sutton, David Groves, Diana R Holdright, David Bradbury, David Brull, and Hugo D Critchley. A cortical potential reflecting cardiac function. *Proceedings of the National Academy of Sciences of the United States of America*, 104:6818–6823, 2007. ISSN 0027-8424. doi: 10.1073/pnas.0609509104. 70, 88
- Jess Hartcher-O'Brien, Salvador Soto-Faraco, and Ruth Adam. Editorial: A Matter of Bottom-Up or Top-Down Processes: The Role of Attention in Multisensory Integration. *Frontiers in Integrative Neuroscience*, 11(February):10–12, 2017. ISSN 1662-5145. doi: 10.3389/fnint.2017.00005. 53
- Christoph S. Herrmann, Ingo Fründ, and Daniel Lenz. Human gamma-band activity: A review on cognitive and behavioral correlates and network models. *Neuroscience & Biobehavioral Reviews*, 34(7):981–992, 2010. ISSN 01497634. doi: 10.1016/j.neubiorev.2009.09.001. 11
- Malcolm Horne. Are people in a persistent vegetative state conscious? *Monash bioethics review*, 28(2):12–1–12, 2009. ISSN 1321-2753. 3
- A. Hyvärinen and E. Oja. Independent component analysis: Algorithms and applications. *Neural Networks*, 13(4-5):411–430, 2000. ISSN 08936080. doi: 10.1016/S0893-6080(00)00026-5. 73

- Mainak Jas, D.A. Denis A. Engemann, Yousra Bekhti, Federico Raimondo, and Alexandre Gramfort. Autoreject: Automated artifact rejection for MEG and EEG data. *NeuroImage*, 159(December 2016):417–429, dec 2016. ISSN 10538119. doi: 10.1016/j.neuroimage.2017.06.030. 29
- Herbert H. Jasper. Report of the committee on methods of clinical examination in electroencephalography. *Electroencephalography and Clinical Neurophysiology*, 10(2):370–375, 1958. ISSN 00134694. doi: 10.1016/0013-4694(58)90053-1. 11
- Bryan Jennett and Fred Plum. Persistent Vegetative State After Brain Damage: A Syndrome in Search of a Name. *The Lancet*, 299(7753):734–737, 1972. ISSN 01406736. doi: 10.1016/S0140-6736(72)90242-5. 3
- J. Richard Jennings and Charles C. Wood. Cardiac Cycle Time Effects on Performance, Phasic Cardiac Responses, and Their Intercorrelation in Choice Reaction Time. *Psychophysiology*, 14(3):297–307, 1977. ISSN 14698986. doi: 10.1111/j.1469-8986.1977.tb01179.x. 70, 89
- Eric Jones, Travis Oliphant, Pearu Peterson, and Others. SciPy.org, 2001. 28
- Ralf J Jox, James L Bernat, Steven Laureys, and Eric Racine. Disorders of consciousness: responding to requests for novel diagnostic and therapeutic interventions. *Lancet neurology*, 11(8):732–8, 2012. ISSN 1474-4465. doi: 10.1016/S1474-4422(12)70154-0. 5
- Guy Kahane and Julian Savulescu. Brain damage and the moral significance of consciousness, 2009. ISSN 03605310. 3
- Andreas Kampfl, Erich Schmutzhard, Gerhard Franz, Bettina Pfausler, Hans Peter Haring, Hanno Ulmer, Stefan Felber, Stefan Golaszewski, and Franz Aichner. Prediction of recovery from post-traumatic vegetative state with cerebral magnetic-resonance imaging. *Lancet*, 351(9118):1763–1767, 1998. ISSN 01406736. doi: 10.1016/S0140-6736(97)10301-4. 6
- N. M. Kane, S. H. Curry, S. R. Butler, and B. H. Cummins. Electrophysiological indicator of awakening from coma, 1993. ISSN 01406736. 16
- Christina M Karns and Robert T Knight. Intermodal auditory, visual, and tactile attention modulates early stages of neural processing. *Journal of cognitive neuroscience*, 21(4): 669–83, 2009. ISSN 0898-929X. doi: 10.1162/jocn.2009.21037. 53
- Robert Kass and Adrian Raftery. Bayes Factors. *J. Amer. Statist. Assoc.*, 90(430):773–795, 1995. 22

- J. R. King and S. Dehaene. Characterizing the dynamics of mental representations: The temporal generalization method, 2014. ISSN 1879307X. 59
- J. R. King, F. Faugeras, A. Gramfort, A. Schurger, I. El Karoui, J. D. Sitt, B. Rohaut, C. Wacongne, E. Labyt, T. Bekinschtein, L. Cohen, L. Naccache, and S. Dehaene. Single-trial decoding of auditory novelty responses facilitates the detection of residual consciousness. *NeuroImage*, 83:726–738, 2013a. ISSN 10538119. doi: 10.1016/j.neuroimage.2013.07.013. 15, 50, 71
- Jean Rémi King, Jacobo D. Sitt, Frédéric Faugeras, Benjamin Rohaut, Imen El Karoui, Laurent Cohen, Lionel Naccache, and Stanislas Dehaene. Information sharing in the brain indexes consciousness in noncommunicative patients. *Current Biology*, 23(19):1914–1919, 2013b. ISSN 09609822. doi: 10.1016/j.cub.2013.07.075. 29
- Jean Rémi King, Alexandre Gramfort, Aaron Schurger, Lionel Naccache, and Stanislas Dehaene. Two distinct dynamic modes subtend the detection of unexpected sounds. *PLoS ONE*, 9(1), 2014. ISSN 1932-6203 (Electronic)r1932-6203 (Linking). doi: 10.1371/journal.pone.0085791. 67
- W M Kistler, J L van Hemmen, and C I De Zeeuw. Time window control: a model for cerebellar function based on synchronization, reverberation, and time slicing. *Progress in brain research*, 124:275–97, 2000. ISSN 0079-6123. doi: 10.1016/S0079-6123(00)24023-5. 11
- Wolfgang Klimesch, Paul Sauseng, and Simon Hanslmayr. EEG alpha oscillations : The inhibition – timing hypothesis. *Brain Research Reviews*, 53:63–88, 2007. ISSN 0165-0173. doi: 10.1016/j.brainresrev.2006.06.003. 11
- Ron Kohavi and George H. John. Wrappers for feature subset selection. *Artificial Intelligence*, 97(1-2):273–324, dec 1997. ISSN 00043702. doi: 10.1016/S0004-3702(97)00043-X. 82
- Albert Kok, Jennifer R. Ramautar, Michiel B. De Ruiter, Guido P.H. Band, and K. Richard Ridderinkhof. ERP components associated with successful and unsuccessful stopping in a stop-signal task. *Psychophysiology*, 41(1):9–20, 2004. ISSN 00485772. doi: 10.1046/j.1469-8986.2003.00127.x. 14
- Nancy Kopell, Mark A. Kramer, Paola Malerba, and Miles A. Whittington. Are Different Rhythms Good for Different Functions? *Frontiers in Human Neuroscience*, 4, 2010. ISSN 1662-5161. doi: 10.3389/fnhum.2010.00187. 12

- S. Kouider and S. Dehaene. Levels of processing during non-conscious perception: a critical review of visual masking. *Philosophical Transactions of the Royal Society B: Biological Sciences*, 362(1481):857–875, 2007. ISSN 0962-8436. doi: 10.1098/rstb.2007.2093. 53
- Beatrice C Lacey and John I Lacey. Two-way communication between the heart and the brain. Significance of time within the cardiac cycle. *American Psychologist*, 33(2):99–113, 1978. ISSN 0003-066X. doi: 10.1037/0003-066X.33.2.99. 70
- Steven Laureys. Death, unconsciousness and the brain, 2005a. ISSN 1471003X. 7
- Steven Laureys. The neural correlate of (un)awareness: Lessons from the vegetative state. *Trends in Cognitive Sciences*, 9(12):556–559, 2005b. ISSN 13646613. doi: 10.1016/j.tics.2005.10.010. 4, 17, 95
- Steven Laureys and Melanie Boly. What is it like to be vegetative or minimally conscious? *Current opinion in neurology*, 20(6):609–613, 2007. ISSN 1350-7540. doi: 10.1097/WCO.0b013e3282f1d6dd. 2
- Steven Laureys and Nicholas D Schiff. NeuroImage Coma and consciousness : Paradigms (re) framed by neuroimaging. *NeuroImage*, 61(2):478–491, 2012. ISSN 1053-8119. doi: 10.1016/j.neuroimage.2011.12.041. 7
- T W Lee, M Girolami, and T J Sejnowski. Independent component analysis using an extended infomax algorithm for mixed subgaussian and supergaussian sources. *Neural computation*, 11:417–441, 1999. ISSN 0899-7667. doi: 10.1162/089976699300016719. 58, 73
- Bigna Lenggenhager, Tej Tadi, Thomas Metzinger, and Olaf Blanke. Video ergo sum: Manipulating bodily self-consciousness. *Science*, 317(5841):1096–1099, 2007. ISSN 00368075. doi: 10.1126/science.1143439. 53
- Antonino Leo, Antonino Naro, Antonio Cannavò, Laura Rosa Pisani, Rocco Bruno, Carlo Salviera, Placido Bramanti, and Rocco Salvatore Calabrò. Could autonomic system assessment be helpful in disorders of consciousness diagnosis? A neurophysiological study. *Experimental Brain Research*, 234(8):2189–2199, 2016. ISSN 14321106. doi: 10.1007/s00221-016-4622-8. 70, 71, 78, 86
- María J Leone, Agustín Petroni, Diego Fernandez Slezak, and Mariano Sigman. The tell-tale heart: heart rate fluctuations index objective and subjective events during a game of chess. *Frontiers in human neuroscience*, 6(October):273, 2012. ISSN 1662-5161. doi: 10.3389/fnhum.2012.00273. 70, 88

- G Litscher. Middle latency auditory evoked potentials in intensive care patients and normal controls. *The International journal of neuroscience*, 83(3-4):253–267, 1995. ISSN 00207454. doi: 10.3109/00207459508986342. 15
- Gilles Louppe. Understanding Random Forests: From Theory to Practice. jul 2014. 48
- Gilles Louppe, Louis Wehenkel, Antonio Sutera, and Pierre Geurts. Understanding variable importances in forests of randomized trees. *Advances in Neural Information Processing Systems 26*, pages 431–439, 2013. ISSN 1098-6596. doi: NIPS2013_4928. 35, 47
- Dorothee Lulé, Quentin Noirhomme, Sonja C. Kleih, Camille Chatelle, Sebastian Halder, Athena Demertzi, Marie Aurélie Bruno, Olivia Gosseries, Audrey Vanhauzenhuyse, Caroline Schnakers, Marie Thonnard, Andrea Soddu, Andrea Kübler, and Steven Laureys. Probing command following in patients with disorders of consciousness using a brain-computer interface. *Clinical Neurophysiology*, 124(1):101–106, 2013. ISSN 13882457. doi: 10.1016/j.clinph.2012.04.030. 49
- B. Lütkenhöner, C. Lammertmann, C. Simões, and R. Hari. Magnetoencephalographic correlates of audiotactile interaction. *NeuroImage*, 15(3):509–522, 2002. ISSN 10538119. doi: 10.1006/nimg.2001.0991. 53
- Charles-Edouard Luyt, Damien Galanaud, Vincent Perlberg, Audrey Vanhauzenhuyse, Robert D Stevens, Rajiv Gupta, Hortense Besancenot, Alexandre Krainik, Gérard Audibert, Alain Combes, Jean Chastre, Habib Benali, Steven Laureys, and Louis Puybasset. Diffusion tensor imaging to predict long-term outcome after cardiac arrest: a bi-centric pilot study. *Anesthesiology*, 117(6):1311–21, 2012. ISSN 1528-1175. doi: 10.1097/ALN.0b013e318275148c. 6
- Scott Makeig, Scott Makeig, Stefan Debener, Stefan Debener, Julie Onton, Julie Onton, Arnaud Delorme, and Arnaud Delorme. Mining event-related brain dynamics. *Trends in Cognitive Sciences*, 8(5):204–210, 2004. ISSN 1364-6613. doi: 10.1016/j.tics.2004.03.008. 12
- Eric Maris and Robert Oostenveld. Nonparametric statistical testing of EEG- and MEG-data. 164:177–190, 2007. doi: 10.1016/j.jneumeth.2007.03.024. 60, 75
- Chris J. McBain and Julie A. Kauer. Presynaptic plasticity: targeted control of inhibitory networks, 2009. ISSN 09594388. 11
- Tom M Mitchell. *Machine Learning*. Number 1. 1997. ISBN 0070428077. doi: 10.1145/242224.242229. 19

R D Morey, J N Rouder, and T Jamil. BayesFactor: Computation of Bayes factors for common designs. *R package version 0.9*, 8, 2014. 22

Dominique Morlet and Catherine Fischer. MMN and Novelty P3 in Coma and Other Altered States of Consciousness: A Review. *Brain topography*, nov 2013. ISSN 1573-6792. doi: 10.1007/s10548-013-0335-5. 89

Lionel Naccache. Minimally conscious state or cortically mediated state? *Brain*, 2017. ISSN 0006-8950. doi: 10.1093/brain/awx324. 50

Lionel Naccache, Louis Puybasset, Raphaël Gaillard, Emilie Serve, and Jean Claude Willer. Auditory mismatch negativity is a good predictor of awakening in comatose patients: A fast and reliable procedure [1]. *Clinical Neurophysiology*, 116(4):988–989, 2005. ISSN 13882457. doi: 10.1016/j.clinph.2004.10.009. 16

Lionel Naccache, Jean-Rémi King, Jacobo Sitt, Denis Engemann, Imen El Karoui, Benjamin Rohaut, Frederic Faugeras, Srivas Chennu, Mélanie Strauss, Tristán Bekinschtein, and Stanislas Dehaene. Neural detection of complex sound sequences in the absence of consciousness? *Brain*, 138, 2015. doi: 10.1093/brain/awv190. 89

Ernst Niedermeyer and F H Lopes Da Silva. *Electroencephalography: Basic Principles, Clinical Applications, and Related Fields*, volume 1. 2004. ISBN 0781751268. 12, 15

Hyeong-Dong Park and Catherine Tallon-Baudry. The neural subjective frame: from bodily signals to perceptual consciousness. *Philosophical transactions of the Royal Society of London. Series B, Biological sciences*, 369(1641):20130208, 2014. ISSN 1471-2970. doi: 10.1098/rstb.2013.0208. 70

Hyeong-Dong Park, Stéphanie Correia, Antoine Ducorps, and Catherine Tallon-Baudry. Spontaneous fluctuations in neural responses to heartbeats predict visual detection. *Nature neuroscience*, 17(4):612–8, 2014. ISSN 1546-1726. doi: 10.1038/nn.3671. 70, 88, 89

Fabian Pedregosa, Gaël Varoquaux, Alexandre Gramfort, Vincent Michel, Bertrand Thirion, Olivier Grisel, Mathieu Blondel, Peter Prettenhofer, Ron Weiss, Vincent Dubourg, Jake Vanderplas, Alexandre Passos, David Cournapeau, Matthieu Brucher, Matthieu Perrot, and Édouard Duchesnay. Scikit-learn: Machine Learning in Python. *Journal of Machine Learning Research*, 12:2825–2830, 2012. ISSN 15324435. doi: 10.1007/s13398-014-0173-7.2. 28, 34

Delphine Pins and Dominic Ffytche. The neural correlates of conscious vision. *Cerebral Cortex*, 13(5):461–474, 2003. ISSN 10473211. doi: 10.1093/cercor/13.5.461. 50

- J Platt. Probabilistic outputs for support vector machines and comparisons to regularized likelihood methods. *Advances in large margin classifiers*, 10(3):61–74, 1999. ISSN 0262194481. doi: 10.1.1.41.1639. 34
- John Polich. Updating P300: An integrative theory of P3a and P3b. *Clinical Neurophysiology*, 118(10):2128–2148, 2007. ISSN 13882457. doi: 10.1016/j.clinph.2007.04.019. 14, 50, 67
- J.B. Posner, Fred Plum, and Clifford Saper. *Plum and Posner’s Diagnosis of Estupor and Coma*, volume 1. 2007. ISBN 9780195321319. doi: 10.1002/1521-3773(20010316)40:6<9823::AID-ANIE9823>3.3.CO;2-C. 2
- P. L. Purdon, E. T. Pierce, E. A. Mukamel, M. J. Prerau, J. L. Walsh, K. F. K. Wong, A. F. Salazar-Gomez, P. G. Harrell, A. L. Sampson, A. Cimenser, S. Ching, N. J. Kopell, C. Tavares-Stoekel, K. Habeeb, R. Merhar, and E. N. Brown. Electroencephalogram signatures of loss and recovery of consciousness from propofol. *Proceedings of the National Academy of Sciences*, 110(12):E1142–E1151, 2013. ISSN 0027-8424. doi: 10.1073/pnas.1221180110. 49
- Timothy E Quill. Terri Schiavo—a tragedy compounded. *The New England journal of medicine*, 352(16):1630–1633, 2005. ISSN 1533-4406. doi: 10.1056/NEJMp058062. 3
- R Development Core Team. R: A Language and Environment for Statistical Computing. *R Foundation for Statistical Computing Vienna Austria*, 0:{ISBN} 3–900051–07–0, 2016. ISSN 16000706. doi: 10.1038/sj.hdy.6800737. 22
- E. Racine, R. Amaram, M. Seidler, M. Karczewska, and J. Illes. Media coverage of the persistent vegetative state and end-of-life-decision-making. *Neurology*, 71(13):1027–1032, 2008. ISSN 1526-632X. doi: 10.1212/01.wnl.0000320507.64683.ee. 3
- M Rappaport, A M Dougherty, and D L Kelting. Evaluation of coma and vegetative states. *Archives of physical medicine and rehabilitation*, 73(7):628–34, 1992. ISSN 0003-9993. 6
- Benjamin Rohaut, Frédéric Faugeras, Nicolas Chausson, Jean Rémi King, Imen El Karoui, Laurent Cohen, and Lionel Naccache. Probing ERP correlates of verbal semantic processing in patients with impaired consciousness. *Neuropsychologia*, 66:279–292, 2015. ISSN 18733514. doi: 10.1016/j.neuropsychologia.2014.10.014. 15
- Benjamin Rohaut, Federico Raimondo, Damien Galanaud, Mélanie Valente, Jacobo Diego J.D. Sitt, and Lionel Naccache. Probing consciousness in a sensory-disconnected

- paralyzed patient. *Brain Injury*, 31(08):1–6, 2017. ISSN 0269-9052. doi: 10.1080/02699052.2017.1327673. 50, 52, 68
- Jeffrey N. Rouder, Richard D. Morey, Paul L. Speckman, and Jordan M. Province. Default Bayes factors for ANOVA designs. *Journal of Mathematical Psychology*, 56(5):356–374, 2012. ISSN 00222496. doi: 10.1016/j.jmp.2012.08.001. 22
- Sepideh Sadaghiani and Andreas Kleinschmidt. *Brain Networks and α -Oscillations: Structural and Functional Foundations of Cognitive Control*, 2016. ISSN 1879307X. 49
- Roy Salomon, Jean Paul Noel, Marta Łukowska, Nathan Faivre, Thomas Metzinger, Andrea Serino, and Olaf Blanke. Unconscious integration of multisensory bodily inputs in the peripersonal space shapes bodily self-consciousness. *Cognition*, 166:174–183, 2017. ISSN 18737838. doi: 10.1016/j.cognition.2017.05.028. 53
- Saeid Sanei and Jonathon. A. Chambers. *EEG Signal Processing*, volume 1. 2007. ISBN 9780470025819. doi: 10.1002/9780470511923. 9, 13
- B M Sayers, H A Beagley, and W R Henshall. The mechanism of auditory evoked EEG responses. *Nature*, 247(441):481–483, 1974. ISSN 0028-0836. doi: 10.1038/247481a0. 12
- Nicholas D. Schiff. Recovery of consciousness after brain injury: a mesocircuit hypothesis, 2010. ISSN 01662236. 49
- C Schnakers and S Laureys. Voluntary Brain Processing in Disorders of Consciousness Reply. *Neurology*, 73(20):1712–1713, 2009. 16
- Caroline Schnakers, Joseph Giacino, Kathleen Kalmar, Sonia Pitet, Eduardo Lopez, Mélanie Boly, Richard Malone, and Steven Laureys. Does the FOUR score correctly diagnose the vegetative and minimally conscious states? [1], 2006. ISSN 03645134. 5
- Caroline Schnakers, Audrey Vanhauzenhuyse, Joseph Giacino, Manfredi Ventura, Melanie Boly, Steve Majerus, Gustave Moonen, and Steven Laureys. Diagnostic accuracy of the vegetative and minimally conscious state: clinical consensus versus standardized neurobehavioral assessment. *BMC neurology*, 9:35, 2009. ISSN 1471-2377. doi: 10.1186/1471-2377-9-35. 5, 52
- Caroline Schnakers, Helene Bessou, Ilona Rubi-Fessen, Alexander Hartmann, Gereon R. Fink, Ingo Meister, Joseph T. Giacino, Steven Laureys, and Steve Majerus. Impact of Aphasia on Consciousness Assessment. *Neurorehabilitation and Neural Repair*, 29(1): 41–47, 2015. ISSN 1545-9683. doi: 10.1177/1545968314528067. 5

Paul W Schoenle and W Witzke. How vegetative is the vegetative state? Preserved semantic processing in VS patients—evidence from N 400 event-related potentials. *NeuroRehabilitation*, 19(4):329–334, 2004. ISSN 1053-8135. 15

Daniel Senkowski, Till R. Schneider, John J. Foxe, and Andreas K. Engel. Crossmodal binding through neural coherence: implications for multisensory processing. *Trends in Neurosciences*, 31(8):401–409, 2008. ISSN 01662236. doi: 10.1016/j.tins.2008.05.002. 53

Claire Sergent, Sylvain Baillet, and Stanislas Dehaene. Timing of the brain events underlying access to consciousness during the attentional blink. *Nature Neuroscience*, 8(10):1391–1400, 2005. ISSN 10976256. doi: 10.1038/nn1549. 50

Claire Sergent, Frédéric Faugeras, Benjamin Rohaut, Fabien Perrin, Mélanie Valente, Catherine Tallon-Baudry, Laurent Cohen, and Lionel Naccache. Multidimensional cognitive evaluation of patients with disorders of consciousness using EEG: A proof of concept study. *NeuroImage: Clinical*, 13:455–469, 2017. ISSN 22131582. doi: 10.1016/j.nicl.2016.12.004. 16, 50

Anil K. Seth. Interoceptive inference, emotion, and the embodied self. *Trends in Cognitive Sciences*, 17(11):565–573, Nov 2013. ISSN 13646613. doi: 10.1016/j.tics.2013.09.007. 92

Anil K. Seth, Keisuke Suzuki, and Hugo D. Critchley. An interoceptive predictive coding model of conscious presence. *Frontiers in Psychology*, 3(JAN), 2012. ISSN 16641078. doi: 10.3389/fpsyg.2011.00395. 70

A Shiel, S A Horn, B A Wilson, M J Watson, M J Campbell, and D L Mclellan. The Wessex Head Injury Matrix (WHIM) main scale: a preliminary report on a scale to assess and monitor patient recovery after severe head injury. *Clinical Rehabilitation*, 14(4):408–416, 2000. ISSN 0269-2155. doi: 10.1191/0269215500cr326oa. 6

Jacobo Diego Sitt, Jean Remi King, Imen El Karoui, Benjamin Rohaut, Frederic Faugeras, Alexandre Gramfort, Laurent Cohen, Mariano Sigman, Stanislas Dehaene, and Lionel Naccache. Large scale screening of neural signatures of consciousness in patients in a vegetative or minimally conscious state. *Brain*, 137(8):2258–2270, 2014. ISSN 14602156. doi: 10.1093/brain/awu141. 17, 26, 27, 28, 29, 30, 31, 32, 35, 36, 41, 82, 84, 90, 96, 103

Erik K. St. Louis and Lauren C Frey. *Electroencephalography*. 2016. ISBN 978-0-9979756-0-4. doi: 10.5698/978-0-9979756-0-4. 9, 10

- Barry E. Stein and Terrence R. Stanford. Multisensory integration: Current issues from the perspective of the single neuron. *Nature Reviews Neuroscience*, 9(4):255–266, 2008. ISSN 1471003X. doi: 10.1038/nrn2331. 52, 53
- Jeroen J. Stekelenburg and Jean Vroomen. Neural Correlates of Multisensory Integration of Ecologically Valid Audiovisual Events. *Journal of Cognitive Neuroscience*, 19(12):1964–1973, 2007. ISSN 0898-929X. doi: 10.1162/jocn.2007.19.12.1964. 53
- Johan Stender, Olivia Gosseries, Marie-Aur lie Bruno, Vanessa Charland-Verville, Audrey Vanhauzenhuyse, Athena Demertzi, Camille Chatelle, Marie Thonnard, Aurore Thibaut, Lizette Heine, Andrea Soddu, M lanie Boly, Caroline Schnakers, Albert Gjedde, and Steven Laureys. Diagnostic precision of PET imaging and functional MRI in disorders of consciousness: a clinical validation study. *Lancet*, 384(9942):514–522, 2014. ISSN 1474-547X. doi: 10.1016/S0140-6736(14)60042-8. 7
- Johan Stender, Kristian Nygaard N. Mortensen, Aurore Thibaut, Sune Darkner, Steven Laureys, Albert Gjedde, and Ron Kupers. The Minimal Energetic Requirement of Sustained Awareness after Brain Injury. *Current Biology*, 26(11):1494–1499, 2016. ISSN 09609822. doi: 10.1016/j.cub.2016.04.024. 7, 95
- M lanie Strauss, Jacobo Diego Sitt, Jean-R mi King, M. Elbaz, Leila Azizi, Marco Buiatti, Lionel Naccache, Virginie Van Wassenhove, and Stanislas Dehaene. Disruption of hierarchical predictive coding during sleep. *Proceedings of the National Academy of Sciences*, page In press, 2015. 89
- Pasquale Striano, Francesca Bifulco, and Giuseppe Servillo. The saga of Eluana Englaro: Another tragedy feeding the media, 2009. ISSN 03424642. 3
- Durk Talsma and Marty G. Woldorff. Selective Attention and Multisensory Integration: Multiple Phases of Effects on the Evoked Brain Activity. *Journal of Cognitive Neuroscience*, 17(7):1098–1114, 2005. ISSN 0898-929X. doi: 10.1162/0898929054475172. 53, 54, 67
- Ole Tange. GNU Parallel: the command-line power tool. *login: The USENIX Magazine*, 36(1):42–47, 2011. doi: 10.5281/zenodo.16303. 28
- Graham Teasdale and Bryan Jennett. ASSESSMENT OF COMA AND IMPAIRED CONSCIOUSNESS. A Practical Scale. *The Lancet*, 304(7872):81–84, 1974. ISSN 01406736. doi: 10.1016/S0140-6736(74)91639-0. 5
- W. A. Teder-S lej rvi, J. J. McDonald, F. Di Russo, and S. A. Hillyard. An analysis of audio-visual crossmodal integration by means of event-related potential (ERP) recordings. *Cognitive Brain Research*, 14(1):106–114, 2002. ISSN 09266410. doi: 10.1016/S0926-6410(02)00065-4. 54, 67

- Giulio Tononi and Christof Koch. The neural correlates of consciousness: An update, 2008. ISSN 00778923. 17
- Giulio Tononi, Melanie Boly, Marcello Massimini, and Christof Koch. Integrated information theory: From consciousness to its physical substrate. *Nature Reviews Neuroscience*, 17(7): 450–461, 2016. ISSN 14710048. doi: 10.1038/nrn.2016.44. 17
- Athina Tzovara, Alexandre Simonin, Mauro Oddo, Andrea O. Rossetti, and Marzia De Lucia. Neural detection of complex sound sequences in the absence of consciousness. *Brain*, 138 (5):1160–1166, 2015. ISSN 14602156. doi: 10.1093/brain/awv041. 89
- M.W. Van Der Molen, R.J.M. Somsen, and J.F. Orlebeke. Phasic heart rate responses and cardiac cycle time in auditory choice reaction time. *Biological Psychology*, 16(3-4):255–271, may 1983. ISSN 03010511. doi: 10.1016/0301-0511(83)90028-5. 70, 89
- F Varela, J P Lachaux, E Rodriguez, and J Martinerie. The brainweb: phase synchronization and large-scale integration. *Nature reviews. Neuroscience*, 2(4):229–239, 2001. ISSN 1471-003X. doi: 10.1038/35067550. 11
- Francisco J. Varela, Evan Thompson, and Eleanor Rosch. *The embodied mind: cognitive science and human experience*. MIT Press, 1991. ISBN 978-0-262-22042-2. 92
- Gaël Varoquaux, Pradeep Reddy Raamana, Denis A. Engemann, Andrés Hoyos-Idrobo, Yannick Schwartz, and Bertrand Thirion. Assessing and tuning brain decoders: Cross-validation, caveats, and guidelines. *NeuroImage*, 145:166–179, jan 2017. ISSN 10538119. doi: 10.1016/j.neuroimage.2016.10.038. 35
- X.-J. Wang. Neurophysiological and Computational Principles of Cortical Rhythms in Cognition. *Physiological Reviews*, 90(3):1195–1268, 2010. ISSN 0031-9333. doi: 10.1152/physrev.00035.2008. 11, 12
- Sarah Wannez, Lizette Heine, Marie Thonnard, Olivia Gosseries, and Steven Laureys. The repetition of behavioral assessments in diagnosis of disorders of consciousness. *Annals of Neurology*, 81(6):883–889, 2017. ISSN 15318249. doi: 10.1002/ana.24962. 52
- Eelco F M Wijdicks, William R. Bamlet, Bobby V. Maramattom, Edward M. Manno, and Robyn L. McClelland. Validation of a new coma scale: The FOUR score. *Annals of Neurology*, 58(4):585–593, 2005. ISSN 03645134. doi: 10.1002/ana.20611. 5
- Shawniqua T. Williams, Mary M. Conte, Andrew M. Goldfine, Quentin Noirhomme, Olivia Gosseries, Marie Thonnard, Bradley Beattie, Jennifer Hersh, Douglas I. Katz, Jonathan D. Victor, Steven Laureys, and Nicholas D. Schiff. Common resting brain dynamics indicate

a possible mechanism underlying zolpidem response in severe brain injury. *eLife*, 2013(2), 2013. ISSN 2050084X. doi: 10.7554/eLife.01157. 49

S L Wilson and H Gill-Thwaites. Early indication of emergence from vegetative state derived from assessments with the SMART—a preliminary report. *Brain injury*, 14(4):319, 2000. ISSN 0269-9052. doi: 10.1080/026990500120619. 6

Jennifer Michelle Windt and Thomas Metzinger. The philosophy of dreaming and self-consciousness: What happens to the experiential subject during the dream state?, 2007. 53